Geosphere

Synvolcanic crustal extension during the mid-Cenozoic ignimbrite flare-up in the northern Sierra Madre Occidental, Mexico: Evidence from the Guazapares Mining District region, western Chihuahua

Bryan P. Murray, Cathy J. Busby, Luca Ferrari and Luigi A. Solari

Geosphere published online 13 September 2013;
doi: 10.1130/GES00862.1

Notes

Geosphere, published online on 13 September 2013 as doi:10.1130/GES00862.1

Synvolcanic crustal extension during the mid-Cenozoic ignimbrite flare-up in the northern Sierra Madre Occidental, Mexico: Evidence from the Guazapares Mining District region, western Chihuahua

Bryan P. Murray[1], Cathy J. Busby[1], Luca Ferrari[2], and Luigi A. Solari[2]
[1]*Department of Earth Science, University of California, Santa Barbara, Webb Hall, Santa Barbara, California 93106-9630, USA*
[2]*Centro de Geociencias, Universidad Nacional Autónoma de México, Boulevard Juriquilla 3001, Querétaro, 76230, México*

ABSTRACT

The timing and spatial extent of mid-Cenozoic ignimbrite flare-up volcanism of the Sierra Madre Occidental silicic large igneous province of Mexico in relation to crustal extension is relatively unknown. Extension in the Sierra Madre Occidental has been variably interpreted to have preceded, postdated, or begun during Early Oligocene flare-up volcanism of the silicic large igneous province. New geologic mapping, zircon U-Pb laser ablation–inductively coupled plasma–mass spectrometry dating, modal analysis, and geochemical data from the Guazapares Mining District region along the western edge of the northern Sierra Madre Occidental silicic large igneous province have identified three informal synextensional formations. The ca. 27.5 Ma Parajes formation is an ~1-km-thick succession composed primarily of welded to nonwelded silicic outflow ignimbrite sheets erupted from distant sources. The 27–24.5 Ma Témoris formation is interpreted as an andesitic volcanic center composed of locally erupted mafic to intermediate composition lavas and associated intrusions, with interbedded andesite-clast fluvial and debris flow deposits, and an upper section of thin distal silicic outflow ignimbrites. The 24.5–23 Ma Sierra Guazapares formation is composed of silicic vent facies ignimbrites to proximal ignimbrites, lavas, plugs, dome-collapse deposits, and fluvially or debris flow–reworked equivalents. These three formations record (1) the accumulation of outflow ignimbrite sheets, presumably erupted from calderas mapped ~50–100 km east of the study area that were active during the Early Oligocene pulse of the mid-Cenozoic ignimbrite flare-up; (2) development of an andesitic volcanic field in the study area, likely related to rocks of the Southern Cordillera basaltic andesite province that were intermittently erupted across all of the northern Sierra Madre Occidental toward the end of and following the Early Oligocene ignimbrite pulse; and (3) the initiation of explosive and effusive silicic fissure magmatism in the study area during the Early Miocene pulse of the mid-Cenozoic ignimbrite flare-up.

The main geologic structures identified in the Guazapares Mining District region are NNW–trending normal faults, with an estimated minimum of 20% total horizontal extension. Normal faults were active during deposition of all three formations (Parajes, Témoris, and Sierra Guazapares), and bound half-graben basins that show evidence of synvolcanic extension (e.g., growth strata) during deposition. Normal faulting began by ca. 27.5 Ma during deposition of the youngest ignimbrites of the Parajes formation, concurrent with the end of the Early Oligocene silicic ignimbrite pulse to the east and before magmatism began in the study area. In addition, preexisting normal faults localized andesitic volcanic vents of the Témoris formation and silicic vents of the Sierra Guazapares formation, and some faults were reactivated during, as well as after, deposition of these formations.

We interpret extensional faulting and magmatism in the Guazapares Mining District region to be part of a regional-scale Middle Eocene to Early Miocene southwestward migration of active volcanism and crustal extension in the northern Sierra Madre Occidental. We show that extension accompanied silicic volcanism in the Guazapares region, and overlapped with the peak of mid-Cenozoic ignimbrite flare-up in the Sierra Madre Occidental; this supports the interpretation that there is a relationship between lithospheric extension and silicic large igneous province magmatism.

INTRODUCTION

Silicic large igneous provinces are significant in the geologic record due to their unusually extensive areal coverage (>100,000 km^2), large volumes (>250,000 km^3), and potential to induce environmental change (e.g., Bryan, 2007; Cather et al., 2009; Jicha et al., 2009; Bryan and Ferrari, 2013). Compositions within silicic large igneous provinces range from basalt to high-silica rhyolite, but are volumetrically dominated (>80%) by dacite-rhyolite compositions, with >75% of the total magmatic volume emplaced during short duration (~1–5 Myr) pulses over a maximum province lifespan of ~50 Myr (Bryan, 2007; Bryan and Ernst, 2008). Previous studies suggest that silicic large igneous provinces may be characteristic of continental regions undergoing broad lithospheric extension and typically initiate as prerifting magmatic events (Bryan et al., 2002; Bryan, 2007; Best et al., 2013; Bryan and Ferrari, 2013). Therefore, determining the timing of extensional deformation in relation to magmatism is an important consideration toward understanding silicic large igneous province processes, as crustal extension is suggested as one mechanism that favors the generation of large silicic magma volumes (Hildreth, 1981; Wark, 1991; Hanson and Glazner, 1995) as well as very large magnitude explosive silicic eruptions (Aguirre-Díaz and Labarthe-Hernández, 2003; Costa et al., 2011).

The Sierra Madre Occidental of western Mexico is the third largest silicic large igneous province of the Phanerozoic and is the largest and best-preserved of the Cenozoic (Fig. 1; Bryan, 2007; Ferrari et al., 2007). It extends for ~1200 km south from the U.S.-Mexico border to the Trans-Mexican Volcanic Belt, forming a high plateau with an average elevation >2000 m, consisting primarily of Oligocene to Early Miocene ignimbrites that cover an

Geosphere; October 2013; v. 9; no. 5; doi:10.1130/GES00862.1; 15 figures; 3 tables; 5 supplemental files.
Received 21 August 2012 ♦ Revision received 19 June 2013 ♦ Accepted 14 August 2013 ♦ Published online 12 September 2013

Geosphere, published online on 13 September 2013 as doi:10.1130/GES00862.1

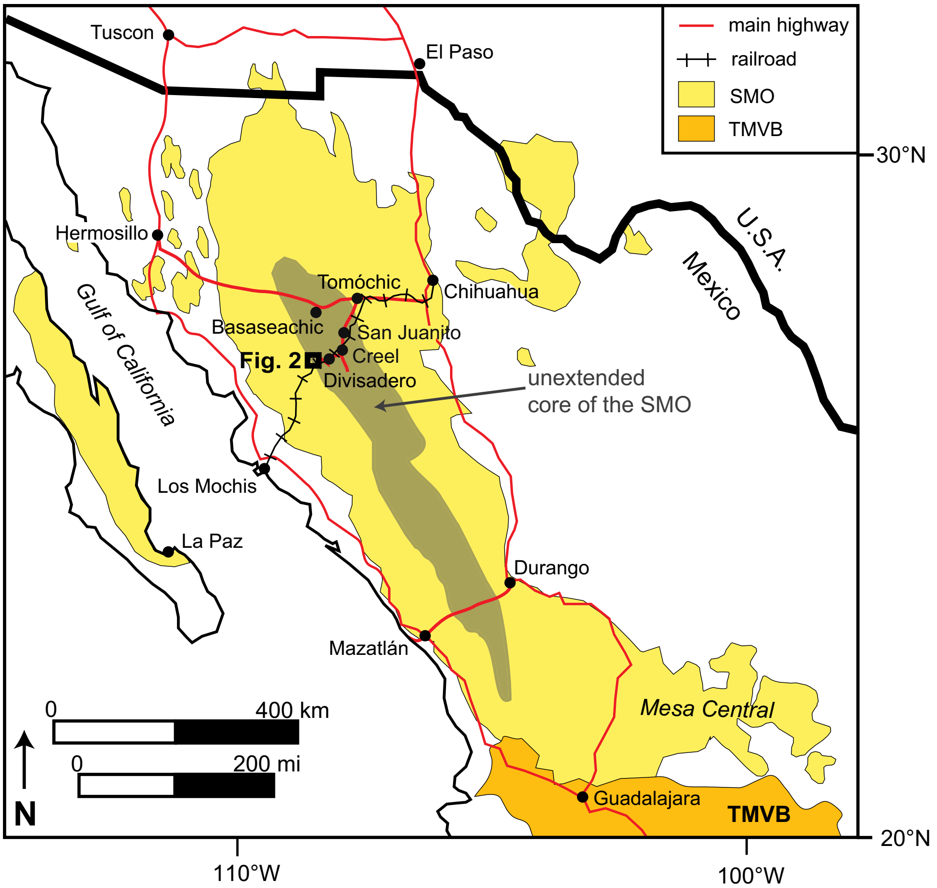

Figure 1. Generalized map of western Mexico showing the extent of the Sierra Madre Occidental (SMO) silicic large igneous province (light yellow) and the relatively unextended core (dark gray) of the SMO (after Henry and Aranda-Gómez, 2000; Ferrari et al., 2002; Bryan et al., 2013). The location of the Guazapares Mining District region (Fig. 2) is indicated. TMVB—Trans-Mexican Volcanic Belt.

estimated area of 300,000–400,000 km^2 with an average thickness of 1 km (McDowell and Keizer, 1977; McDowell and Clabaugh, 1979; Aguirre-Díaz and Labarthe-Hernández, 2003). The volcanism of the Sierra Madre Occidental silicic large igneous province is contemporaneous with, and is considered part of, the extensive mid-Cenozoic ignimbrite flare-up that affected much of the southwestern North American Cordillera from the Middle Eocene to Late Miocene (e.g., Coney, 1978; Armstrong and Ward, 1991; Ward, 1991; Ferrari et al., 2002; Lipman, 2007; Cather et al., 2009; Henry et al., 2010; Best et al., 2013). The core of the Sierra Madre Occidental is relatively unextended in comparison to the surrounding Late Oligocene to Miocene extensional belts of the southern Basin and Range to the east and the Gulf Extensional Province to the west (Fig. 1; Nieto-Samaniego et al., 1999; Henry and Aranda-Gómez, 2000). Rocks related to the silicic large igneous province extend beyond the Sierra Madre Occidental proper (Fig. 1) to the Mesa Central and parts of the southern Basin and Range in eastern Chihuahua and Durango (Gunderson et al., 1986; Aguirre-Díaz and McDowell, 1991, 1993), as well as southwesternmost mainland Mexico and Baja California Sur (Umhoefer et al., 2001; Ferrari et al., 2002).

A large part of the Sierra Madre Occidental remains unmapped and undated (>90%; Swanson et al., 2006). Previous work in the Sierra Madre Occidental has been primarily restricted to the southern region of the igneous province (e.g., Nieto-Samaniego et al., 1999; Ferrari et al., 2002), the vicinity of the Mazatlán–Durango highway in the central region (e.g., McDowell and Keizer, 1977; McDowell and Clabaugh, 1979; Henry and Fredrikson, 1987), and the areas around the Hermosillo–Chihuahua City highway and the Tomóchic–Creel road in the northern region (e.g., Swanson, 1977; Swanson and McDowell, 1984, 1985; Wark et al., 1990; Cochemé and Demant, 1991; Wark, 1991; McDowell and Mauger, 1994; Albrecht and Goldstein, 2000; Swanson et al., 2006; McDowell, 2007; McDowell and McIntosh, 2012) (Fig. 1). As a result, the age relationships between ignimbrite flare-up volcanism and crustal extension remain unclear. Previous studies have suggested that significant crustal extension in the region did not occur until after the peak of large volume ignimbrite flare-up volcanism, which was inferred to have occurred between ca. 32 and 28 Ma (Early Oligocene; e.g., McDowell and Clabaugh, 1979; Wark et al., 1990; McDowell and Mauger, 1994; Gans, 1997; Grijalva-Noriega and Roldán-Quintana, 1998). However, other studies have inferred that initial regional extension is recorded by the onset of large volume Early Oligocene ignimbrite flare-up volcanism (e.g., Aguirre-Díaz and McDowell, 1993), or that extensional deformation began before the flare-up (e.g., Dreier, 1984; Ferrari et al., 2007). Uncertainty regarding the timing of extension relative to ignimbrite flare-up volcanism is also a problem in the Basin and Range of the western U.S., where previous studies have inferred that extension preceded, postdated, or began during ignimbrite flare-up volcanism (e.g., Gans et al., 1989; Best and Christiansen, 1991; Axen et al., 1993; Best et al., 2013).

The Guazapares Mining District region of western Chihuahua, Mexico, is located ~250 km southwest of Chihuahua City in the northern Sierra Madre Occidental (Fig. 1). The excellent rock exposure and topographic relief in this previously unmapped area make it ideal for studying the relationships between silicic large igneous province volcanism and crustal extension. In this paper we show that extension preceded the onset of magmatism in the study area. We demonstrate that extension was active in the study area during deposition of ca. 27.5 Ma outflow ignimbrites, presumably derived from calderas of similar ages identified to the north and east by other workers. Extension continued during growth of a ca. 27–24.5 Ma andesitic volcanic center in the study area, followed by continued extension during ca. 24.5–23 Ma silicic flare-up magmatism in the study area. This study shows how extensional structures controlled the siting of the andesitic and silicic volcanic vents and shallow-level intrusions. This study also shows that the onset of extension in the study area overlaps with the end of peak Oligocene silicic magmatism to the east, and that extension in the study area preceded and coincided with a second peak of magmatism in the Miocene, which is represented in the study area. Last, we show that our data support the interpretation that silicic flare-up magmatism swept southwestward with time, due to rollback and/or removal of the slab that was subducting beneath western Mexico.

GEOLOGIC SETTING

Previous regional-scale studies in the Sierra Madre Occidental subdivided volcanic rocks into: (1) the Late Cretaceous to Eocene Lower Volcanic Complex of dominantly andesitic composition; (2) the Eocene to Early Miocene Upper Volcanic Supergroup of dominantly silicic composition; and (3) the Early Oligocene to Early Miocene basaltic andesite volcanic rocks of the Southern Cordillera basaltic andesite province (McDowell and Keizer, 1977; Cameron et al., 1989; Ferrari et al., 2007). The Lower Volcanic Complex is believed to underlie most of the Upper Volcanic Supergroup (Aguirre-Díaz and McDowell, 1991; Ferrari et al., 2007), although the thick ignimbrite cover of the Upper Volcanic Supergroup obscures much of the geologic relationships between these two subdivisions in most areas. The volcanic rocks of the Lower Volcanic Complex generally consist of intermediate composition lavas and lesser silicic tuffs, and are interpreted as the products of normal steady-state (i.e., non–flare-up-style) continental subduction-related magmatism broadly contemporaneous with the Laramide orogeny in western North America (McDowell and Keizer, 1977; McDowell et al., 2001).

The ~1-km-thick Upper Volcanic Supergroup broadly refers to the products of large-volume flare-up–style (i.e., high output rate and large eruptive volumes) silicic magmatism, also known as the mid-Cenozoic ignimbrite flare-up, and defines the extent of the Sierra Madre Occidental silicic large igneous province (McDowell and Keizer, 1977; Bryan, 2007; Ferrari et al., 2007). The Upper Volcanic Supergroup is composed of Eocene to Early Miocene silicic ignimbrites, lavas, and intrusions, and lesser intermediate to mafic lavas (McDowell and Keizer, 1977; McDowell and Clabaugh, 1979; Aguirre-Díaz and McDowell, 1991, 1993; Ferrari et al., 2002, 2007; McDowell, 2007). The large volume of silicic ignimbrites and high output rate suggest multiple caldera and fissure sources for these volcanic deposits (e.g., Swanson and McDowell, 1984; Aguirre-Díaz and Labarthe-Hernández, 2003; Swanson et al., 2006; McDowell, 2007). Ferrari et al. (2002, 2007) proposed that there were at least two main pulses of large volume silicic ignimbrite flare-up volcanism in the Sierra Madre Occidental during the mid-Cenozoic, one during the Early Oligocene (ca. 32–28 Ma) and another during the Early Miocene (ca. 24–20 Ma). The Early Oligocene ignimbrite pulse is inferred to have occurred throughout the Sierra Madre Occidental, while the Early Miocene ignimbrite pulse was inferred to be volumetrically more significant in the southern Sierra Madre Occidental and less abundant, with more mafic compositions, in the north (Ferrari et al., 2002, 2007; Bryan et al., 2013). The Early Oligocene pulse is estimated to have contributed at least half to three-quarters (>200,000 km^3) of the erupted volume of the Upper Volcanic Supergroup, but at least 50,000–100,000 km^3 was erupted during the Early Miocene pulse (Cather et al., 2009; Bryan et al., 2013). McDowell and McIntosh (2012) suggested that most ignimbrites in the northern and central Sierra Madre Occidental were erupted during discrete time intervals (36–33.5 Ma and 31.5–28 Ma). In addition, an older Eocene pulse of ignimbrite eruptions between 46 and 42 Ma is only recognized along the eastern margin of the Sierra Madre Occidental, and an interval of ca. 24 Ma ignimbrite eruptions that coincides with the Early Miocene pulse of Ferrari et al. (2002, 2007) is observed in the western regions of the igneous province (McDowell and McIntosh, 2012), west of our study area.

During the final stages of and after each silicic ignimbrite pulse of the Upper Volcanic Supergroup, basaltic andesite lavas were intermittently erupted across all of the northern Sierra Madre Occidental (Ferrari et al., 2007). In the northern part of the Sierra Madre Occidental these rocks were generally considered part of the Southern Cordillera basaltic andesite province (Cameron et al., 1989) with ages ranging from 33 to 17.6 Ma, although they mostly are Oligocene (Cameron et al., 1989, and references therein; Ferrari et al., 2007). The rocks of the Southern Cordillera basaltic andesite province have been interpreted as magmatism recording the initiation of crustal extension across the region (e.g., Cameron et al., 1989; Cochemé and Demant, 1991; Gans, 1997; McDowell et al., 1997; González León et al., 2000; Ferrari et al., 2007).

Several prior studies recognized significant crustal extension in the Sierra Madre Occidental immediately following the Early Oligocene ignimbrite pulse of the Upper Volcanic Supergroup (e.g., McDowell and Clabaugh, 1979; Wark et al., 1990; McDowell and Mauger, 1994; Gans, 1997; Grijalva-Noriega and Roldán-Quintana, 1998). The earliest evidence of extensional faulting in the northern Sierra Madre Occidental is found in central Chihuahua (younger than 29 Ma), immediately following the Early Oligocene ignimbrite pulse (McDowell and Mauger, 1994). In east-central Sonora, the earliest age of crustal extension is possibly as old as 27 Ma and synvolcanic deposition in many normal-fault basins was active by 24 Ma, following the peak of Early Oligocene ignimbrite flare-up volcanism (Gans, 1997; McDowell et al., 1997; Gans et al., 2003). However, extension in the Sierra Madre Occidental may have begun as early as the Eocene, prior to the eruption of the Early Oligocene ignimbrite pulse, based on the orientation and age of epithermal vein deposits (Dreier, 1984) and a moderate angular unconformity between the Lower Volcanic Complex and Upper Volcanic Supergroup (e.g., Ferrari et al., 2007). Direct evidence of Early Eocene (pre–Upper Volcanic Supergroup) extensional faulting is observed in the Mesa Central region to the east of the core of the southern Sierra Madre Occidental and includes a moderate angular unconformity within continental clastic and andesitic volcanic sequences and subvolcanic intrusions along normal faults (Aranda-Gómez and McDowell, 1998; Aguillón-Robles et al., 2009; Tristán-González et al., 2009), as well as ca. 32 Ma synvolcanic normal faults that were active until ca. 24 Ma (Aguirre-Díaz and McDowell, 1993; Luhr et al., 2001). However, Eocene-age extensional faulting has not been documented in the Sierra Madre Occidental proper.

The Guazapares Mining District of western Chihuahua is located at the western edge of the relatively unextended core of the northern Sierra Madre Occidental, at the boundary with the highly extended Gulf Extensional Province (Fig. 1). Previous geologic studies in this ~300 km^2 region were restricted to regional 1:50,000 and 1:250,000 geologic mapping by the Mexican Geological Survey (Minjárez Sosa et al., 2002; Ramírez Tello and Garcia Peralta, 2004) and mining company reports (e.g., Roy et al., 2008; Wood and Durgin, 2009; Gustin, 2011, 2012). On these maps and reports, Paleocene–Eocene Lower Volcanic Complex andesitic rocks were inferred to underlie the Oligocene Upper Volcanic Supergroup silicic ignimbrites, but we show here that these rocks (which we informally refer to as the Témoris formation) are both underlain and overlain by silicic ignimbrites, and therefore cannot be assigned to the Lower Volcanic Complex. Prior to this study there were no geochronological data from the Guazapares Mining District region and the closest reported dates were from Upper Volcanic Supergroup ignimbrites ~50 km to the northeast near Divisadero (ca. 30 Ma; Swanson et al., 2006).

LITHOLOGY AND STRATIGRAPHY

New geologic mapping in the Guazapares Mining District region (Figs. 2, 3, and 4; Supplemental Figure 1[1]) provides the basis for the

[1]Supplemental Figure 1. Geologic map of Guazapares Mining District region, northern Sierra Madre Occidental, Chihuahua, Mexico. If you are viewing the PDF of this paper or reading it offline, please visit http://dx.doi.org/10.1130/GES00862.S1 or the full-text article on www.gsapubs.org to view Supplemental Figure 1.

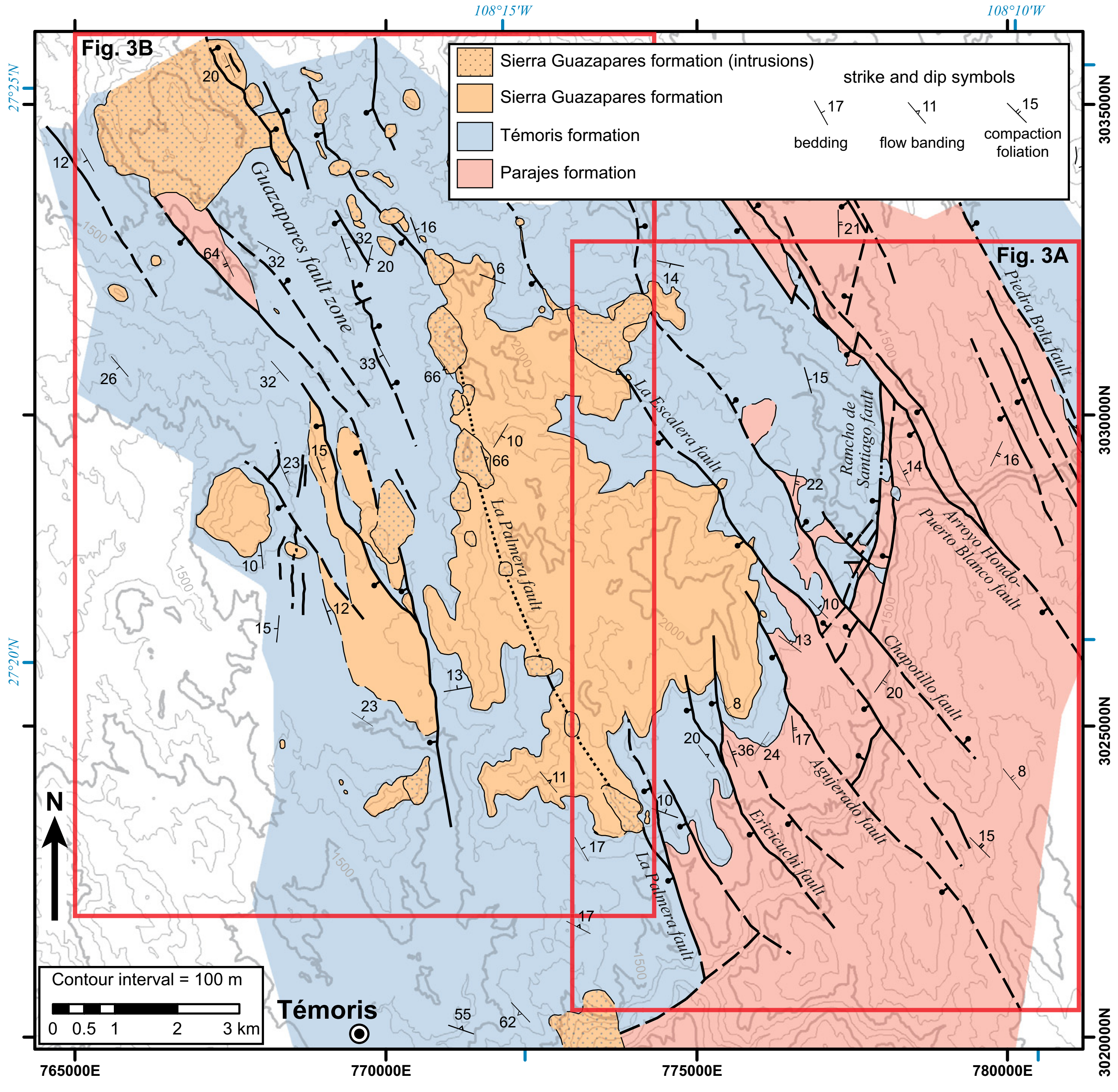

Figure 2. Simplified geologic map of the Guazapares Mining District region, showing the extents of the three formations discussed herein (see Fig. 5) and the locations of major faults. Boxes indicate the locations of the detailed geologic maps of Figure 3. See Supplemental Figure 1 (see footnote 1) for more detailed geologic mapping of the study area. Coordinates in black are Universal Transverse Mercator, North American Datum 1927.

subdivision of three informally named formations described in the following (from oldest to youngest): (1) the Parajes formation, consisting mainly of silicic outflow ignimbrites; (2) the Témoris formation, composed mainly of mafic to intermediate composition lavas and intrusions; and (3) the Sierra Guazapares formation, consisting of silicic vent-proximal ignimbrites, lavas, and subvolcanic intrusions (Fig. 5).

The volcanic and volcaniclastic terminologies used in this paper are those of Fisher and Schmincke (1984), Fisher and Smith (1991), and Sigurdsson et al. (2000). Following Fisher and Schmincke (1984), volcaniclastic refers to all fragmental rocks made dominantly of volcanic detritus; these include (1) pyroclastic fragmental deposits, inferred to have been directly fed from an eruption, e.g., pyroclastic fall, ignimbrites,

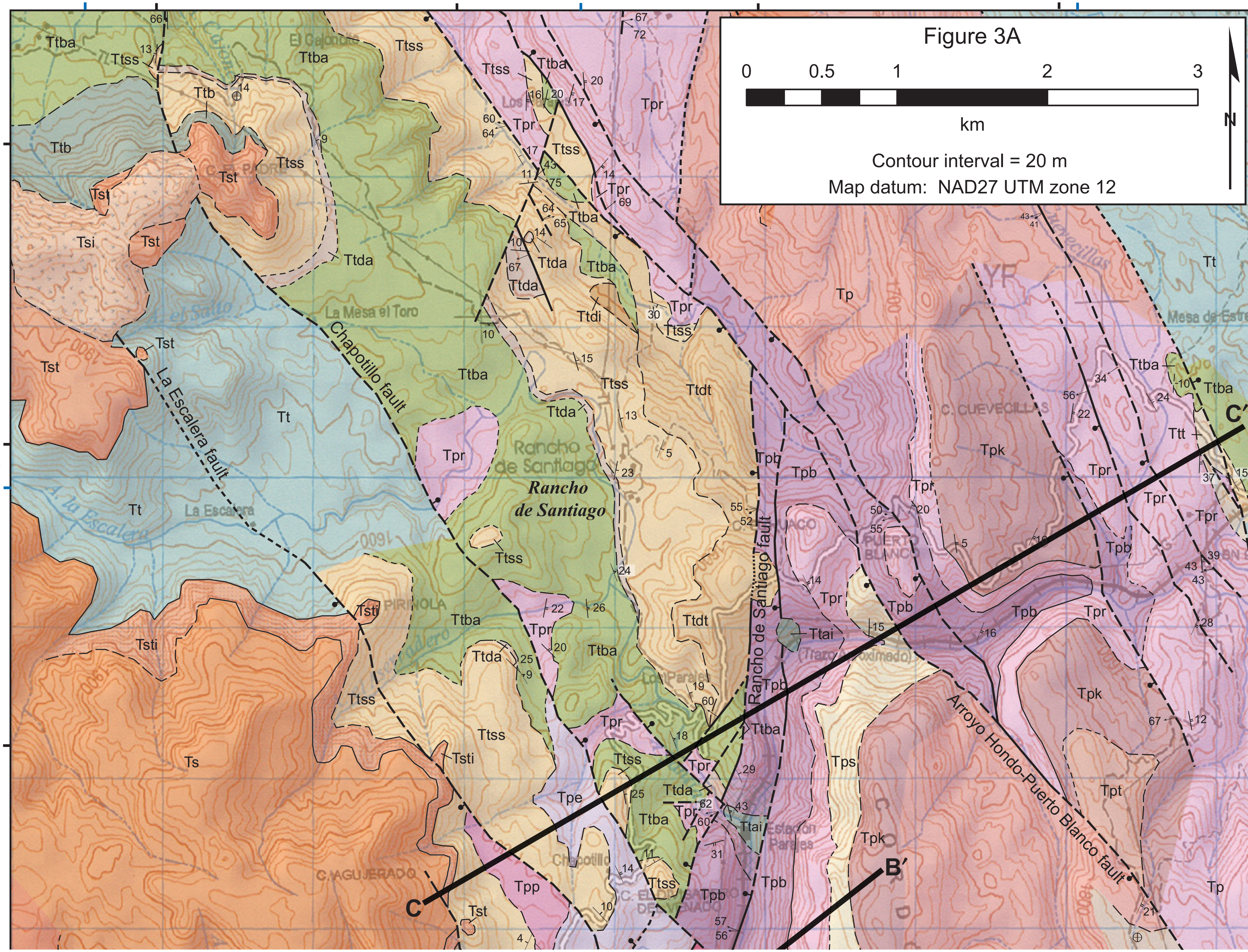

Figure 3 (*on this and following four pages*). Geologic maps of portions of the Guazapares Mining District region. Topographic base map is from Instituto Nacional de Estadística, Geografía e Informática (INEGI); original 1:50,000 scale ITRF92 (International Terrestrial Reference Frame 1992) datum projected to NAD27 UTM (Universal Transverse Mercator, North American Datum 1927) zone 12. The entire geologic map for the study area is presented in Supplemental Figure 1 (see footnote 1). (A) Geologic map of the southeastern portion of the Guazapares Mining District region between Puerto La Cruz and Rancho de Santiago, east of Témoris. The locations of cross-sections A–A′, B–B′, and C–C′ (Fig. 4) are indicated.

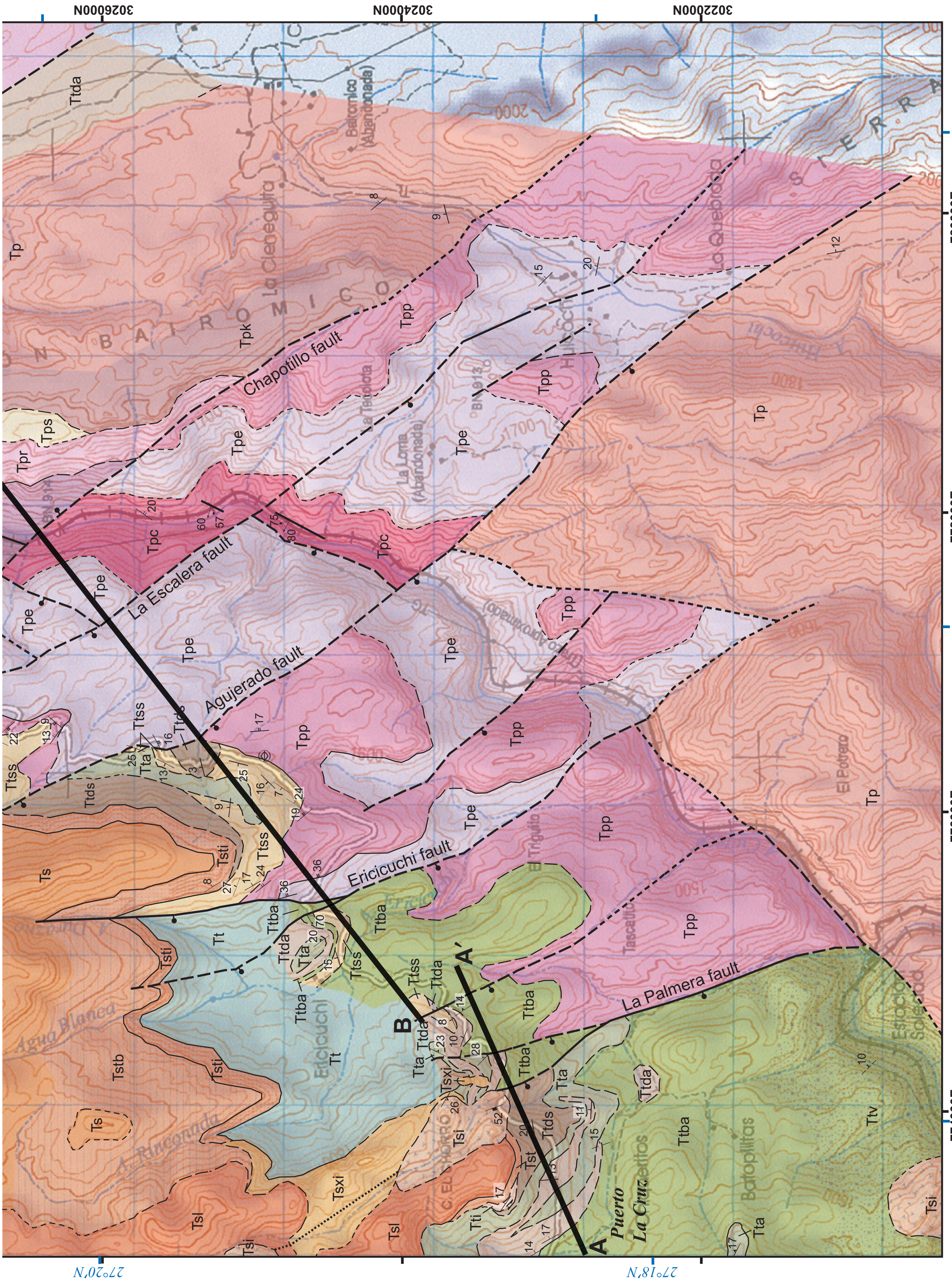

Figure 3A (*continued*).

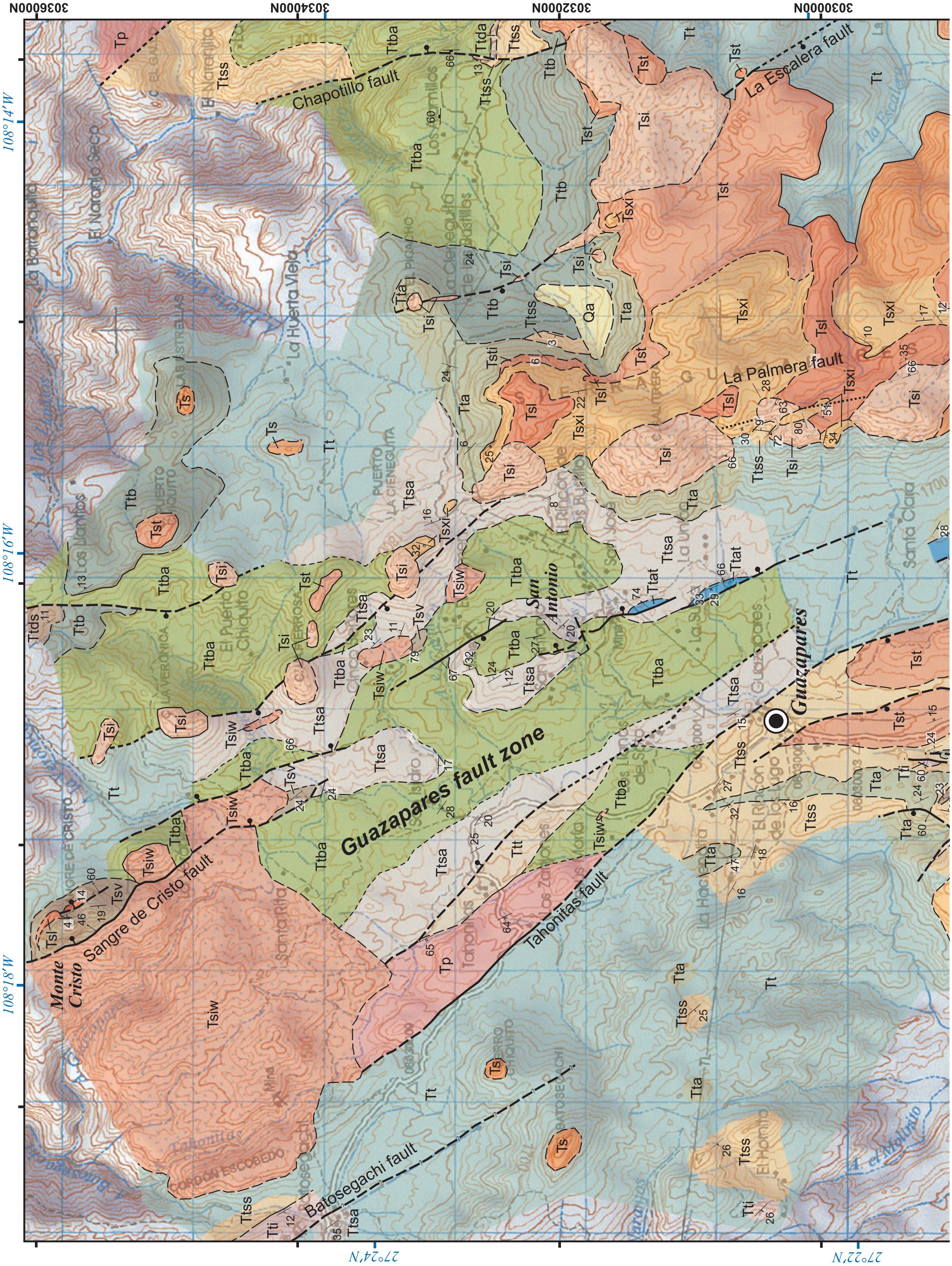

Figure 3 (*continued*). (B) Geologic map of the Guazapares fault zone between Témoris and Monte Cristo.

Geosphere, published online on 13 September 2013 as doi:10.1130/GES00862.1

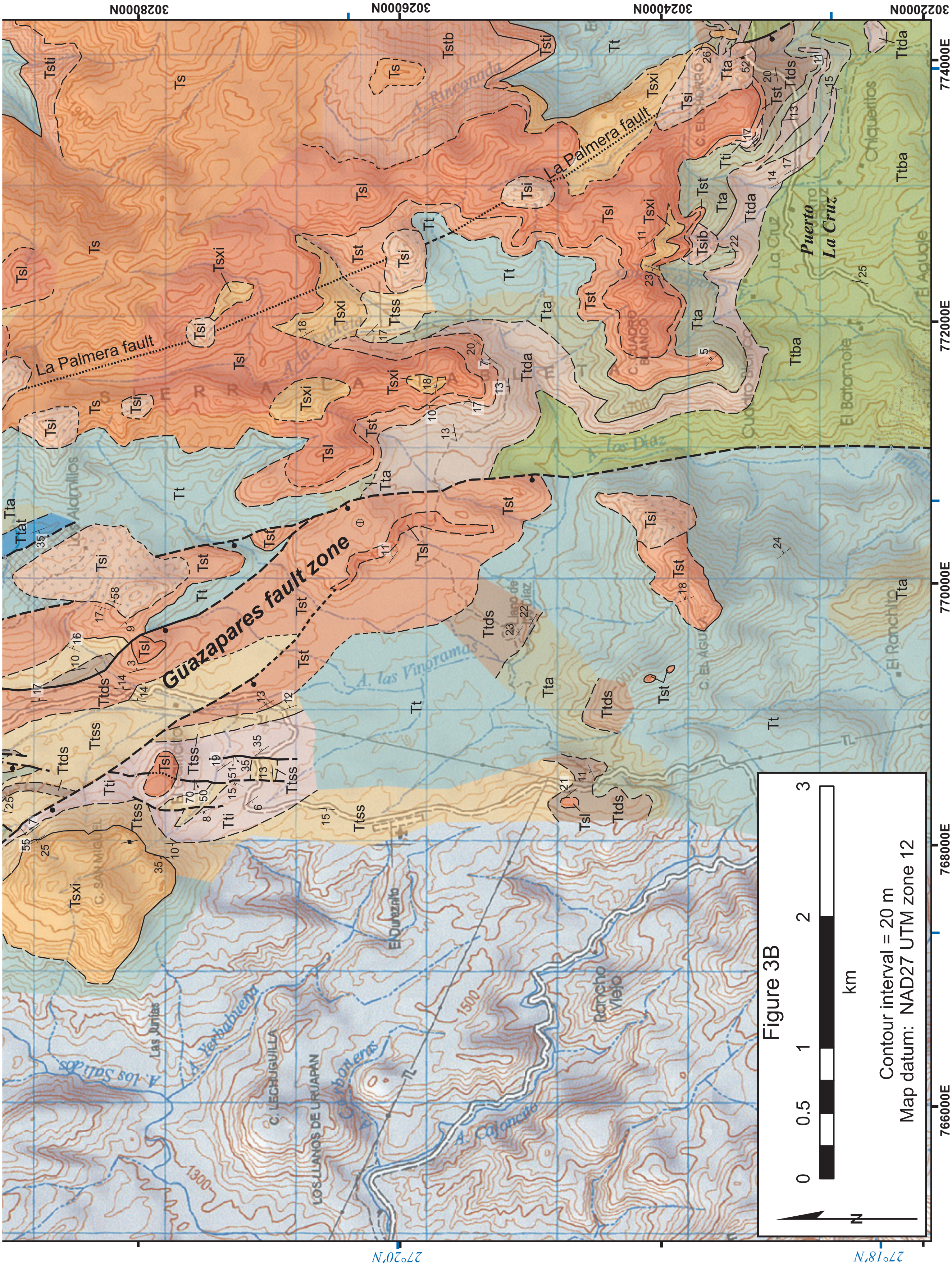

Figure 3B (*continued*).

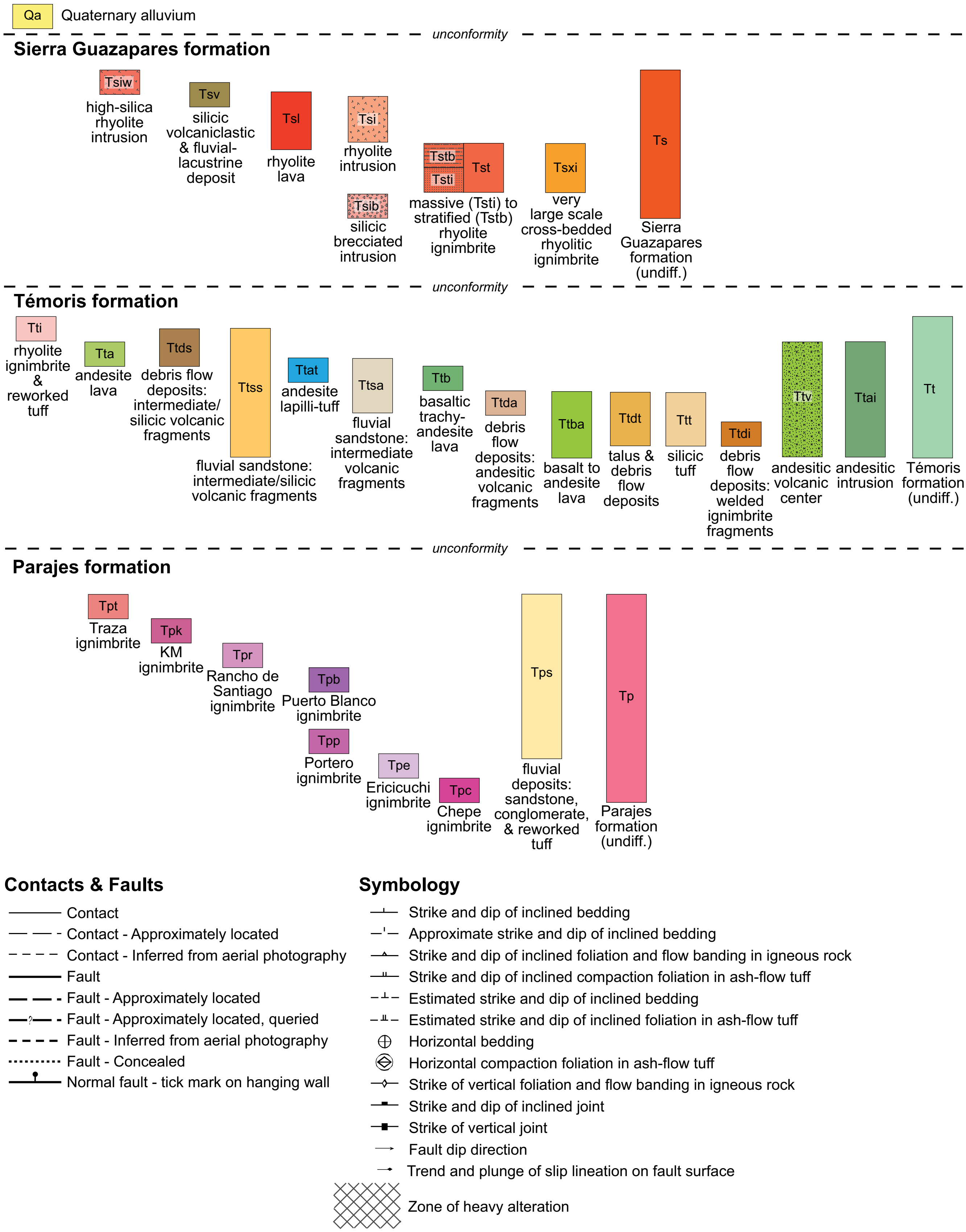

Figure 3 (*continued*). (C) Geologic map key, with lithostratigraphic correlation chart for the map units of the Guazapares Mining District region, based on depositional relationships and geochronology presented in this study. The lithology of the map units is described in Table 1.

Geosphere, published online on 13 September 2013 as doi:10.1130/GES00862.1

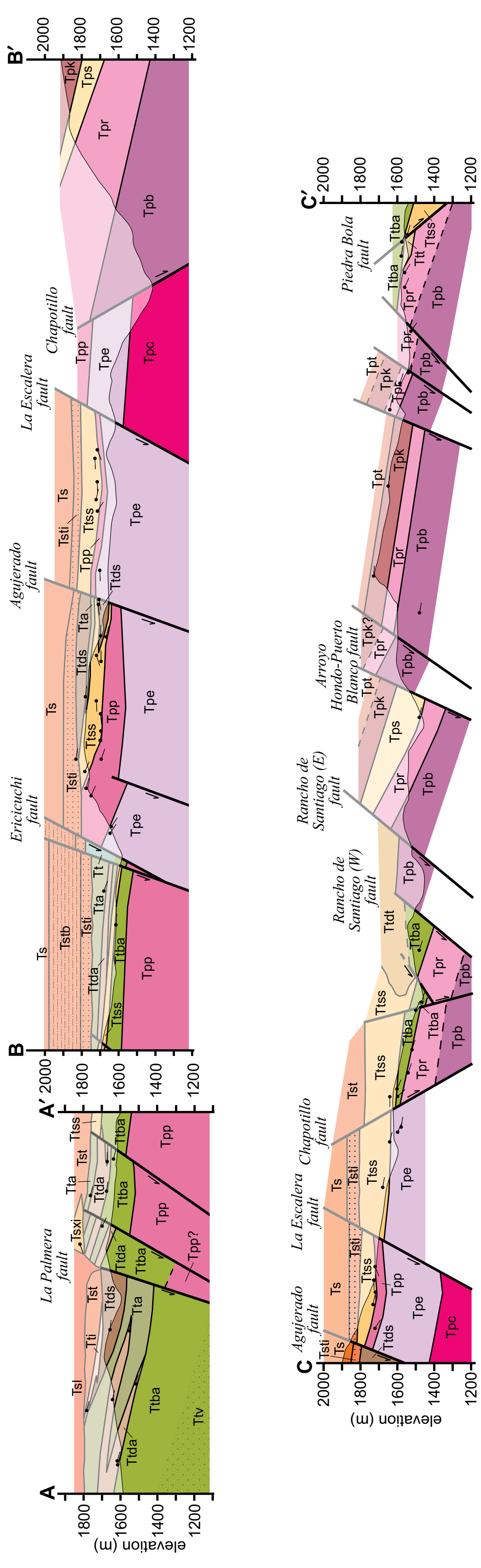

Figure 4. Geologic cross sections for the area between Puerto La Cruz and east of Rancho de Santiago (Fig. 3A), showing major normal faults and the synvolcanic half-graben basins bounded by the La Palmera, Agujerado, Rancho de Santiago, and Arroyo Hondo–Puerto Blanco faults. Sections are same scale as Figure 3A, with no horizontal or vertical exaggeration. Rock units inferred above topography are indicated by subdued color shades, and bedding orientation is shown by tick marks. See Figure 3C for rock unit abbreviations.

autoclastic flow breccias; (2) reworked fragmental deposits, inferred to result from downslope reworking of unconsolidated eruption-fed fragmental deposits, e.g., block-and-ash-flow deposits commonly pass downslope into debris flow and fluvial deposits; and (3) epiclastic deposits, made of volcanic fragments inferred to have been derived from erosion of preexisting rock. When the distinctions cannot be made, the general term volcaniclastic is applied. Delicate pyroclastic detritus such as pumice, shards, or euhedral crystals cannot be derived from erosion of preexisting rock, so their presence in fluvial or debris flow deposits indicates that at least some of the deposit consists of reworked pyroclastic material, indicating broadly coeval explosive volcanism. Similarly, if a debris flow deposit is dominated by one volcanic clast type, it can be inferred to record reworking of a block-and-ash-flow deposit or flow breccia. However, the presence of a broad range of volcanic clast types is not proof of an epiclastic origin, because a wide variety of volcanic clast types can become incorporated into an eruption-triggered debris flow; in that case, a distinction between reworked and epiclastic cannot be made, and the deposit is simply a volcaniclastic debris flow deposit. Debris-flow deposits with blocks of welded ignimbrite, however, cannot be derived by any downslope reworking process known in outflow ignimbrite fields, and instead likely record erosion of preexisting rocks, so those can be classified as epiclastic (note that intracaldera ignimbrites commonly have blocks of welded ignimbrite cannibalized from the caldera wall during ongoing collapse; see discussion in Schermer and Busby, 1994).

The three formations in the Guazapares Mining District region are subdivided into 30 distinct lithologic units by outcrop and thin section characteristics, mineralogy, chemical composition, and inferred volcanic or sedimentary processes (Fig. 3C; Table 1). These lithologic units include volcanic rocks (e.g., lavas, ignimbrites), volcaniclastic rocks (e.g., sandstone, conglomerate, breccia), and hypabyssal intrusions (e.g., plugs, dikes). Modal point-count analyses were carried out for 39 samples, chosen to represent most of the volcanic and hypabyssal map units (Fig. 6). Reconnaissance whole-rock geochemical analyses were performed on 15 relatively unaltered samples of volcanic rock and hypabyssal intrusions from the Témoris and Sierra Guazapares formations (Fig. 7; Table 2).

Parajes Formation

The Parajes formation is primarily exposed in the eastern part of the study area; continuous stratigraphic sequences are found in the vicinity

Geosphere, published online on 13 September 2013 as doi:10.1130/GES00862.1

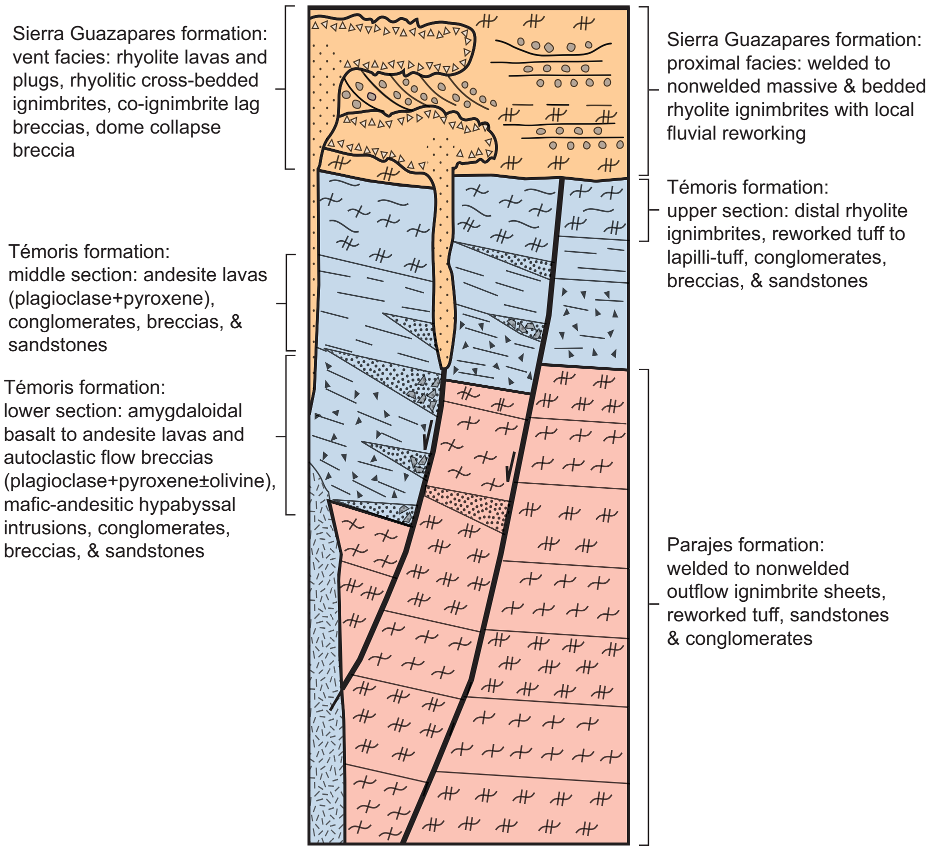

Figure 5. Generalized stratigraphic column of the Guazapares Mining District region, depicting the characteristics and depositional relationships between the Parajes formation, Témoris formation, and the Sierra Guazapares formation.

of Rancho de Santiago (Fig. 3A). The base of this formation is not exposed in the study area. The formation is composed of seven lithologically distinct silicic ignimbrites, with lesser locally interbedded sandstone, conglomerate, and reworked tuff (Figs. 6 and 8; Table 1). Individual ignimbrites are informally named in this study, and are distinguished based on phenocryst assemblages and outcrop characteristics such as degree of welding, weathering style, color, and percentage and type of pumice and/or fiamme and lithic fragments (Fig. 6; Table 1).

Description

Each ignimbrite of the Parajes formation has a densely welded to partially welded lower part that passes upward into a less welded to nonwelded top (Fig. 8A), forming a single cooling unit, as well as a single flow unit with normal coarse-tail grading of lithic fragments and inverse coarse-tail grading of pumice. Where the bases of ignimbrites are exposed, 0.5–2-m-thick basal vitrophyres are present. The ignimbrites are generally crystal poor to crystal moderate (<20%), with a dacitic phenocryst assemblage (no chemical analyses were done) consisting primarily of plagioclase and pyroxene phenocrysts, with minor amounts of hornblende, biotite, and quartz in some ignimbrites; sanidine is lacking in all of the ignimbrites of the Parajes formation (Fig. 6). The thickness of individual ignimbrites range from ~20 to ~210 m; the total thickness of the Parajes formation is ~1 km (Table 1). Some ignimbrites appear to thicken due to ponding in paleotopographic lows (e.g., Rancho de Santiago [Tpr] and KM [Tpk] ignimbrites); ponded thicknesses are 2.5 times greater than nonponded parts of the same ignimbrite (Figs. 3A and 4; Table 1).

Each ignimbrite of the Parajes formation has distinguishing outcrop and/or compositional characteristics, described in ascending stratigraphic order (Fig. 6; Table 1). The Chepe, Ericicuchi, and Portero ignimbrites form the oldest continuous stratigraphic sequence, which is only found on the southwest (footwall) side of the Chapotillo fault in the Guazapares Mining District region (Fig. 3A). The Chepe ignimbrite (Tpc) is the only crystal-rich (~30%) ignimbrite in the study area, with embayed quartz and biotite phenocrysts to 2 mm in diameter. The Ericicuchi ignimbrite (Tpe) has dark gray fiamme to 1 cm in length, typically with orange rims, and it has a mafic phenocryst assemblage that includes pyroxene, hornblende, and biotite. The Portero ignimbrite (Tpp) is characterized by a pink groundmass with eutaxitic texture in the densely welded lower portion, dark reddish-gray fiamme to 30 cm in length, and trace quartz phenocrysts.

The Puerto Blanco, Rancho de Santiago, KM, and Traza ignimbrites form a second, younger continuous stratigraphic sequence that is only found on the northeast (hanging wall) side of the Chapotillo fault (Fig. 3A); the depositional relationship between the two stratigraphic sequences on either side of the fault is not known, but is considered younger than the previously described sequence on the footwall based on the sense of fault offset (Fig. 4) and inferred regional correlations (described in the Discussion following). The base of the Puerto Blanco ignimbrite (Tpb) is not exposed; however, the exposed portion of its lower part, as well as its upper part, are nonwelded, with a welded middle. The Puerto Blanco ignimbrite (Tpb) has the greatest amount and size of lithic fragments (10%–40%, to 5 cm) compared to the other ignimbrites of the Parajes formation, with normal coarse-tail grading and upsection decrease in lithic fragments (from ~40% to 10%); it also shows an upsection increase in phenocrysts (from <5% to 20%) and an upsection increase in fiamme, which are distinctively yellow. The Rancho de Santiago ignimbrite (Tpr) is similar in appearance and composition to the Portero ignimbrite (Tpp) described above, but has gray fiamme with dark gray rims (Fig. 8B); these are generally 3 cm (to 1 m) in length. It has a 2-m-thick basal vitrophyre at the contact with the underlying Puerto Blanco ignimbrite. The KM ignimbrite (Tpk) is similar to the underlying Rancho de Santiago ignimbrite (Tpr), but is distinguished by the presence of a brownish-red, ~10-m-thick, crystal-poor (<5%) lower welded section and an overall lower lithic fragment content (5%–10%). The youngest unit of the Parajes formation is the Traza ignimbrite (Tpt), which is similar in appearance to both the Chepe and Puerto Blanco ignimbrites, but is distinguished by having gray fiamme and a moderate crystal content (20%) with trace quartz and no biotite.

Sedimentary rocks occur locally between ignimbrite units. An ~150-m-thick sequence of reworked tuff and cross-bedded sandstone with fragments of tuff and pumice (Tps) is between the Rancho de Santiago ignimbrite (Tpr) and KM ignimbrite (Tpk) southwest of the Arroyo Hondo–Puerto Blanco fault (Figs. 3A and 4).

TABLE 1. LITHOLOGIC DESCRIPTIONS OF THE MAP UNITS OF THE GUAZAPARES MINING DISTRICT

Map unit*	Lithology	Description
Qa	Alluvium	Unconsolidated very poorly sorted debris flow deposits. Gray to light gray; boulders to 5 m. Derived primarily from the Sierra Guazapares formation.
Tsiw	High-silica rhyolite intrusion	Hypabyssal intrusions (dikes and plugs). White to light pink; aphyric to 10% phenocrysts (to 1 mm): plagioclase, biotite, trace quartz. Subvertical flow banding. In Monte Cristo region (text Fig. 3B), intruded into gray andesitic feldspar porphyry (likely part of Témoris formation). Similar in appearance to rhyolitic dome collapse breccia (Tsv).
Tsv	Silicic volcaniclastic and fluvial-lacustrine deposits†	Volcaniclastic lithofacies (too small to show at map scale of text Fig. 3; Supplemental Fig. 1 [see text footnote 1]). Rhyolitic dome-collapse breccia: clast-supported rhyolitic block to lapilli breccia; white to light orange; primarily monomictic; angular lapilli to blocks (>2 m) with some flow banding. Aphyric to trace quartz and plagioclase phenocrysts. Contains zones of as much as to 20% andesitic blocks that are as large as 1.5 m. Block breccia transitions laterally into lapilli breccia, with the block fragment size decreasing northeastward away from the Sangre de Cristo fault (text Fig. 3B) from >2 m blocks to lapilli-sized fragments supported in an ash matrix of same composition. Massive to bedded silicic lapilli-tuff: nonwelded lapilli-tuff, light red to gray; <5% phenocrysts; plagioclase, biotite; trace to 20% lithic fragments (intermediate volcanic). Slight fluvial reworking (planar lamination, sorting, cut-and-fill structures), bedding to 5 m thick. Local white reworked ash layers and red very fine grained thinly bedded sandstone. Lacustrine deposits: fine- to medium-grained sandstone with graded bedding (Bouma Sequences A, B) and small-scale basal scouring; mudstone with planar lamination to very thinly bedded; water-lain ash layers. Tan to white. Soft sediment slumping and folding. Fluvial sandstone: medium- to coarse-grained sandstone; white to light gray; moderate to poor sorting; subangular silicic volcanic lithic fragments; massive with faint laminations, cut-and-fill and trough cross-bedding structures. Minor clast-supported breccia with subangular cobble to boulder silicic lapilli-tuff fragments interpreted as hyperconcentrated debris flows of reworked silicic volcanic material.
Tsi	Rhyolite intrusion	Hypabyssal intrusions (plugs and dikes). Light red to pink, typically with light pink subvertical flow banding; aphanitic groundmass with 5%–20% phenocrysts: plagioclase (to 3 mm), biotite (1 mm), trace quartz. Likely source for rhyolite lavas (Tsl).
Tsib	Silicic brecciated intrusion	Hypabyssal intrusion. White to light gray; silicic blocks (to 20 cm) supported in crystal-rich aphanitic groundmass with 40% phenocrysts: plagioclase, hornblende, quartz; locally massive and nonbrecciated.
Tsl	Rhyolite lava	Lava flows. Light gray to reddish-gray, with light pink banding; 5%–20% phenocrysts: plagioclase (to 4 mm), biotite (to 2 mm), quartz. Lavas consist of a 3–15-m-thick autoclastic breccia base of flow-banded blocks, a coherent middle portion (at least 30 m thick) with well-developed to minor flow banding, and a flow-top autoclastic breccia with flow-banded blocks and sediment infilling the spaces between blocks. Spherulites and quartz-filled vugs are common, and thundereggs are typically found within the top portion of a lava. An ~4-m-thick, basal block and ash flow is locally observed. Rhyolite hypabyssal intrusions (Tsi) are likely the source for these lavas.
Tst	Massive to stratified rhyolite ignimbrite	Nonwelded to partially welded tuff to lapilli tuff. Light pink, tan, or white groundmass; 5%–25% phenocrysts (to 2 mm): plagioclase, biotite; trace to 25% (locally 40%–50%) yellow-white long-tube pumice fragments (to 15 mm); <5%–40% lithic fragments (red, orange, gray intermediate volcanic, trace white silicic volcanic; to 20 mm). Crudely to well stratified; thickly to very thickly bedded (<1 m to ~10 m thick); mild to intense fluvial reworking locally observed (clast rounding, sorting, cross-bedding, and cut-and-fill structures). Tstb: more fluvially reworked and more thinly bedded than Tsti. Tsti: primary silicic nonwelded ignimbrite with thicker massive bedding and less intense reworked sections.
Tsxi	Very large scale cross-bedded rhyolitic ignimbrite	Nonwelded lapilli-tuff to tuff-breccia. Light pink, tan, or white groundmass; 5%–10% phenocrysts (<1 mm): plagioclase, biotite, quartz; 5%–10% (locally to 50%) tan to white long-tube pumice fragments (to 20 mm); alternating lithic-rich (>50%) and lithic-poor (<30%) stratification with ~0.5–50 cm lithic fragments (gray and red intermediate volcanic and white silicic volcanic). Cross-bedding with ~5-m-thick sets (to ~20 m thick).
Tti	Rhyolite ignimbrite and reworked tuff	Nonwelded to partially welded lapilli-tuff and fluvially reworked tuff/lapilli-tuff. Light pink to white groundmass; 5%–10% phenocrysts: plagioclase, biotite (to 2 mm), trace quartz, trace K-feldspar; <5-50% white and tan long-tube pumice fragments (5–10 mm); 5%–30% lithic fragments (gray and red intermediate volcanic; <5 mm to 30 mm). Individual ignimbrites are generally 5–10 m thick with compaction foliation. Reworked tuffs and lapilli-tuffs are well to crudely stratified, very thin to medium bedded; contain well to very poorly sorted, subangular to subrounded intermediate and silicic volcanic clasts.
Tta	Andesite lava	Nonvesicular lava flows. Gray; 5%–10% phenocrysts (typically weathered out): plagioclase, clinopyroxene. Average lava flow thickness ~15 m; lavas generally have flow-top and bottom autoclastic breccias and resistant flow-banded coherent interior.
Ttat	Andesite lapilli-tuff	Lapilli-tuff. Gray groundmass; trace phenocrysts: plagioclase; 15%–30% intermediate volcanic and silicic tuff lithic fragments (to 4 mm).
Ttb	Basaltic trachyandesite lava	Amygdaloidal lava flows. Dark gray to brick red; 5%–20% phenocrysts: plagioclase (some flow-alignment of laths), olivine (altered to iddingsite), clinopyroxene; zeolite amygdules. Average lava flow thickness ~2 m, lavas have vesicular top and bottom, locally with coherent flow interior. Local multilobed flows with blocky autoclastic flow breccia (text Fig. 9D).
Ttba	Basalt to andesite lava	Predominantly amygdaloidal lava flows. Gray to dark gray with local red hematitic and green propylitic alteration; 5%–25% phenocrysts: plagioclase (some flow alignment of laths), clinopyroxene; zeolite amygdules. Average lava flow thickness ~5 m, lavas are typically brecciated and vesicular with secondary zeolite infilling vesicles and autoclastic flow breccia interstices fragments, with lesser flow-banded and nonvesicular lavas with flow-top and bottom autoclastic breccias.
Ttv	Andesitic volcanic center (lavas, dikes, hypabyssal intrusions)	Complexly intruded hematite-stained basalt to andesite lavas (Ttba, Tta), andesitic block and ash flows, aphyric basaltic andesite hypabyssal intrusions with quartz veinlets, and andesitic dikes or intrusions with subvertical flow banding and to 10% phenocrysts (plagioclase, clinopyroxene). Dark gray to reddish-gray.
Ttai	Andesitic intrusions	Hypabyssal intrusions (dikes and sills). Dark gray with local red hematitic and green propylitic alteration; aphanitic groundmass with 5%–10% phenocrysts: plagioclase, clinopyroxene.
Ttt	Silicic tuff	Nonwelded to partially welded tuff. White to light tan groundmass; trace to 10% phenocrysts (<1 mm): plagioclase, biotite, ± hornblende, ± quartz; trace to 25% lapilli-sized lithic fragments (red intermediate volcanic).

(*continued*)

TABLE 1. LITHOLOGIC DESCRIPTIONS OF THE MAP UNITS OF THE GUAZAPARES MINING DISTRICT (*continued*)

Map unit*	Lithology	Description
Ttss	Fluvial sandstone: intermediate and silicic volcanic fragments	Feldspathic litharenite. Tan to red; moderately to poorly sorted, subrounded to subangular, predominantly fine to medium grained, to very coarse grained. Clasts consist of feldspar and intermediate and silicic volcanic lithic fragments with trace biotite. Contains very thin layers of matrix-supported granule to pebble pumice and silicic tuff fragments. Thinly to thickly bedded, with horizontal bedding and trough cross-bedding. Local red siltstone and clast-supported granule to pebble conglomerates with silicic tuff and intermediate volcanic fragments.
Ttds	Debris flow deposits: intermediate and silicic volcanic fragments	Matrix-supported polymictic breccia and conglomerate. Tan to red; massive to medium to very thickly bedded, average bed thickness ~5 m; subangular to angular pebble to large cobble intermediate volcanic and lesser silicic tuff clasts, fine- to medium-grained sand matrix (locally silicic ash rich with quartz and biotite crystals). Channel cut and scour surfaces between individual beds; interbedded with sandstone (Ttss) lenses.
Ttsa	Fluvial sandstone: intermediate volcanic fragments	Feldspathic litharenite. Dark tan to reddish-purple; moderately to poorly sorted, subrounded to subangular, medium- to coarse-grained with trace granules. Clasts consist of feldspar and intermediate volcanic lithic fragments. Contains lenses of clast-supported pebble conglomerates and matrix-supported pebble to cobble breccia with intermediate volcanic fragments. Thinly to thickly bedded.
Ttda	Debris flow deposits: intermediate volcanic fragments	Matrix-supported breccia and conglomerate. Tan; massive to very thickly bedded, nongraded, average bed thickness ~10 m; angular to subrounded pebble to boulder (to 1.5 m) intermediate volcanic clasts, medium-grained sand matrix. Channel cut and scour surfaces between individual beds.
Ttdt	Talus and debris flow deposits	Debris flows: matrix-supported breccia; tan to gray; massive to very crudely stratified; angular pebble to boulder intermediate volcanic clasts (mostly small boulder, <0.5 m to 2 m), with welded silicic ignimbrite clasts found upsection (to 5 m), fine- to medium-grained sand matrix. Talus: clast-supported monolithic breccia; tan to gray; massive; angular cobble to boulder intermediate volcanic clasts (most >0.5 m, to 4 m), limited fine- to-medium-grained sand matrix. Localized slide blocks of bedded sandstone to 15 m thick (text Fig. 9B).
Ttdi	Debris flow deposits with welded silicic ignimbrite fragments	Matrix-supported polymictic breccia. Tan to red; massive; primarily subangular to angular cobble to boulder silicic welded ignimbrite clasts, lesser pebble intermediate volcanic clasts, fine- to medium-grained sand to silt matrix. Larger (1–2 m) ignimbrite boulders weather to form small hoodoos (text Fig. 9A).
Tpt	Traza ignimbrite	Welded to nonwelded lapilli-tuff. Dark tan (welded) to white (nonwelded) groundmass; 20% phenocrysts: plagioclase, pyroxene, trace quartz; gray fiamme; 30% lithic fragments (red intermediate volcanic, gray silicic volcanic and welded tuff; to 50 mm). Thickness >40 m. Basal 1-m-thick vitrophyre, transitions upsection from welded to nonwelded, top not exposed.
Tpk	KM ignimbrite	Densely welded to nonwelded lapilli-tuff. Brownish-red (welded) and white to light gray (nonwelded) groundmass; <5% phenocrysts: plagioclase, trace quartz; 30% gray fiamme (to 30 mm); 5%–10% lithic fragments (red and gray intermediate volcanic). Thickness ~40–100 m. Basal 0.5-m-thick black vitrophyre below an ~10-m-thick red densely welded lower portion that transitions upsection into a white partially welded to nonwelded top. Weathered-out pumice lenses (to 10 cm) near top.
Tpr	Rancho de Santiago ignimbrite	Welded to nonwelded lapilli-tuff. Welded portion: red to pinkish-gray groundmass; weak eutaxitic texture; 5%–20% phenocrysts: plagioclase (to 3 mm), pyroxene, ± hornblende, ± quartz; 10%–20% gray fiamme with dark gray rims (altered to pink with orange rims near faults), typically to 30 mm, maximum 1 m length; trace to 5% lithic fragments (red intermediate volcanic and gray silicic volcanic). Nonwelded portion: white to tan groundmass; <5% phenocrysts: plagioclase, clinopyroxene, hornblende; noncompacted pumice fragments (to 35 mm); 10%–25% lithic fragments (red and brown intermediate volcanic and gray silicic volcanic). Thickness ~80 to 200 m. Basal 2-m-thick vitrophyre unit with 2 black vitrophyres separated by ~0.5-m-thick welded tuff. Transitions upsection from welded to nonwelded top. Weathered-out pumice lenses (to 25 mm) in upper middle portion of unit. Fewer phenocrysts upsection. Larger size of lithic fragments and fiamme found in easternmost exposures.
Tpb	Puerto Blanco ignimbrite	Welded to nonwelded lapilli-tuff. Nonwelded lower portion: tan to white groundmass; <5% phenocrysts: plagioclase, with trace biotite, hornblende, pyroxene, quartz; 15% white pumice fragments (to 30 mm); 30%–40% lithic fragments (red and gray intermediate volcanic, to 50 mm). Welded portion: tan groundmass; 10%–15% phenocrysts: plagioclase, biotite, with trace hornblende, quartz; 5% yellow fiamme (to 10 cm), mostly occur as weathered-out lenses in outcrop; 15%–20% lithic fragments (red and gray intermediate volcanic, to 30 mm). Nonwelded top: white to light pink groundmass; 15%–20% phenocrysts: plagioclase, biotite; 10%–15% yellowish-white long-tube pumice fragments; 10% lithic fragments (red and gray intermediate volcanic; to 15 mm). More than 190 m thick, base not exposed.
Tpp	Portero ignimbrite	Densely welded to welded lapilli-tuff. Pink groundmass; eutaxitic texture; trace to 25% phenocrysts: plagioclase, pyroxene, ± hornblende, trace quartz; 20% dark reddish-gray fiamme (to 30 cm); trace to 10% lithic fragments (red and gray volcanic; to 15 mm). Thickness ~20 to 180 m. Basal 1-m-thick vitrophyre, top eroded. Increased amount of phenocrysts, lithic fragments, and vapor-phase alteration upsection.
Tpe	Ericicuchi ignimbrite	Welded to nonwelded lapilli-tuff. Reddish-gray (welded) to light gray or white (nonwelded) groundmass; compaction foliation; 5%–15% phenocrysts: plagioclase, pyroxene, ± biotite, ± hornblende, trace quartz; 5%–10% dark gray fiamme with orange rims (to 10 mm), noncompacted white to brown pumice in nonwelded portion; trace to 10% (locally to 30%) lithic fragments (red, purple, and orange intermediate and gray silicic volcanic; to 2 mm, locally to 30 mm). Thickness ~210 m. Base located in inaccessible cliff exposures, transitions upsection from welded interior to nonwelded top.
Tpc	Chepe ignimbrite	Densely welded lapilli-tuff. Light red groundmass; eutaxitic texture; 30% phenocrysts: quartz (embayed), plagioclase, biotite (to 2 mm), hornblende; 15% pink-orange fiamme. More than 140 m thick, base not exposed. Likely correlative to the Divisadero tuff of Swanson et al. (2006) (see text).
Tps	Fluvial reworked tuff, sandstone, and conglomerate	Reworked tuff: white; white pumice fragments; 5%–10% crystal fragments: plagioclase, biotite, hornblende; <5% lithic fragments (~1 cm), thinly to thickly bedded. Sandstone: orange to tan; moderately well to poorly sorted, fine- to medium-grained, white pumice and tuff fragments; cross-bedding and graded bedding; local well-sorted pumice-rich granule lenses. Conglomerate: reddish-orange; matrix-supported; massive; monomictic; subrounded pebble to cobble silicic ignimbrite (welded to nonwelded) clasts, fine- to medium-grained sand matrix.

*Text Figure 3; Supplemental Figure 1 (see text footnote 1).
†Further descriptions of the silicic volcaniclastic and fluvial-lacustrine deposits (Tsv) are given in the Supplemental Data File (see text footnote 3).

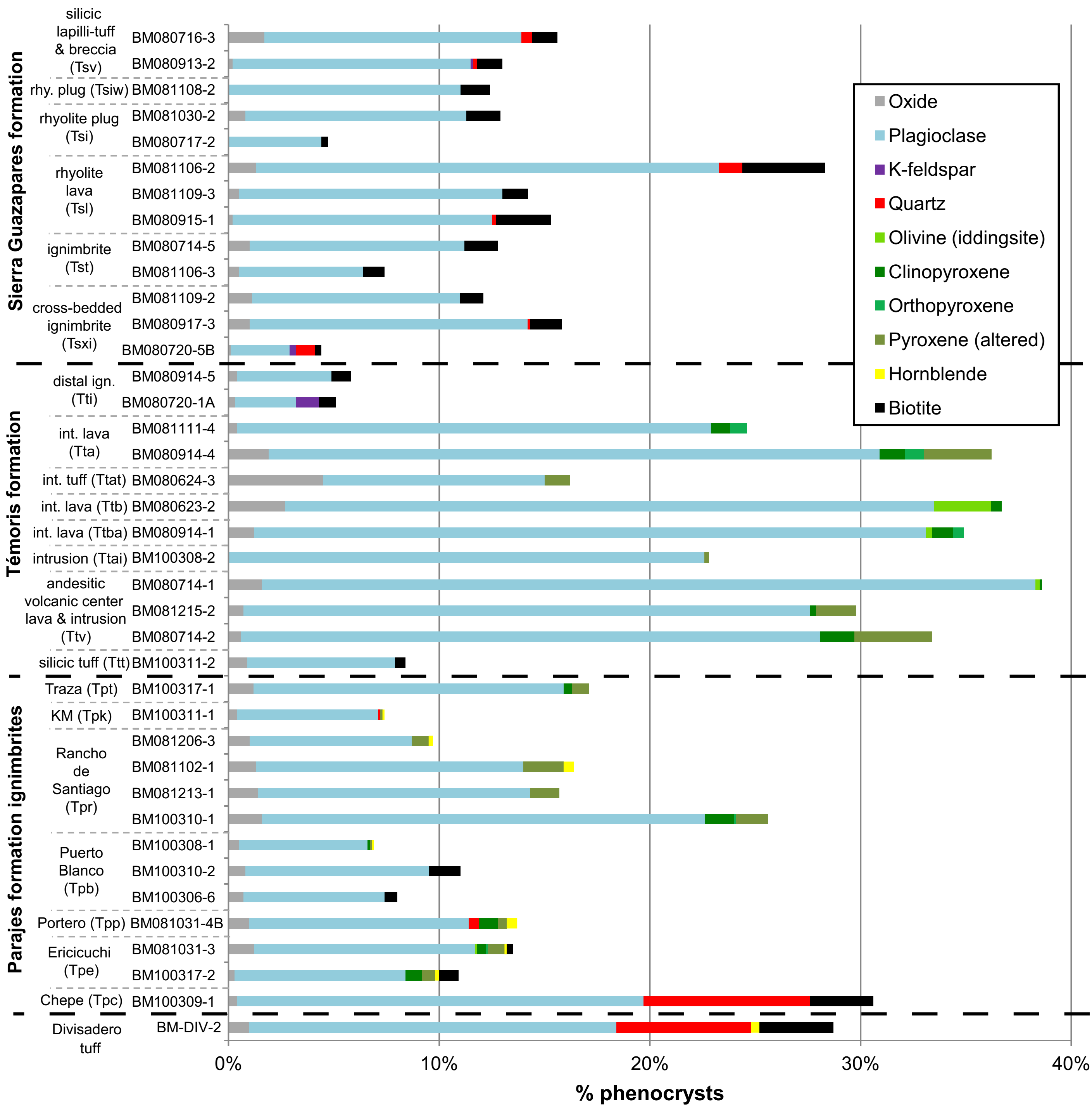

Figure 6. Modal point-count analyses of representative volcanic and intrusive rocks from the three formations of the Guazapares Mining District region showing the percentage of phenocrysts in each sample. Map unit symbols correspond to Figure 3 and Table 1. DIV-2 is a sample of the upper Divisadero tuff (e.g., Swanson et al., 2006) collected from Divisadero, ~50 km ENE of the Guazapares Mining District region, and analyzed during this study for compositional comparison with welded ignimbrites of the Parajes formation. One thin section was analyzed per sample, with 1000 point counts per thin section. Global positioning system coordinates of the samples and details of individual modal point-count analyses, including the proportions of lithic, pumice, and volcanic glass fragments in each sample, are shown in Supplemental Table 1 (see footnote 2).

Geosphere, published online on 13 September 2013 as doi:10.1130/GES00862.1

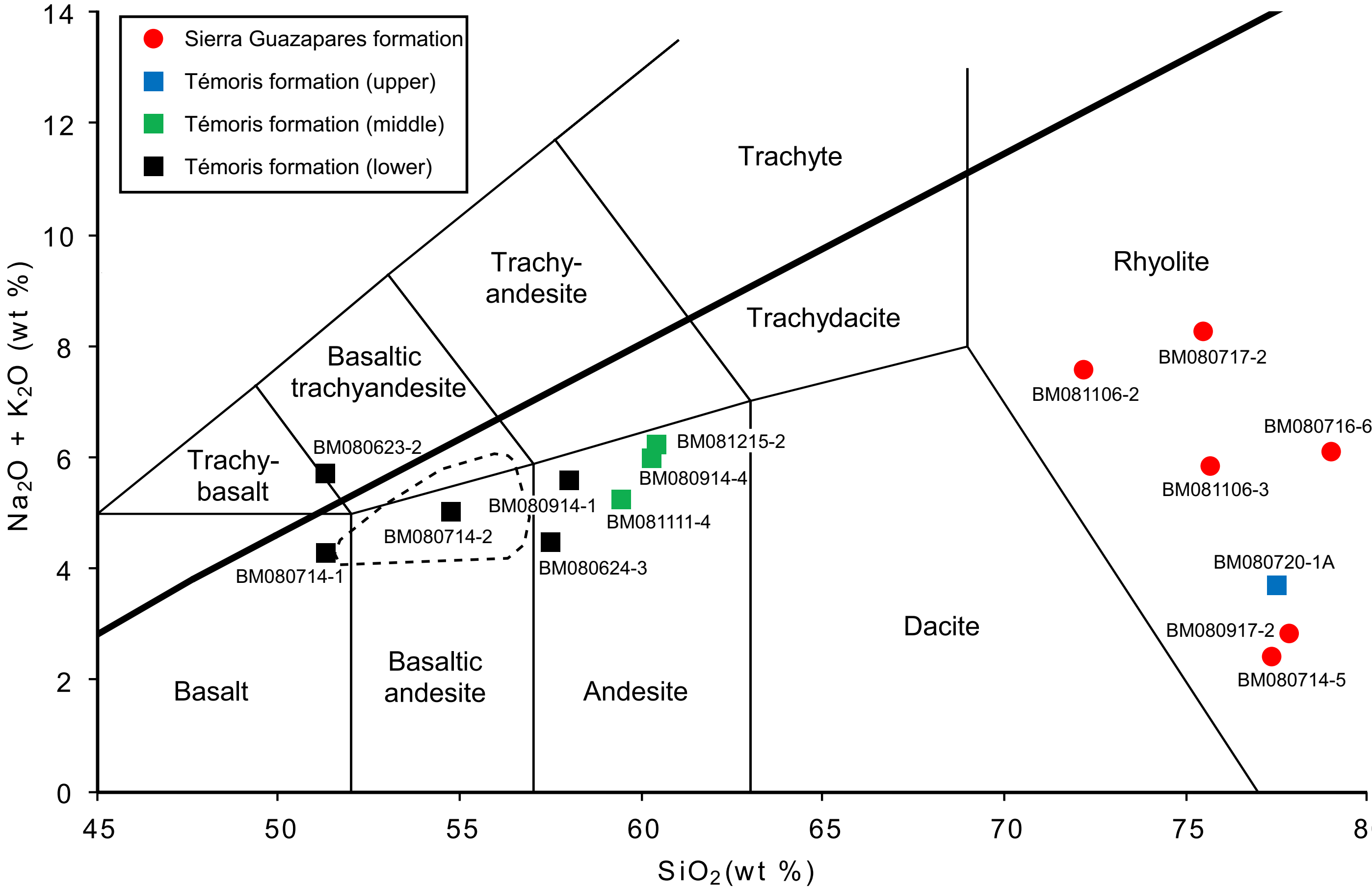

Figure 7. Total alkali-silica classification diagram (after Le Bas et al., 1986) for selected volcanic rocks of the Guazapares Mining District region. The boundary between the alkaline and subalkaline fields (thicker line) is after Irvine and Baragar (1971). Samples were analyzed from the Témoris formation and the Sierra Guazapares formation. Details of each analysis and global positioning system coordinates of samples are given in Table 2 and sample locations are plotted in Supplemental Figure 1 (see footnote 1). The field of the Southern Cordillera basaltic andesites, based on Figure 5 of McDowell et al. (1997), is included here for comparison (dashed line).

Also present at this stratigraphic interval in the Mesa de Cristal area east of Rancho de Santiago (Supplemental Fig. 1 [see footnote 1]) is a monomictic matrix-supported pebble to cobble conglomerate with welded ignimbrite clasts similar in appearance to ignimbrites of the Parajes formation (Fig. 8C). In addition, a thin (<1 m) layer of fine- to medium-grained sandstone is present along the contact between the Ericicuchi ignimbrite (Tpe) and Portero ignimbrites (Tpp) (Fig. 8D).

Interpretation

The Parajes formation represents medial facies of silicic outflow ignimbrite sheets, based on the sheet-like geometry of the flow units, the moderate thicknesses of flow units (each <~200 m thick, locally thicker where ponded by paleotopography), the presence of welding textures and vitrophyres, and the lack of associated lithic lag breccias. No caldera or vent-proximal lithofacies have been identified for these outflow ignimbrites, so the locations of their sources are not known. However, lithic fragments and fiamme within in the Rancho de Santiago ignimbrite (Tpr) increase in size eastward, suggesting that the source for this ignimbrite is located toward this direction. Based on flow thicknesses and degree of welding relative to distance from the source recorded in large-volume silicic ignimbrites in the western U.S. (e.g., Smith, 1960; Lipman, 2007), the ignimbrites of the Parajes formation were likely erupted from calderas located within 50–100 km. The large size and concentration of lithic fragments within the Puerto Blanco ignimbrite (Tpb) are suggestive of a somewhat closer source.

Sedimentary rocks (Tps) interbedded with the ignimbrites of the Parajes formation record both erosion of welded units and reworking of unconsolidated pyroclastic debris, with deposition by fluvial and debris flow processes (Figs. 8C, 8D). The debris flow deposits are massive, poorly sorted matrix-supported conglomerates, while fluvial sandstones and fluvially reworked tuffs have trough cross-bedding, normal grading, and well-sorted granule conglomerate lenses. The clasts in these sedimentary rocks are predominantly silicic volcanic fragments, including welded and nonwelded tuff and pumice (e.g., Fig. 8C); there are no andesitic volcanic fragments in these rocks. This suggests that the Parajes formation ignimbrites were uplifted and partly eroded prior to deposition of overlying andesitic rocks of the Témoris formation.

Témoris Formation

The Témoris formation overlies the Parajes formation in angular unconformity, and is best exposed in the central and western portions of the study area in the vicinity of Puerto La Cruz and Guazapares (Fig. 3). This formation

Geosphere, published online on 13 September 2013 as doi:10.1130/GES00862.1

TABLE 2. WHOLE-ROCK GEOCHEMICAL ANALYSES FROM VOLCANIC ROCKS AND INTRUSIONS

Sample	Map unit	Formation	SiO_2	TiO_2	Al_2O_3	FeO	MnO	MgO	CaO	Na_2O	K_2O	P_2O_5	Rock name	UTM (E)	UTM (N)
BM080716–6	Tsiw	Sierra Guazapares	79.00	0.15	13.32	0.82	0.03	0.45	0.11	2.37	3.73	0.02	high-silica rhyolite	767384	3035292
BM080717–2	Tsi	Sierra Guazapares	75.47	0.18	14.27	0.75	0.05	0.33	0.65	4.18	4.08	0.03	rhyolite	770929	3030949
BM081106–2	Tsl	Sierra Guazapares	72.18	0.39	15.35	2.00	0.07	0.63	1.69	3.64	3.93	0.12	rhyolite	769571	3028001
BM080917–2	Tsl	Sierra Guazapares	77.84	0.21	13.20	0.96	0.06	1.22	3.64	0.42	2.41	0.02	rhyolite (altered)*	772612	3023830
BM081106–3	Tst	Sierra Guazapares	75.67	0.25	13.58	1.34	0.03	0.61	2.63	1.29	4.56	0.04	rhyolite	769700	3028097
BM080714–5	Tst	Sierra Guazapares	77.36	0.25	13.51	1.14	0.06	1.06	4.19	0.67	1.75	0.00	rhyolite (altered)*	773778	3023239
BM080720–1A	Tti	Témoris (upper)	77.50	0.24	13.28	1.25	0.09	1.16	2.77	0.54	3.16	0.01	rhyolite (altered)*	768484	3027285
BM081111–4	Tta	Témoris (middle)	59.44	0.98	18.82	5.96	0.12	2.27	6.84	3.69	1.55	0.33	andesite	775962	3025047
BM080914–4	Tta	Témoris (middle)	60.28	0.98	17.82	6.68	0.09	2.14	5.71	3.84	2.15	0.31	andesite	773279	3023255
BM081215–2	Ttv	Témoris (middle)	60.42	1.29	16.68	6.92	0.20	2.27	5.44	4.33	1.89	0.56	andesite	772106	3020880
BM080624–3	Ttat	Témoris (lower)	57.49	1.02	16.93	7.55	0.15	4.92	7.19	3.26	1.22	0.27	andesite	770411	3028744
BM080623–2	Ttb	Témoris (lower)	51.29	1.88	17.85	10.40	0.15	4.68	6.98	3.50	2.21	1.08	basaltic trachyandesite	769959	3035621
BM080914–1	Ttba	Témoris (lower)	58.00	1.00	19.27	6.40	0.15	2.31	6.95	3.79	1.80	0.33	andesite	773051	3023001
BM080714–1	Ttv	Témoris (lower)	51.30	1.38	20.09	9.40	0.20	3.65	9.30	3.36	0.93	0.38	basalt	771758	3021619
BM080714–2	Ttv	Témoris (lower)	54.76	1.13	19.50	7.85	0.12	3.56	7.72	3.65	1.37	0.33	basaltic andesite	771841	3021629

Note: Calculated on anhydrous basis, normalized to 100%. Universal Transverse Mercator (UTM; E—east, N—north) coordinates are based on the North American Datum 1927 (NAD27) zone 12. Map unit labels correspond to Table 1. Locations of the samples are shown on Supplemental Figure 1 (see text footnote 1).

*Na_2O and K_2O leaching, likely due to hydrothermal alteration of albite and orthoclase.

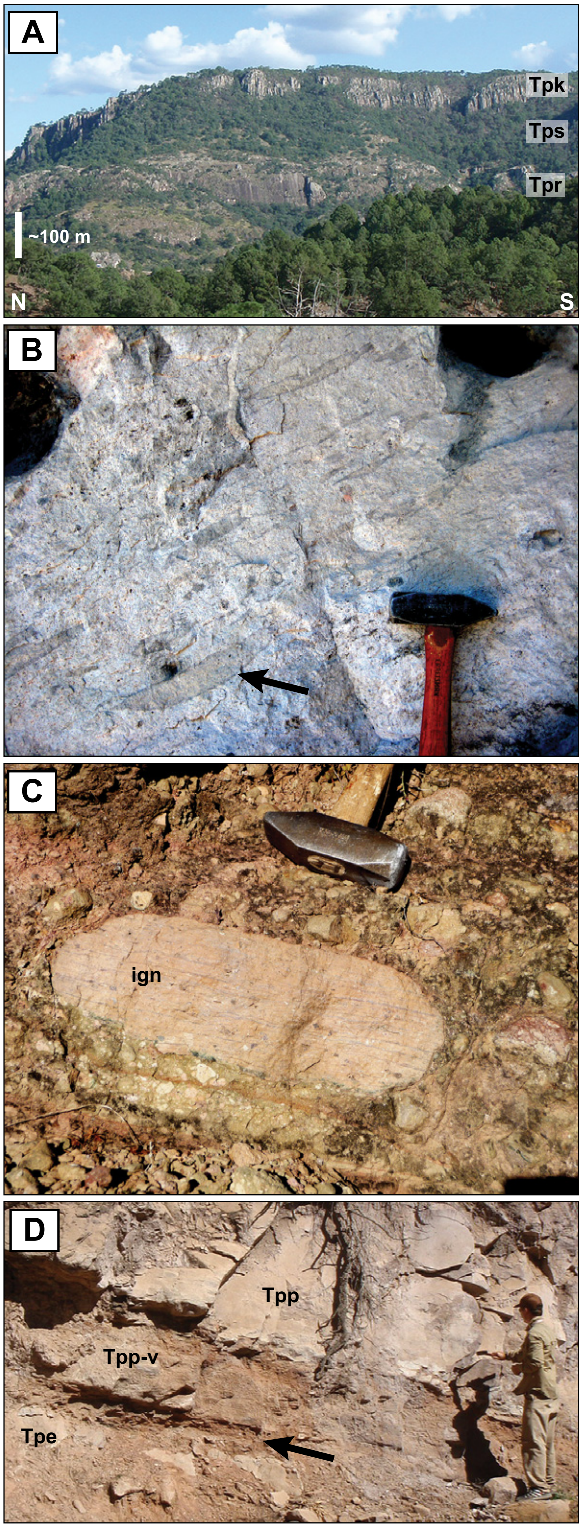

Figure 8. Representative photographs of the Parajes formation; locations of photos are given in Universal Transverse Mercator, North American Datum 1927 coordinates (NAD27 UTM zone 12). Unit abbreviations as in Table 1. (A) View east toward Cordón Bairomico from Chapotillo (777340E 3027305N; Fig. 3A), with the cliff-forming welded portions of the KM ignimbrite (Tpk) and Rancho de Santiago ignimbrite (Tpr) separated by an ~150-m-thick sequence of reworked tuff and sandstone (Tps). (B) Welded ignimbrite near the base of the Rancho de Santiago ignimbrite (Tpr), with large dark-rimmed gray fiamme (e.g., arrow) at 780913E 3028802N. Head of hammer is ~12.5 cm. (C) Subrounded welded ignimbrite clast with eutaxitic texture (ign) below hammer (head is ~12.5 cm), likely derived from the Parajes formation, in a monomictic matrix-supported pebble to cobble conglomerate (Tps) deposited above the Rancho de Santiago ignimbrite (Tpr) near Mesa de Cristal (777551E 3033189N; Supplemental Fig. 1 [see footnote 1]). (D) Depositional contact between the nonwelded upper portion of the Ericicuchi ignimbrite (Tpe) and the densely welded lower portion the Portero ignimbrite (Tpp) with basal ~1-m-thick vitrophyre (Tpp-v) at 775567E 3024552N. A thin (<1 m) layer of fine- to medium-grained sandstone is observed along the contact between the two units (arrow).

Geosphere, published online on 13 September 2013 as doi:10.1130/GES00862.1

is primarily composed of mafic to intermediate composition lavas (flow-banded and/or vesicular) and hypabyssal intrusions, intercalated conglomerates, breccias, and sandstones dominated by mafic to intermediate volcanic lithic fragments, and lesser thin silicic nonwelded ignimbrites and reworked silicic tuff (Figs. 6, 7, and 9; Tables 1 and 2). This formation has undergone mild hematitic and propylitic alteration, with infilling of vesicles and autoclastic flow breccia interstices with zeolite minerals; the most intense alteration is in the rocks within the Guazapares fault zone (Fig. 3B).

Description

The basal deposits of the Témoris formation consist of sandstones with silicic tuff fragments (Ttss), matrix- to clast-supported breccias with welded silicic ignimbrite boulders (Ttdi, Ttdt; Figs. 9A, 9B), and lesser interbedded silicic tuffs (Ttt). The welded ignimbrite clasts were derived from the underlying Parajes formation, indicating continued erosion of this formation. One ignimbrite of the Parajes formation (Portero ignimbrite, Tpp), located east of Ericicuchi near 12R 775504E 3024974N (Universal Transverse Mercator coordinates, North American Datum 1927; Fig. 3A), contains clastic dikes directly below the Parajes–Témoris formation contact. These dikes are composed of overlying Témoris formation sandstone that infills fissures formed in the top of the Portero ignimbrite.

The Témoris formation is subdivided into three sections based on volcanic rock compositions and types (Figs. 6, 7, and 10; Tables 1 and 2; Supplemental Table 1[2]). These subdivisions have gradational contacts and consist of (1) a lower section of pyroxene-plagioclase ± olivine-bearing amygdaloidal basalt, basaltic andesite, and andesite lavas and autoclastic flow breccias (Ttba, Ttb; Figs. 9C, 9D); (2) a middle section of pyroxene-plagioclase–bearing flow-banded andesite lavas (Tta; Fig. 9E); and (3) an upper section of several thin (<5-m-thick) primary and reworked rhyolite ignimbrites (Tti; Figs. 9F, 9G); this upper section is only locally preserved beneath the angular unconformity with the overlying Sierra Guazapares formation. Conglomerates, breccias, and sandstones with well-sorted gravel lenses and trough cross-bedding are interbedded with and laterally interfinger with all of the volcanic rocks listed above (Figs. 9B, 9F–9K, and 10; Table 1). These volcaniclastic deposits contain detritus similar in composition to the interstratified lavas and ignimbrites: amygdaloidal and flow-banded basaltic andesite to andesite clasts dominate the lower and middle sections of the Témoris formation (Ttda, Ttsa, Ttdt), while the upper section of the Témoris formation has mixed mafic-intermediate and silicic volcanic clasts, including pumice fragments in tuffaceous sandstones and tuffaceous conglomerates (Ttss, Ttds, Tti). Lavas and autoclastic flow breccias locally infill channels incised into the underlying sedimentary rock (Fig. 9E), and wet sediment-magma interactions (peperitic) are locally observed where lavas were apparently emplaced over wet sand (Fig. 9L).

In the area around Témoris, the Témoris formation thickens from ~100–400 m to >700 m (Fig. 3; Supplemental Fig. 1 [see footnote 1]). There, basalt to andesite lavas of the lower and middle sections of the Témoris formation are heavily hematite stained and are complexly intruded by numerous andesitic dikes and aphyric hypabyssal rocks (Ttv; Table 1).

Interpretation

The rocks of the Témoris formation are interpreted as the products of vent to proximal mafic to intermediate composition magmatism and distal silicic ignimbrite volcanism. Deposition in a terrestrial environment, likely part of alluvial fan systems (e.g., Kelly and Olsen, 1993; Blair and McPherson, 1994; Hampton and Horton, 2007; Murray et al., 2010), is indicated by interstratified matrix-supported debris flow breccias and conglomerates (Ttda, Ttds, Ttdi), clast-supported avalanche and/or talus breccias (Ttdt), well-sorted stratified and cross-bedded fluvial sandstones and conglomerates (Ttas, Ttss), and some lavas infilling fluvial channels and forming peperites within them

Figure 9 (*on following two pages*). Representative photographs of the Témoris formation; locations of photos are given in Universal Transverse Mercator, North American Datum 1927 coordinates (NAD27 UTM zone 12). Unit abbreviations as in Table 1. (A) Matrix-supported polymictic breccia with cobble- to boulder-sized welded silicic ignimbrite clasts (ign) and lesser pebble-sized mafic to intermediate volcanic clasts (below ign boulder) from the basal section of the Témoris formation (Ttdi), weathering to form a small hoodoo in the Rancho de Santiago area (776990E 3031055N). The large (1–2 m) welded ignimbrite boulders (ign) were likely derived from the Parajes formation. (B) Clast-supported monolithic breccia of angular intermediate volcanic cobble- to boulder-sized clasts (Ttdt), which includes a 15-m-thick slide block of bedded sandstone (ss), in the Rancho de Santiago half-graben basin adjacent to the Rancho de Santiago fault (777781E 3028522N; Fig. 3A). (C) Autoclastic flow breccia on top of andesitic lava (Ttba) at 769403E 3032339N. (D) Blocky autoclastic flow breccia in basaltic trachyandesite lavas (Ttb) at 771976E 3032195N. (E) Andesite lava (Tta) with basal autoclastic flow breccia infilling a channel (arrow) incised into underlying reddish orange sandstone (Ttsa) and debris flow deposits (Ttda) in the middle section of the Témoris formation in the Puerto La Cruz area (773685E 3022996N). (F) Lithic-rich 2–3-m-thick ignimbrite deposit (Tti), with ~30% mafic-intermediate and silicic volcanic lithic fragments to 3 cm, deposited over medium-bedded sandstone (Ttss) at 768484E 3027278N. (G) Medium-bedded matrix-supported tuffaceous conglomerate (reworked tuff) from the upper section of the Témoris formation (Ttds), with subangular to subrounded mafic-intermediate and silicic volcanic clasts. Located in the Puerto La Cruz measured section (~25 m; Fig. 10D) at 773391E 3023300N. Head of hammer is ~12.5 cm. (H) Sandstone (Ttsa) filling in depression on top of amygdaloidal basalt lava (Ttba) at 771675E 3021604N. (I) Matrix-supported polymictic conglomerate with subangular to subrounded mafic-intermediate and silicic volcanic clasts (Ttds), interbedded fine- to medium-grained sandstone (Ttss), located in the half-graben basin adjacent to the Agujerado fault (776328E 3025345N; Fig. 3A). A white pumice-rich lens (wht) is located near base of the 33-cm-long hammer, and a thin (~1 cm) siltstone layer is located directly above the head of hammer (arrow). (J) Matrix-supported polymictic breccia from the upper section of the Témoris formation (775590E 3025137N), with subangular to subrounded mafic-intermediate volcanic and silicic ignimbrite clasts (Ttds). Breccia grades upsection into sandstone with a thin white pumice-rich lens located below the head of the 38-cm-long hammer (arrow). (K) Downdip view of sandstone from the upper section of the Témoris formation (Ttss), with trough cross-bedding (e.g., arrow) and lenses of white pumice and tuff fragments at 767952E 3027759N. Hammer in photo is 38 cm long. (L) Wet sediment–lava intermixing (peperitic) along the depositional contact between orange-tan sandstone (Ttss) and reddish-gray basaltic andesite (Ttba) at 776571E 3032292N. Hammer in photo is 38 cm long.

[2]Supplemental Table 1. Modal point-count analyses. If you are viewing the PDF of this paper or reading it offline, please visit http://dx.doi.org/10.1130/GES00862.S2 or the full-text article on www.gsapubs.org to view Supplemental Table 1.

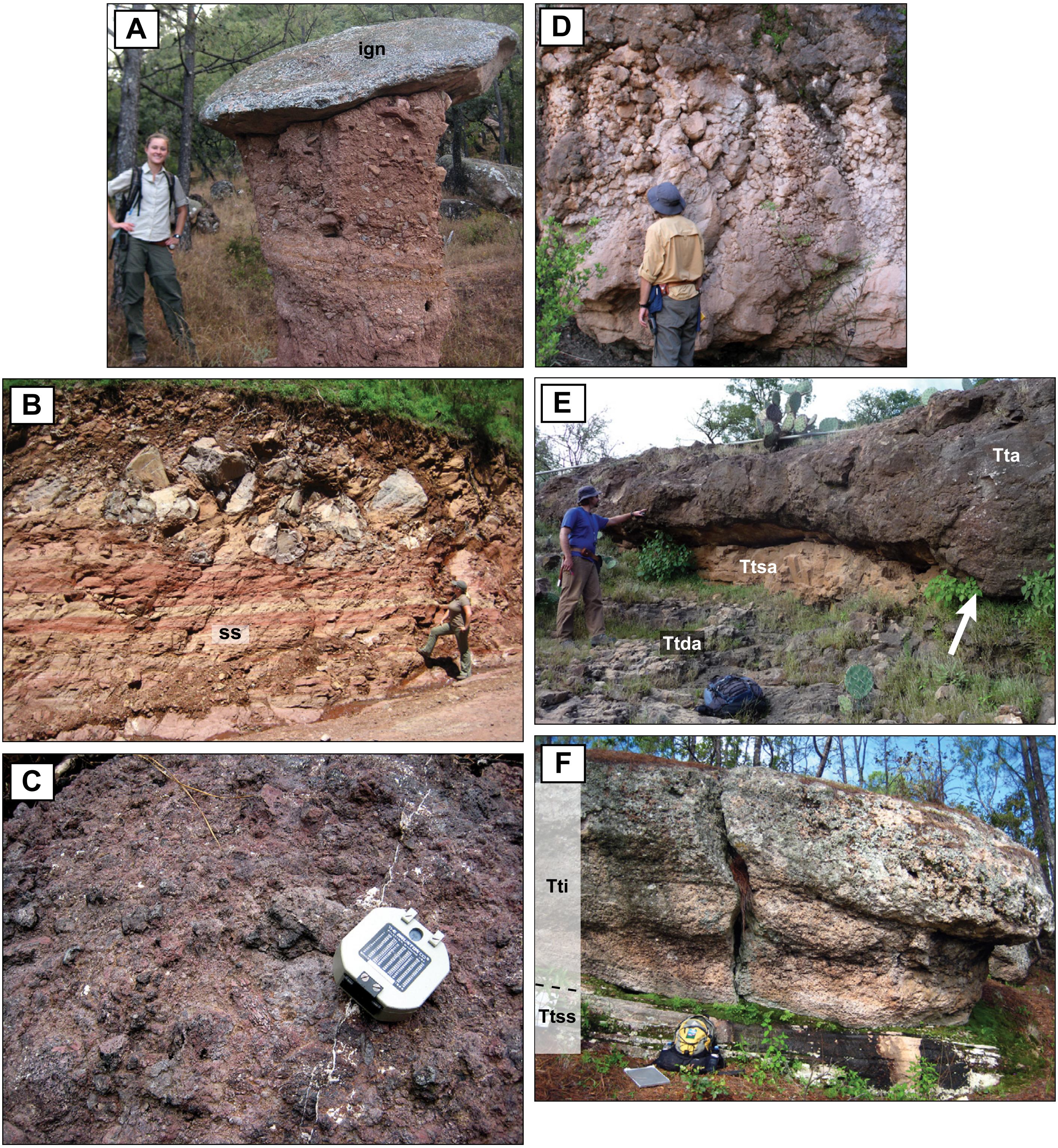

Figure 9.

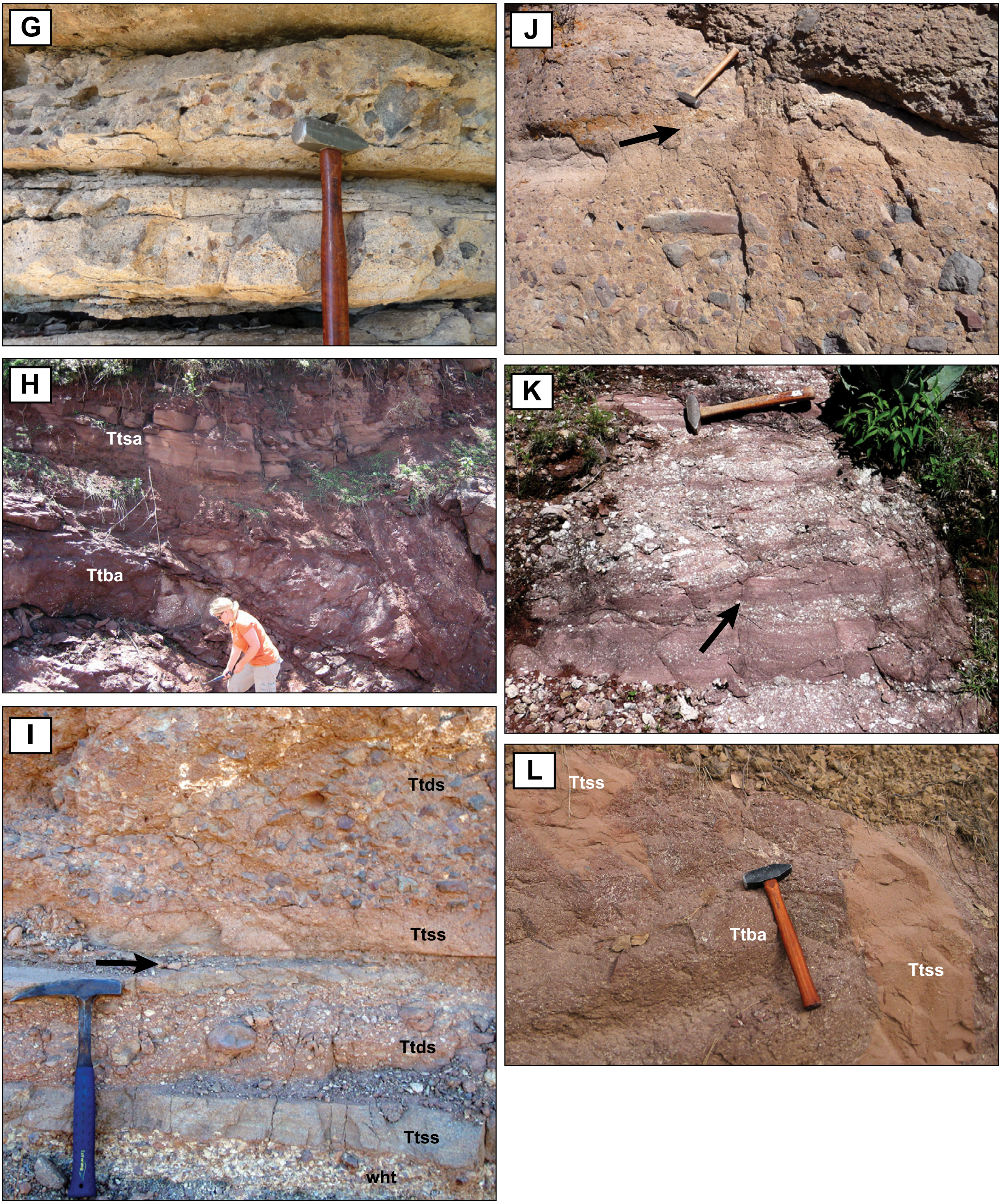

Figure 9 (***continued***).

Geosphere, published online on 13 September 2013 as doi:10.1130/GES00862.1

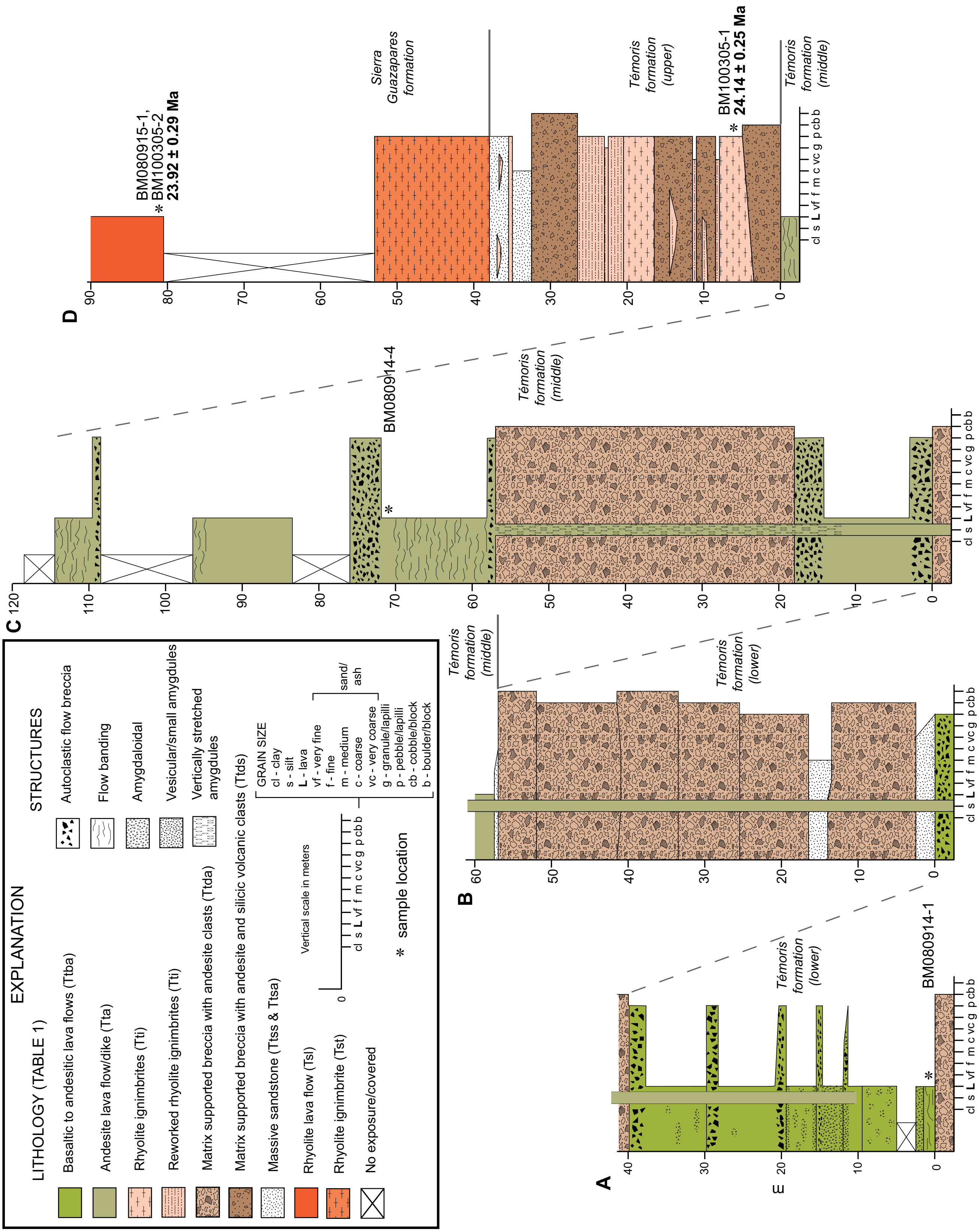

Figure 10. Four continuous measured stratigraphic sections (A–D) of the Témoris formation to Sierra Guazapares formation in the Puerto La Cruz area, east of Témoris (see Fig. 3A), with lithologies, depositional structures, and stratigraphic positions of analyzed samples (Figs. 6 and 13; Tables 2 and 3; Supplemental Table 2 [see footnote 4]). The three subdivisions of the Témoris formation and the boundary between the Témoris and Sierra Guazapares formations are indicated.

(Fig. 9). The composition of fragments in the fluvial and debris flow deposits is similar to that of the interstratified volcanic rocks, indicating intrabasinal reworking of eruptive products. The upper section of rhyolite ignimbrites in the Témoris formation likely erupted from distal sources, because they are thin and nonwelded, with a high proportion of interstratified fluvially reworked tuff (Tti; Figs. 9F, 9G; Table 1).

We interpret the Témoris area to be the site of an andesitic volcanic center in the Témoris formation, based on dramatic thickening of the lava section, abundant plugs and dikes, and increased alteration (Fig. 3; Supplemental Fig. 1 [see footnote 1]). This andesitic volcanic center, roughly defined by map unit Ttv, greatly thickens toward its subvolcanic intrusion–dominated core located along the ridge east of Témoris, with a minimum volume of 9 km^3 based on the mapped area and exposed thickness (Fig. 3; Supplemental Fig. 1 [see footnote 1]). A feeder dike emanating from the volcanic center can be traced upward into an andesitic lava flow in the Puerto La Cruz area (Fig. 10). In addition, andesitic dikes crosscut rocks of the Témoris formation away from the volcanic center, locally along faults.

Sierra Guazapares Formation

The Sierra Guazapares formation comprises much of the central and northwestern part of the study area, with best exposures located along the NS–trending ridge east of Guazapares (Fig. 3; Supplemental Fig. 1 [see footnote 1]). This formation is composed of plagioclase-biotite ± quartz ± sanidine–bearing rhyolitic ignimbrites, rhyolite lavas, flow-banded rhyolite hypabyssal intrusions, and lesser silicic volcaniclastic deposits (Figs. 3, 6, 7, and 11; Table 1). The Sierra Guazapares formation is flat-lying to gently dipping (<10°) and overlies the Témoris formation in low to moderate angular unconformity (Fig. 12A). The Sierra Guazapares formation is >200 m thick; it is not known how much of the formation is preserved, because the top is eroded. The formation locally infills lows cut into older stratigraphic units, recording paleotopography produced by erosion or faulting.

Description

The dominant lithofacies of the Sierra Guazapares formation is massive to stratified nonwelded to partially welded rhyolite ignimbrites (Tst; Fig. 11A; Table 1). Locally, these ignimbrites show evidence of reworking, including sorting and rounding of lithic, pumice, and crystal fragments, stratification and cut-and-fill structures, and small- to medium-scale cross-lamination (Fig. 11B).

Very large scale cross-bedded rhyolitic ignimbrites (Tsxi) form a distinctive lithofacies of the Sierra Guazapares formation (Fig. 11C, 11D; Table 1). These deposits are mainly restricted to a linear belt ~11 km long and 3 km wide within and immediately adjacent to the Guazapares fault zone–La Palmera fault (Fig. 3B), and laterally grade away from this linear belt into massive to stratified ignimbrites (Tst; Figs. 3 and 5; Supplemental Fig. 1 [see footnote 1]). The very large scale cross-bedded ignimbrites have average set heights of ~5 m; some are as great as ~20 m (Figs. 11C, 11D). The cross-bedding in these ignimbrites is defined by alternating lithic-rich (>50%) and lithic-poor (<30%) layers (Fig. 11D). The lithic fragments are very coarse grained, with blocks to 50 cm in diameter; these are dominantly mafic to intermediate volcanic rocks likely derived from the underlying Témoris formation (Fig. 11E). The matrix of the very large scale cross-bedded ignimbrites is an unsorted mixture of angular pumice, euhedral crystals, and glass shards, and the very large scale cross-beds lack internal laminations, sorting, or other fine-scale sedimentary structures indicative of reworking by water.

Rhyolite lavas (Tsl) and hypabyssal intrusions (Tsi, Tsiw, Tsib) occur in the same linear belt along the Guazapares fault zone–La Palmera fault as the very large scale cross-bedded ignimbrites, and also occur along additional NNW–striking faults in the region (Figs. 2 and 3; Supplemental Fig. 1 [see footnote 1]). The silicic hypabyssal intrusions (Fig. 11F) are typically plugs with related dikes that intrude the ignimbrites (Tst, Tsxi) of the Sierra Guazapares formation, and some of the plugs pass continuously upward into rhyolite lavas (Tsl) (Fig. 12B). The rhyolite lavas typically overlie the ignimbrites, but are locally interstratified (Fig. 11G).

In addition to silicic ignimbrites, lavas, and plugs, the Sierra Guazapares formation also includes a volcaniclastic unit (Tsv) in the Monte Cristo area (Fig. 3B). This unit includes a rhyolitic dome-collapse breccia associated with a rhyolite dome complex (Tsiw) that overlies and interfingers with normal graded sandstones, mudstones with soft-sediment deformation features, and moderately to poorly sorted sandstone with trough cross-bedding and cut-and-fill structures (Table 1; Supplemental Data File[3]).

Interpretation

We interpret the very large scale cross-bedded ignimbrites to be vent-proximal lag breccias deposited from energetic, turbulent pyroclastic density currents erupted during several events from a major fissure vent along the Guazapares fault zone–La Palmera fault (Figs. 2 and 3). Their linear map distribution indicates they

[3]Supplemental Data File. Mining claims of the Guazapares fault zone. If you are viewing the PDF of this paper or reading it offline, please visit http://dx.doi.org/10.1130/GES00862.S3 or the full-text article on www.gsapubs.org to view the Supplemental Data File.

Figure 11 (*on following page*). Representative photographs of the Sierra Guazapares formation; locations of photos are given in Universal Transverse Mercator, North American Datum 1927 coordinates (NAD27 UTM zone 12). Unit abbreviations as in Table 1. (A) Massive to stratified rhyolite ignimbrites (Tsti) forming prominent cliff north of Ericicuchi. Photo taken from 775509E 3024976N. (B) Tuffaceous sandstone (reworked tuff) with cross-bedding (arrow) in stratified rhyolite ignimbrite unit (Tst); very fine to medium grained, well to moderately sorted, subrounded. Head of hammer is 12.5 cm (771650E 3031928N). (C) View west from 769131E 3028438N at very large scale cross-bedded rhyolitic ignimbrite unit (Tsxi) forming an ~30-m-tall cliff face (arrow) at Cerro San Miguel on west side of Guazapares fault zone (Fig. 3B). (D) Very large scale cross-bedded rhyolitic ignimbrite (Tsxi), with person (outlined) standing on set boundary. The orientation of cross-stratification is emphasized by black dashed lines. Dark colored band to left of person (arrow) is a lithic-rich layer with ~50% lithic fragments (part E); lighter colored bands contain ~10%–20% lithic fragments (771904E 3026715N). (E) Close-up of lithic-rich layer in silicic surge-like ignimbrite (Tsxi) in part D, with reddish mafic-intermediate volcanic fragments (e.g., arrow), likely derived in part from the Témoris formation, having diameters ranging from 0.5 to 50 cm. White pumice and crystal fragments are present in an ash matrix (771904E 3026715N). (F) Subvertically flow-banded crystal-poor to aphyric rhyolitic hypabyssal intrusion (Tsi), Cerro Salitrera plug (770909E 3030955N; Fig. 3B). Red dashed lines emphasize orientation of flow banding. (G) Depositional contact between a rhyolite lava (Tsl; lower right) and overlying very large scale cross-bedded rhyolitic ignimbrite (Tsxi; upper left). Map board (~30 cm in length) is located along the contact. The top of the rhyolite lava consists of an autoclastic flow breccia that has a red sandy matrix surrounding the flow-banded blocks, interpreted as sand infilling in the top of the lava prior to eruption of the rhyolitic ignimbrite (772569E 3023871N).

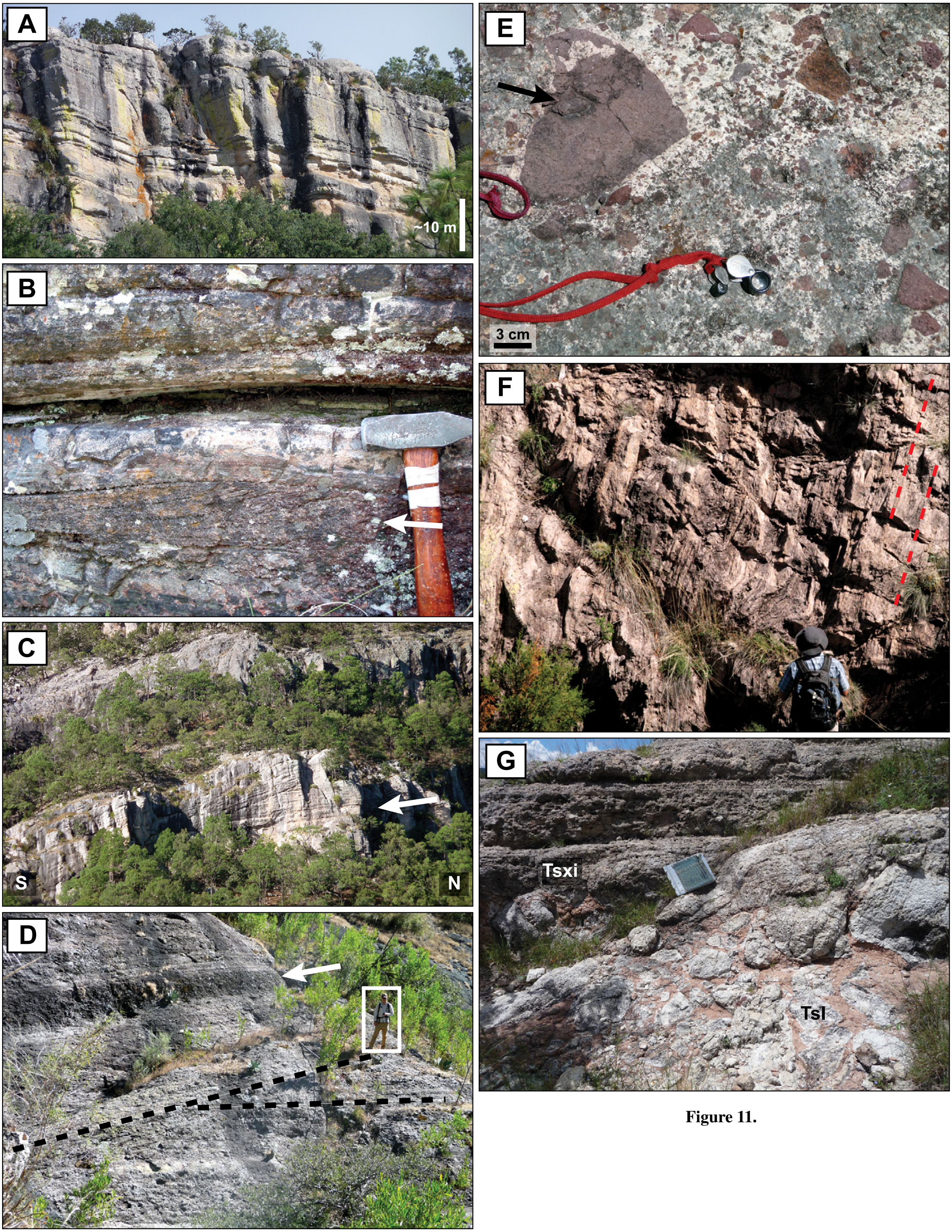

Figure 11.

Geosphere, published online on 13 September 2013 as doi:10.1130/GES00862.1

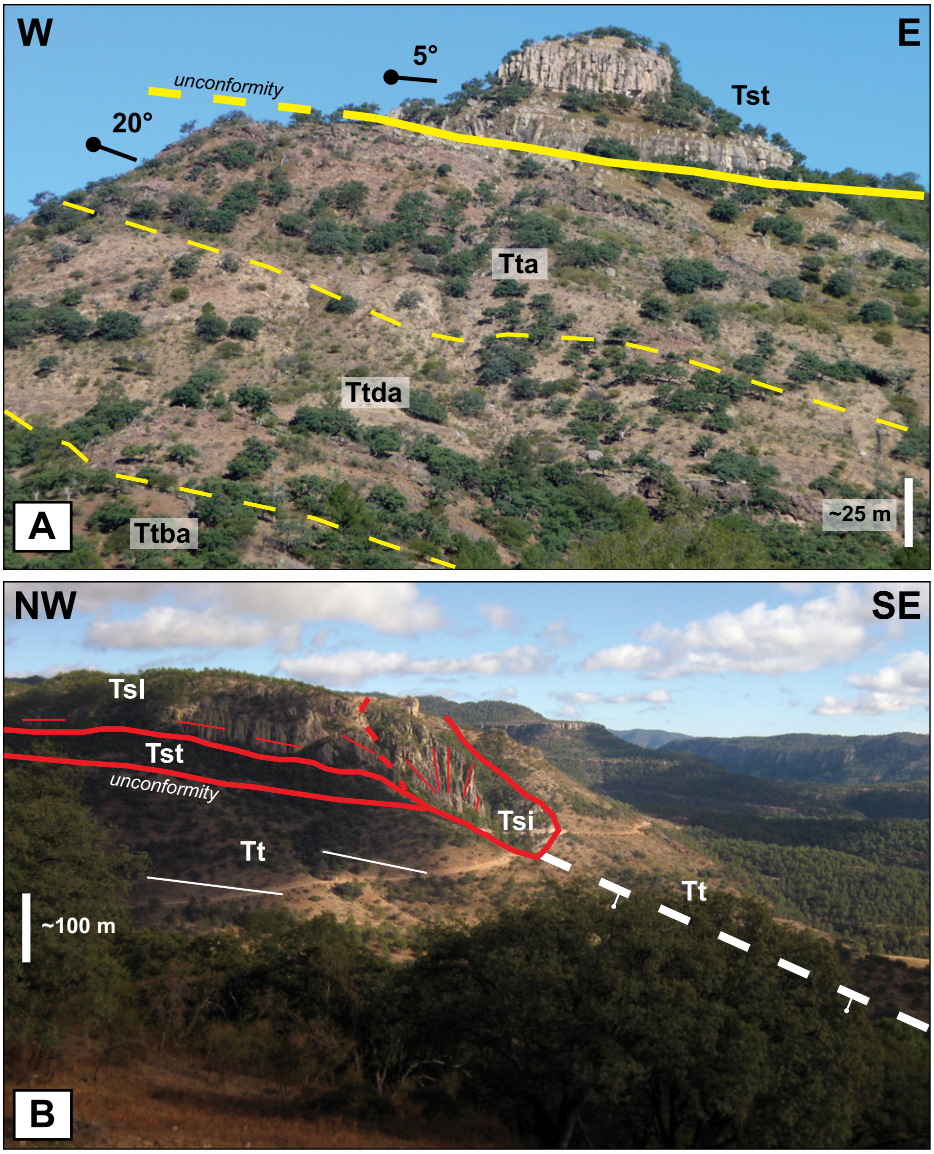

Figure 12. Interpreted photographs of depositional relationships between the Témoris formation and the Sierra Guazapares formation; locations of photos are given in Universal Transverse Mercator, North American Datum 1927 coordinates (NAD27 UTM zone 12). Unit abbreviations as in Table 1. (A) Angular unconformity between gently dipping (~5° NE) massive and stratified rhyolite ignimbrites of the Sierra Guazapares formation (Tst) and the underlying moderately dipping (~20° E) lavas (Ttba, Tta) and debris flow deposits (Ttda) of the Témoris formation. View is north toward Cerro Cuadro Blanco (Fig. 3B) from 772093E 3022247N. (B) View northeast from 772915E 3021769N toward silicic plug (Tsi) that intrudes the La Palmera fault and is the source for the silicic lava (Tsl) that flowed to the northwest over silicic ignimbrites of the Sierra Guazapares formation (Tst) and tilted rocks of the Témoris formation (Tt). The dip of flow banding (thin red lines) in the lava increases in proximity to the plug, where the flow banding is subvertical.

were erupted from fissure vents, rather than a central vent, and likely formed coarse-grained ramparts. Interstratified silicic lavas and plugs are concentrated along either side of the same fault zone, in the same linear map distribution, supporting the interpretation that the Guazapares fault zone–La Palmera fault controlled the siting of an 11-km-long silicic fissure vent.

The very large scale cross-bedded ignimbrites (Tsxi) represent a gradation between the pyroclastic surge and pyroclastic flow end members of pyroclastic density current classification (e.g., Fisher and Schmincke, 1984; Branney and Kokelaar, 2002). The abundant very coarse-grained lithic layers in these cross-bedded ignimbrites are similar to lithic lag breccias described from other vent to proximal ignimbrites (e.g., Fisher and Schmincke, 1984; Carey, 1991; Freundt et al., 2000; Branney and Kokelaar, 2002). The angularity of the lithic components and their derivation from the underlying Témoris formation suggests that they were fragmented and incorporated into the pumice-rich pyroclastic material as it ascended through the vent. However, the very large scale cross-stratification is unusual for ignimbrite lithic lag breccias. Very large scale cross-bedding has been described in vent to proximal ignimbrites in other localities, including Mount St. Helens (e.g., Rowley et al., 1985), Tenerife (e.g., Brown and Branney, 2004), Santorini (e.g., Gertisser et al., 2009), and Volcán Villarrica, Chile (e.g., Silva Parejas et al., 2010); however, these cross-bedded ignimbrites are generally dominated by ash- to lapilli-sized material and do not contain the large lithic blocks such as in the very large scale cross-bedded ignimbrite (Tsxi) described here.

Given their coarse-grained nature and large-scale cross-stratification, the very large scale cross-bedded ignimbrites (Tsxi) suggest deposition from highly energetic low-concentration pyroclastic flows in a vent to proximal setting, due to the high amount of turbulent energy required to produce these very large bedforms while transporting the large lithic fragments (e.g., Wright et al., 1981; Carey, 1991; Branney and Kokelaar, 2002). The gradational lateral transition from very large scale cross-bedded ignimbrites (Tsxi) into massive to stratified ignimbrites (Tst) within 1–2 km of the Guazapares fault zone–La Palmera fault (Fig. 3; Supplemental Fig. 1 [see footnote 1]) suggests decreased turbulence and an increased pyroclastic sedimentation rate farther from the vent.

Lithostratigraphic Summary

The three informal formations defined in the Guazapares Mining District region represent three distinct volcanic episodes:

1. The Parajes formation consists of welded to nonwelded silicic outflow ignimbrite sheets that were erupted from caldera sources within 50–100 km of the study area, with intercalated volcaniclastic rocks derived from erosion of these ignimbrites.

2. The lower and middle Témoris formation consists dominantly of locally erupted mafic to intermediate composition lavas and associated subvolcanic intrusions, including an andesitic center in the area around Témoris, as well

as fault-controlled dikes that likely fed flows outside the main center. The lower and middle Témoris formation also contains interstratified volcaniclastic fluvial and debris flow deposits. Detritus at the base of the formation that was derived from the underlying Parajes formation silicic ignimbrites records erosion of that formation, perhaps along fault scarps. In contrast, the andesitic detritus that dominates higher in the section could record resedimentation of primary eruptive products, such as the collapsing fronts of lavas, or block-and-ash flows or tephras, although erosion of constructional volcanic features or fault scarps is also probable, particularly for polymictic deposits. The distal thin nonwelded silicic ignimbrites and sedimentary rocks of the upper section of the Témoris formation record waning of local mafic to intermediate volcanism prior to the onset of local silicic volcanism, and indicate continuing or recurring silicic ignimbrite-forming eruptions from distant sources.

3. The Sierra Guazapares formation records the local eruption of silicic volcanic rocks within the Guazapares Mining District region. These include ignimbrites with vent facies lithic lag breccias that formed very large scale cross-beds along either side of an 11-km-long fault-controlled fissure, which also controlled the emplacement of silicic plugs and eruption of silicic lavas. The Sierra Guazapares formation also includes silicic dome-collapse breccias and interstratified silicic lavas and volcaniclastic rocks that interfinger with lacustrine deposits preserved in a half-graben basin.

GEOLOGIC STRUCTURES AND BASIN DEVELOPMENT

The main geologic structures in the Guazapares Mining District region are primarily NNW–trending normal faults, including the Guazapares fault zone and faults to the northeast of Témoris (Figs. 2, 3, and 4; Supplemental Fig. 1 [see footnote 1]). The Guazapares fault zone extends from Témoris northward to the Monte Cristo mining claim, and is a complex system of NNW–striking normal faults with numerous splays that dip both east and west, with several changes of fault dip polarity along strike (Fig. 3B; Supplemental Fig. 1 [see footnote 1]; Supplemental Data File [see footnote 3]). This fault zone hosts the majority of mineralization within the mining district (e.g., Gustin, 2012). The normal faults located northeast of Témoris have significant vertical offset and bound half-graben basins (Figs. 3A and 4). Although many of the half graben faults die out upsection, making them relatively easy to recognize, faults of the Guazapares fault zone were reactivated many times, and cut all formations (Figs. 2 and 5), making their earlier history more difficult to document.

Synvolcanic Half-Graben Basins

Several normal faults bound half-graben basins in the Guazapares Mining District region, including the NNW–striking, west-dipping Arroyo Hondo–Puerto Blanco, La Palmera, and Agujerado faults; the NNE–striking, west-dipping Rancho de Santiago fault; and the NNW–striking, east-dipping Sangre de Cristo fault (Figs. 3 and 4). In general, these half-graben basins contain sedimentary and volcanic deposits that thicken and/or coarsen toward basin-bounding normal faults, which either terminate at the fault or thin onto the footwall, indicating synextensional deposition (Fig. 4). Angular unconformities occur between each of the formations, and fanning dips (e.g., Fig. 12A) indicate synextensional deposition, with the Parajes and Témoris formations dipping more steeply than the gently dipping to flat-lying Sierra Guazapares formation.

The upper part of the Parajes formation (younger than the Puerto Blanco ignimbrite [Tpb]) was likely deposited into synvolcanic extensional basins, based on the variable thicknesses of individual outflow ignimbrite sheets and distribution of interbedded sedimentary rocks across faults. Evidence for synextensional deposition includes (1) the presence of reworked tuff, sandstone, and conglomerate (Tps) above the Rancho de Santiago ignimbrite (Tpr) within the half-graben basin adjacent to Arroyo Hondo–Puerto Blanco fault and in the Mesa de Cristal area, which thicken toward and terminate at faults and are not present on the footwall blocks, and (2) thickening of the Rancho de Santiago ignimbrite (Tpr) within the half-graben basin bounded by the Arroyo Hondo–Puerto Blanco fault (~200 m thick), relative to the ~80 m thickness on the footwall block (Figs. 3A, 4, and 8C; Supplemental Fig. 1 [see footnote 1]).

Synextensional deposition of the Témoris formation is evident in the three half-graben basins bounded by the La Palmera, Agujerado, and Rancho de Santiago–Arroyo Hondo–Puerto Blanco faults (Figs. 3A and 4). In these basins, the Témoris formation is deposited in angular unconformity on the more steeply dipping Parajes formation, and the thickness and average grain size of sedimentary deposits increases dramatically eastward toward each of the basin-bounding normal faults (Fig. 4). In the half-graben bounded by the Agujerado fault, a coarse-grained debris flow (Ttds) deposited proximal to the basin-bounding fault interfingers basinward with finer grained sandstone and siltstone (Ttss; Figs. 3A and 4B).

The largest of the three synvolcanic half-grabens of the Témoris formation is the Rancho de Santiago basin, which is unique in that it developed as a half-graben bounded by two west-dipping normal faults on the eastern side of the basin; the southernmost fault is the NNE–striking Rancho de Santiago fault, which is crosscut on the north end by the NNW–striking Arroyo Hondo–Puerto Blanco fault (Fig. 3A). In this basin, a clast-supported breccia (Ttdt) containing large (to 4 m) intermediate volcanic and lesser silicic ignimbrite rock fragments, as well as slide blocks of fractured but intact sedimentary strata to 15 m thick and 20 m long, is adjacent to the Rancho de Santiago fault (Figs. 3A, 4C, and 9B; Table 1). This breccia is interpreted as talus and avalanche deposits that were shed from the uplifted footwall fault scarps directly into the half-graben basin to the west.

Synvolcanic extension during emplacement of the Sierra Guazapares formation is recorded by silicic dome-collapse deposits, reworked tuffs, and fluvial-lacustrine deposits (Tsv) preserved within the half-graben basin bounded by the Sangre de Cristo fault in the Monte Cristo mining claim at the northern mapped end of the Guazapares fault zone (Fig. 3B; Table 1; Supplemental Data File [see footnote 3]). In this basin, a rhyolitic breccia thickens and coarsens toward the Sangre de Cristo fault and interfingers basinward with basal lacustrine sedimentary rocks. Additional evidence of synvolcanic extension in this basin includes the development of a normal fault within the hanging-wall block of the Sangre de Cristo fault that provided a conduit for a small silicic plug and coulee (Tsl) to intrude and flow over the actively depositing volcaniclastic unit (Tsv; Fig. 3B; Supplemental Data File [see footnote 3]).

Relative Timing and Amount of Extensional Deformation

Extensional deformation in the Guazapares Mining District region was concurrent with deposition of at least the upper part of the Parajes formation, the Témoris formation, and the Sierra Guazapares formation, with continued extension following deposition of the Sierra Guazapares formation. Pre–Sierra Guazapares formation extension is suggested by the low to moderate angular unconformities between the Témoris formation and the underlying Parajes formation and the overlying Sierra Guazapares formation (Fig. 12A). Older normal faults that offset the Parajes and Témoris formations localized the vents and silicic plugs of the Sierra Guazapares formation, which utilized these

Geosphere, published online on 13 September 2013 as doi:10.1130/GES00862.1

preexisting structures as pathways for magma accent (e.g., La Palmera and La Escalera faults, Guazapares fault zone; Figs. 2, 3, and 12B; Supplemental Fig. 1 [see footnote 1]). In addition, unfaulted Sierra Guazapares formation lavas bury some faults that offset the Parajes and Témoris formations (Figs. 2 and 3).

Further evidence of pre–Sierra Guazapares formation extension includes greater fault offsets of the older formations compared to offset of the Sierra Guazapares formation (Figs. 3A and 4). The minimum vertical displacement of the base of the Témoris formation across the Ericicuchi fault is >300 m, ~110 m across the Agujerado fault, and >450 m across the La Palmera fault (Fig. 4). In comparison, these faults offset the Sierra Guazapares formation to a lesser degree: the base of the Sierra Guazapares formation is only offset ~60 m across the Ericicuchi fault, ~30 m across the Agujerado fault, and ~100 m across the La Palmera fault (Fig. 4). This shows that a significant amount of extensional deformation (at least 350 m vertical displacement) occurred prior to the eruption of the Sierra Guazapares formation.

A minimum of 20% total horizontal extension is estimated in the Guazapares Mining District region (for the area shown in Fig. 4), based on the vertical displacement of stratigraphic units across normal faults. This amount of extension is significantly lower than that of the Gulf Extensional Province to the west in Sonora, where ~90% extension is estimated to have occurred (Gans, 1997). The structural style also differs between these two areas; high-angle normal faults are found in the Guazapares Mining District region, while highly extended core complexes are located in Sonora (e.g., Gans, 1997; Wong et al., 2010).

Although not directly quantifiable, several faults within the Guazapares Mining District region appear to accommodate considerable amounts of deformation based solely on the juxtaposition of stratigraphic units. The La Palmera fault has significant vertical offset (over 450 m) based on the offset of the Parajes–Témoris formation contact; the Parajes formation is exposed on the footwall, but is not exposed in the hanging wall, which suggests that it is deeply buried beneath Témoris formation deposits there (Figs. 2 and 4). A distinct lithologic boundary in the Parajes formation occurs across the Chapotillo fault, as the younger outflow ignimbrite sheets in the hanging wall of this fault are not exposed on the footwall to the southwest (Fig. 3A). Postdepositional drag folding related to normal fault deformation is observed in the Témoris formation adjacent to many of the NNW–striking faults with significant offset (e.g., La Palmera, Agujerado, and La Escalera faults; Figs. 3A and 4); the underlying Parajes formation has small-scale normal faulting to accommodate this deformation.

AGE CONSTRAINTS

Methodology

We report new U-Pb zircon ages from each of the three informally defined formations, providing constraints on the age of the previously undated volcanic rocks of the Guazapares Mining District region. Laser ablation–inductively coupled plasma–mass spectrometry (LA–ICP-MS) U-Pb analyses were performed at the Laboratorio de Estudios Isotópicos, Centro de Geociencias, Universidad Nacional Autónoma de México on zircons separated from 13 silicic rock samples (Fig. 13; Table 3; Supplemental Table 2[4]). The zircons were hand-picked under binocular microscope, mounted in an epoxy cast, polished, and imaged by cathodoluminescence (CL). The zircons selected for U-Pb geochronology were analyzed following the procedure reported by Solari et al. (2010), employing a Resonetics M050 excimer laser ablation workstation coupled to a Thermo XSeries II ICP-MS. Based on CL imaging, one ablation site was selected on each zircon analyzed, located either in the middle, near rim, or core of the crystal (Supplemental Fig. 2[5]). The Plešovice standard zircon (ca. 337 Ma; Sláma et al., 2008) was used as a bracketing standard, interdispersed and measured after every five unknown zircons. The observed uncertainties of the ^{206}Pb/^{238}U, ^{207}Pb/^{206}Pb, and ^{208}Pb/^{232}Th ratios, during the different sessions in which the current samples were analyzed, as measured on the Plešovice standard zircon, were 0.65%, 1.0%, and 1.1%, respectively. These values are quadratically propagated to the quoted uncertainties of the unknown zircons, to take into account the heterogeneities of the natural standard zircon. A second standard (NIST 610) is used to recalculate the elemental concentrations for each zircon, measured together with the isotopes of interest for U-Pb geochronology. The common Pb correction cannot be performed measuring the ^{204}Pb isotope with the current setup; common Pb is evaluated using the ^{207}Pb/^{206}Pb ratio, graphing the results using Tera-Wasserburg diagrams (Tera and Wasserburg, 1972). If a correction is needed, the algebraic method of Andersen (2002) is used. Filters are then applied to reduce outliers: largely discordant analyses (e.g., >50% discordant) and those with >4% 1σ error on the corrected ^{206}Pb/^{238}U ratio are eliminated. A further screening is applied to check for possible microscopic inclusions of minerals other than zircons that could have been inadvertently hit during the analysis. This screening is performed during data reduction, employing a script written in R (UPb.age; Solari and Tanner, 2011). Additional screenings are performed, checking for analyses with high P and light rare earth elements, which could be indicative of apatite inclusions, and those few analyses that present high concentrations of U and Th (generally >1000 ppm), which could yield to a Pb loss and a consequent discordant or, in any case, younger and geologically meaningless ages.

Concordia plots, probability density distribution and histogram plots, mean age, and age-error calculations were performed using Isoplot v. 3.70 (Ludwig, 2008). The mean ^{206}Pb/^{238}U age is especially useful for the Tertiary ages

[4]Supplemental Table 2. Zircon U-Pb laser ablation–inductively coupled plasma–mass spectrometry analytical results. If you are viewing the PDF of this paper or reading it offline, please visit http://dx.doi.org/10.1130/GES00862.S4 or the full-text article on www.gsapubs.org to view Supplemental Table 2.

[5]Supplemental Figure 2. Cathodoluminescence images of zircons from U-Pb laser ablation–inductively coupled plasma–mass spectrometry analyses. If you are viewing the PDF of this paper or reading it offline, please visit http://dx.doi.org/10.1130/GES00862.S5 or the full-text article on www.gsapubs.org to view Supplemental Figure 2.

Figure 13 (*on following two pages*). Summary of zircon U-Pb laser ablation–inductively coupled plasma–mass spectrometry analyses for samples listed in Table 3; mean ^{206}Pb/^{238}U ages of the youngest zircon population (interpreted emplacement age) for each sample is listed. Tera-Wasserburg concordia plots with inset probability density distribution plots are arranged by major stratigraphic division and lithologic unit. MSWD—mean square of weighted deviates. (A, B) Ericicuchi ignimbrite (Tpe), Parajes formation. (C) Puerto Blanco ignimbrite (Tpb), Parajes formation. (D) Silicic tuff interbedded in sandstone from the basal deposits of the Témoris formation. (E, F) Silicic ignimbrites (Tti) from near the top of the Témoris formation. (G) Very large scale cross-bedded rhyolitic ignimbrite (Tsxi), Sierra Guazapares formation. (H–J) Rhyolitic lavas (Tsl), Sierra Guazapares formation. (K, L) Rhyolitic plugs (Tsi), Sierra Guazapares formation. (M) Rhyolitic dome-collapse breccia from the Monte Cristo mining claim, Sierra Guazapares formation. Details on the experiments and mean age plots are given in Supplemental Table 2 (see footnote 4).

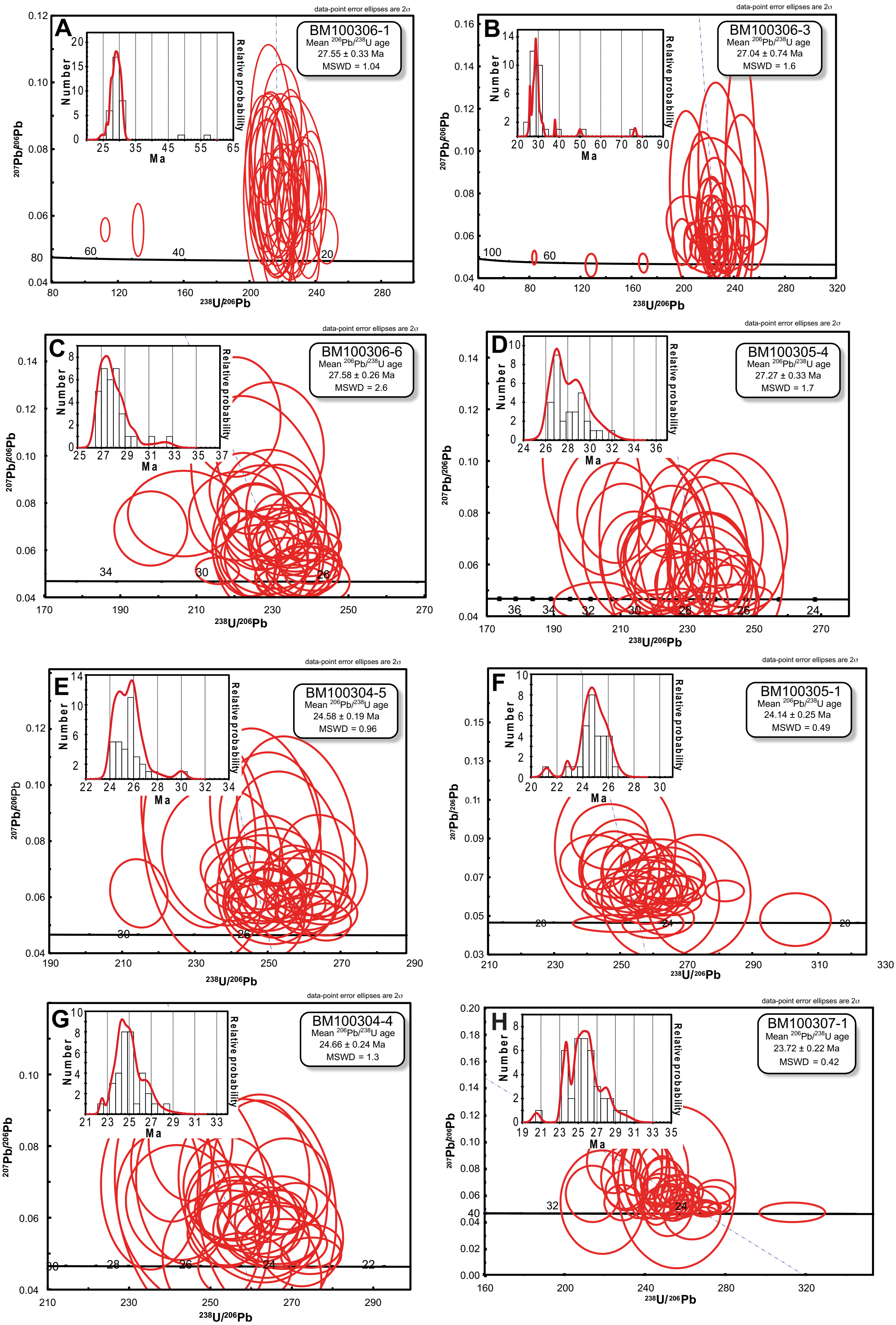
A
BM100306-1
Mean $^{206}Pb/^{238}U$ age
27.55 ± 0.33 Ma
MSWD = 1.04
B
BM100306-3
Mean $^{206}Pb/^{238}U$ age
27.04 ± 0.74 Ma
MSWD = 1.6
C
BM100306-6
Mean $^{206}Pb/^{238}U$ age
27.58 ± 0.26 Ma
MSWD = 2.6
D
BM100305-4
Mean $^{206}Pb/^{238}U$ age
27.27 ± 0.33 Ma
MSWD = 1.7
E
BM100304-5
Mean $^{206}Pb/^{238}U$ age
24.58 ± 0.19 Ma
MSWD = 0.96
F
BM100305-1
Mean $^{206}Pb/^{238}U$ age
24.14 ± 0.25 Ma
MSWD = 0.49
G
BM100304-4
Mean $^{206}Pb/^{238}U$ age
24.66 ± 0.24 Ma
MSWD = 1.3
H
BM100307-1
Mean $^{206}Pb/^{238}U$ age
23.72 ± 0.22 Ma
MSWD = 0.42
data-point error ellipses are 2σ
Number
Relative probability
Ma
$^{207}Pb/^{206}Pb$
$^{238}U/^{206}Pb$

Figure 13.

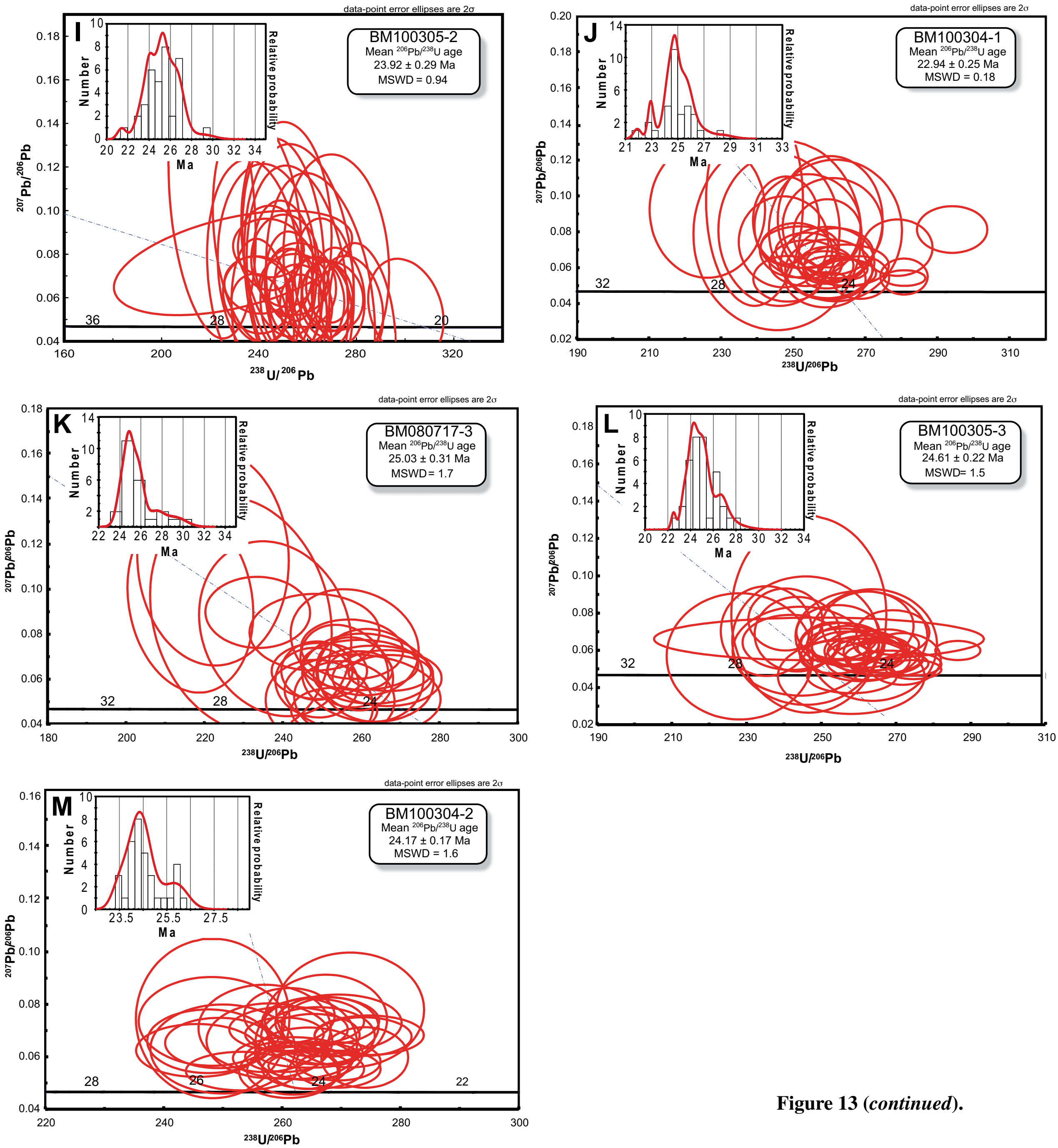

Figure 13 (*continued*).

presented here, because the ^{207}Pb measurement is problematic in these young zircons and the consequent uncertainty on the ^{207}Pb/^{206}Pb ratio is not a good indicator of geologically meaningful discordance. In Tertiary zircons, it is also common to observe scattering of the mean ^{206}Pb/^{238}U ages that yields MSWD (mean square of weighted deviates) values that are largely >1, an indication that a mixed age population possibly exists. An example of this scenario was presented by Bryan et al. (2008). In order to recognize possible different age components in samples that showed an initial MSWD of >3, the deconvolution method, based on the mixture modeling method of Sambridge and Compston (1994), was implemented in Isoplot.

When two mixture components are recognized, their respective mean ^{206}Pb/^{238}U ages are plotted together with errors and recalculated MSWD. The mean ^{206}Pb/^{238}U age of the older mixture component in a sample represents the crystallization age of inherited zircons within the host magma, while the younger mean ^{206}Pb/^{238}U age population represents the phenocryst crystallization age of the sample. This youngest age population of each sample is interpreted as the preferred eruption or emplacement age of the rock, as it is consistent (within error) with stratigraphic relationships in the study area. Age results are presented in the following and summarized in Figure 13 and Table 3; detailed analytical data are given in Supplemental Table 2 (see footnote 4).

TABLE 3. SUMMARY OF ZIRCON U-Pb LA-ICP-MS RESULTS

Sample	Map unit	Lithology	Age* (Ma)	±2σ (Ma)	n	MSWD	UTM (E)	UTM (N)
BM100304–2	Tsv	rhyolite breccia	24.17	0.17	24	1.6	767557	3035421
			25.76	*0.45*	9	1.9		
BM100305–3	Tsi	rhyolite plug	24.61	0.22	23	1.5	774042	3023376
BM080717–3	Tsi	rhyolite plug	25.03	0.31	18	1.7	770970	3030952
BM100304–1	Tsl	rhyolitic lava flow	22.94	0.25	3	0.18	767453	3035862
			25.07	*0.24*	22	1.5		
BM100305–2	Tsl	rhyolite lava flow	23.92	0.29	8	0.94	773462	3023389
			25.69	*0.32*	23	1.5		
BM100307–1	Tsl	rhyolite lava flow	23.72	0.22	5	0.97	771277	3030018
			25.78	*0.27*	17	1.7		
BM100304–4	Tsxi	cross-bedded ignimbrite	24.66	0.24	19	1.3	767878	3027817
BM100305–1	Tti	rhyolite lapilli tuff	24.14	0.25	10	0.49	773365	3023281
			25.58	*0.29*	17	1.6		
BM100304–5	Tti	rhyolite lapilli tuff	24.58	0.19	12	0.96	768511	3027340
			26.07	*0.25*	20	1.5		
BM100305–4	Ttss	silicic tuff	27.27	0.33	18	1.7	776588	3031515
			29.73	*0.70*	11	2.1		
BM100306–6	Tpb	nonwelded silicic ignimbrite	27.58	0.26	31	2.6	778205	3029101
BM100306–3	Tpe	nonwelded silicic ignimbrite	27.04	0.74	6	2.5	776541	3026289
			29.01	*0.32*	16	1.6		
BM100306–1	Tpe	nonwelded silicic ignimbrite	27.55	0.33	6	1.04	775513	3024576
			29.59	*0.33*	22	1.6		

Note: LA-ICP-MS—laser ablation–inductively coupled plasma–mass spectrometry. Ages in italics represent the zircon antecryst (proposed by Charlier et al., 2004; crystals that predate crystallization and eruption of a host magma, but formed during an earlier phase of related magmatism) age population in a given sample. The youngest age population of each sample is interpreted as the preferred eruption or emplacement age. n—number; MSWD—mean square of weighted deviates. Universal Transverse Mercator (UTM; E—east, N—north) coordinates are based on the North American Datum 1927 (NAD27) zone 12. Map unit labels correspond to Table 1. Details of each analysis are given in Supplemental Table 1 (see text footnote 2).

*Mean $^{206}Pb/^{238}U$ age.

Parajes Formation

Three samples were dated from the Parajes formation (Figs. 13A–13C; Table 1), including two samples from the Ericicuchi ignimbrite (Tpe) and one sample from the Puerto Blanco ignimbrite (Tpb). Sample BM100306–1 is Ericicuchi ignimbrite (Tpe), which has separated zircons that are bipyramidal to short and stubby, and to 220 µm in length. Under CL, the zircons show uniform areas with limited luminescence; in a few cases, oscillatory zoning is present around possible inherited cores. The U-Pb geochronological analysis, as well as the screening and filtering, shows the presence of inherited cores that are slightly discordant but older than 40 Ma. Most of the analyzed, nearly concordant crystals range from ca. 26 Ma to 31 Ma (Fig. 13A). Two zircon age populations can be distinguished: the oldest population has a mean age of 29.59 ± 0.33 Ma (n = 22, MSWD = 1.6), whereas the youngest has a mean age of 27.55 ± 0.33 Ma (n = 6, MSWD = 1.04). A second sample from the Ericicuchi ignimbrite (sample BM100306–3; Fig. 13B) yielded fewer and smaller zircon crystals (to 180 µm in length) that are euhedral to subhedral with a prevalence of stubby morphologies with short pyramidal terminations. These zircons show bright CL zoning around darker cores. The U-Pb geochronology for this sample also revealed the presence of inherited cores of ca. 76, 50, and 38 Ma and two main zircon age populations consisting of an older grouping having a mean age of 29.01 ± 0.32 Ma (n = 16, MSWD = 1.6) and a younger grouping with a mean age of 27.04 ± 0.74 Ma (n = 6, MSWD = 2.5). The third sample of the Parajes formation is from the Puerto Blanco ignimbrite (Tpb; sample BM100306–6; Fig. 13C). The zircons in this sample are larger (to 260 µm in length) with elongated shapes that are mostly prismatic with well-developed pyramids. Under CL they show evident bright rims developed outside darker zones. The dated zircons define a homogeneous group with few outliers and have a mean age of 27.58 ± 0.26 Ma (n = 31, MSWD = 2.6).

Témoris Formation

Three samples of silicic tuffs from basal and upper sections of the Témoris formation were dated (Figs. 13D–13F; Table 3). Sample BM100305–4 was collected from the basal section of the Témoris formation (Fig. 13D) and has zircons to 300 µm in length that are prismatic and elongated. Under CL, the zircons are characterized by darker cores surrounded by bright zones. Despite similar crystal morphologies, two zircon age populations are identified; the oldest group has a mean age of 29.73 ± 0.70 Ma (n = 11, MSWD = 2.1), whereas the youngest mean age is 27.27 ± 0.33 Ma (n = 18, MSWD = 1.7). Sample BM100304–5 was collected from the upper section of the Témoris formation (Tti; Fig. 13E) and has zircons that are indistinguishable in size, morphology, and CL imaging from those of the previous sample. Two well-constrained zircon age populations are also defined; the oldest has a mean age of 26.07 ± 0.25 Ma (n = 20, MSWD = 1.5), whereas the youngest mean age is 24.58 ± 0.19 Ma (n = 12, MSWD = 0.96). Sample BM100305–1 is from the uppermost section of the Témoris formation (Tti), ~35 m below the Sierra Guazapares formation contact (Figs. 10 and 13F). Its zircons are also prismatic and very elongated, although they are somewhat smaller (to 200 µm in length) in this sample. Under CL, the zircons are also characterized by darker cores surrounded by bright zones. U-Pb analyses identified two zircon age populations in this sample; the oldest group yields a mean age of 25.58 ± 0.29 Ma (n = 17, MSWD = 1.6), whereas the youngest group yields a mean age of 24.14 ± 0.25 Ma (n = 10, MSWD = 0.49).

Sierra Guazapares Formation

Seven samples from the various lithologies of the Sierra Guazapares formation were chosen for U-Pb geochronology (Figs. 13G–13M; Table 3). Sample BM100304–4 was collected from the very large scale cross-bedded ignimbrite unit (Tsxi; Fig. 13G). It has somewhat small (to 150 µm) euhedral zircons that range in shape from prismatic to stubby and bipyramidal morphologies. CL imaging is not different from the previously described samples, although cores are not as evident as in other samples. The dated zircons define only one coherent group, in which the mean age is 24.66 ± 0.24 Ma (n = 19, MSWD = 1.3).

Three rhyolite lava (Tsl) samples were analyzed. Sample BM100307–1 (Fig. 13H) is characterized by prismatic euhedral zircons (to 300 µm in length) with the same CL characteristics as those previously described. Two zircon age groups are also defined; the oldest group yields a mean age of 25.78 ± 0.27 Ma (n = 17, MSWD = 1.7), whereas the mean age of the youngest group is 23.72 ± 0.22 Ma (n = 5, MSWD = 0.42). Sample BM100305–2 (Fig. 13I) also has prismatic zircons (to 200 µm in length) with most showing oscillatory zoning. U-Pb zircon dating of this sample defines two age populations; the oldest group with a mean age of 25.69 ± 0.32 Ma (n = 23, MSWD = 1.5) and the youngest group with a mean age of 23.92 ± 0.29 Ma (n = 8, MSWD = 0.94). Sample BM100304–1 (Fig. 13J) was collected from a small lava in the Monte Cristo area (Fig. 3B). It also has prismatic zircons (to 180 µm in length), although in this sample they are somewhat more needle shaped. Two age populations are identified in this sample; the oldest has a mean age of 25.07 ± 0.24 Ma (n = 22, MSWD = 1.5), whereas a few grains define the youngest group with a mean age of 22.94 ± 0.25 Ma (n = 3, MSWD = 0.18).

Two samples collected from rhyolite plugs (Tsi) were analyzed. Sample BM080717–3 (Fig. 13K) is characterized by stubby to bipyramidal zircons (to 150 μm in length) that are sector zoned under CL. Its U-Pb dating yields only one age group, with a mean age of 25.03 ± 0.31 Ma (n = 18, MSWD = 1.7). The zircons belonging to the sample BM100305–3 (Fig. 13L) are prismatic and large (to 340 μm in length). The U-Pb dating yields a homogeneous age group, with a mean age of 24.61 ± 0.22 Ma (n = 23, MSWD = 1.5).

Sample BM100304–2 was collected from a rhyolitic breccia locally exposed in the Monte Cristo area (Tsv; Figs. 3B and 13M). Its zircons are prismatic and large (to 250 μm in length). Two age populations are recognized; the oldest group has a mean age of 25.76 ± 0.45 Ma (n = 9, MSWD = 1.9), whereas the youngest group has a mean age of 24.17 ± 0.17 Ma (n = 24, MSWD = 1.6).

Age Interpretations

Previous dating of silicic volcanic rocks in the Sierra Madre Occidental using zircon U-Pb LA-ICP-MS showed that zircon ages are occasionally older (to 1–4 Myr) than the ages obtained from the same rocks using K/Ar and $^{40}Ar/^{39}Ar$ dating methods (Bryan et al., 2008). The older zircon ages in their study are attributed to the presence of antecrysts, a term proposed by Charlier et al. (2004) to describe crystals that predate the crystallization and eruption of a host magma, but formed during an earlier phase of related magmatism. In a region of long-lived magmatism like the Sierra Madre Occidental, the antecryst ages could predate the phenocryst age by more than 10 Myr, making it difficult to distinguish antecrysts from xenocrysts (Bryan et al., 2008). In addition, the occurrence of antecrysts tends to be greater in the younger silicic volcanic rocks of a sequence, when the probability of remelting partially molten or solidified upper crustal rocks formed during a preceding magmatic phase is higher (Bryan et al., 2008).

The presence of antecrysts in a zircon population for a sample will tend to produce initial MSWD values much greater than unity and probability density function curves of zircon ages that are positively skewed and asymmetric, and/or have broad, bimodal, or polymodal peaks. In comparison, a well-defined unimodal peak likely indicates the crystallization age of phenocrysts with limited antecrysts, which is a close approximation to the eruption age of the host magma (Charlier et al., 2004; Bryan et al., 2008).

The ages obtained for most of the samples dated for this study in the Guazapares Mining District region suggest the presence of antecrysts in the zircon population. The probability density function curves tend to be positively skewed and asymmetric, and several have broad or bimodal peaks (Fig. 13; Supplemental Table 2 [see footnote 4]). The oldest zircon population in a sample represents the crystallization age of antecrysts, which generally correspond to zircons with crystal core to middle ablation sites. In comparison, the youngest zircon population indicates the age of phenocryst crystallization and typically represents the zircons with middle to near-rim ablation sites. The antecryst age populations in these samples tend to be ~1.5–2 Myr older than the phenocryst age populations (Table 3); antecryst ages tend to cluster around 29.5 Ma for samples from the Parajes formation and 25.5 Ma for samples from the overlying Témoris and Sierra Guazapares formations.

DISCUSSION

Volcanic and Tectonic Evolution

The new geologic mapping and geochronology presented in this study show that the three informal formations in the Guazapares Mining District region (Fig. 5) record Late Oligocene to Early Miocene synextensional volcanic activity during the mid-Cenozoic ignimbrite flare-up in the northern Sierra Madre Occidental: (1) the synextensional deposition of outflow ignimbrite sheets (Parajes formation) ca. 27.5 Ma, which were likely erupted from calderas ~50–100 km from the study area; these overlap in time with the end of peak ignimbrite flare-up volcanism to the east; (2) synextensional growth of an andesitic volcanic center (Témoris formation) between ca. 27 Ma and ca. 24.5 Ma; and (3) synextensional silicic fissure magmatism (Sierra Guazapares formation), including vent facies ignimbrites, lavas, and intrusions, between ca. 24.5 and ca. 23 Ma (Fig. 14).

Stratigraphic and structural evidence show that the outflow ignimbrite sheets of the Parajes formation younger than the 27.58 ± 0.26 Ma Puerto Blanco ignimbrite (Tpb) were deposited in a developing half-graben basin (Fig. 14A). It is uncertain whether the older outflow ignimbrite sheets in the formation (older than 27.5 Ma) were deposited in half-graben basins. The Parajes formation was tilted by extension and partly eroded from normal fault footwalls prior to and during deposition of the overlying Témoris formation (Figs. 4, 8C, and 9A).

The ca. 27–24.5 Ma Témoris formation records the onset of magmatism in the area, which was primarily andesitic, with compositions ranging from basalt to andesite (Fig. 7). Like the Parajes formation, the Témoris formation was deposited in synvolcanic half-graben basins (Fig. 14B). Fluvial and debris flow processes developed alluvial fan systems that prograded into the half-grabens to become interbedded with andesitic lavas. At least some of these alluvial deposits were likely eroded from andesitic lavas exposed in uplifted normal fault footwall blocks, although some of the detritus could also have been reworked from unconsolidated primary volcanic fragmental eruptive products (Fig. 14B). Normal faults in the study area control the siting of some vents of the Témoris formation, including andesitic feeder dikes along normal faults and the andesitic volcanic center (Ttv) in the area around Témoris, which is located at the southern projection of the Guazapares fault zone (Figs. 2 and 3; Supplemental Fig. 1 [see footnote 1]). The presence of distal silicic ignimbrites (Tti) in the uppermost part of the mafic to andesitic Témoris formation, below the silicic ignimbrite-dominated Sierra Guazapares formation (Figs. 5, 10, and 12A) records a hiatus between local andesitic and silicic magmatism in the region, modified by extension, tilting, and erosion, to produce an angular unconformity.

The ca. 24.5–23 Ma Sierra Guazapares formation records the onset of silicic magmatism within the Guazapares Mining District region. Based on composition and geochronology (Figs. 6, 7, and 13; Table 3), the vent to proximal facies along the Guazapares fault zone–La Palmera fault records several eruption events of high-energy explosive volcanism that resulted in deposition of very large scale cross-bedded ignimbrites with lag breccias (Tsxi) in a wedge that defines a linear, fault-controlled fissure-type vent system (Figs. 3 and 14C). The eruptive style of each event of the Sierra Guazapares formation likely transitioned into effusive volcanism, with the emplacement of rhyolite plugs along the fissures and the deposition of related rhyolite lavas over the ignimbrites (e.g., Fig. 12B). This sequence of fissure-fed ignimbrites and effusive lava and plugs is similar to the fissure ignimbrite eruption model proposed by Aguirre-Díaz and Labarthe-Hernández (2003) to explain the origin of large volume silicic ignimbrites and related effusive volcanic deposits in other extended regions of the Sierra Madre Occidental. Their model suggests that during crustal extension, a volatile-rich silicic magma chamber reaches high crustal levels and encounters preexisting normal faults that provide a conduit for magma ascent. Magma decompression follows, resulting in an explosive eruption event with deposition of proximal pyroclastic volcanic facies adjacent to the fault-controlled vents; silicic lava domes and dikes follow the pyroclastic rocks and close the vents as the magma becomes depleted of volatiles

Geosphere, published online on 13 September 2013 as doi:10.1130/GES00862.1

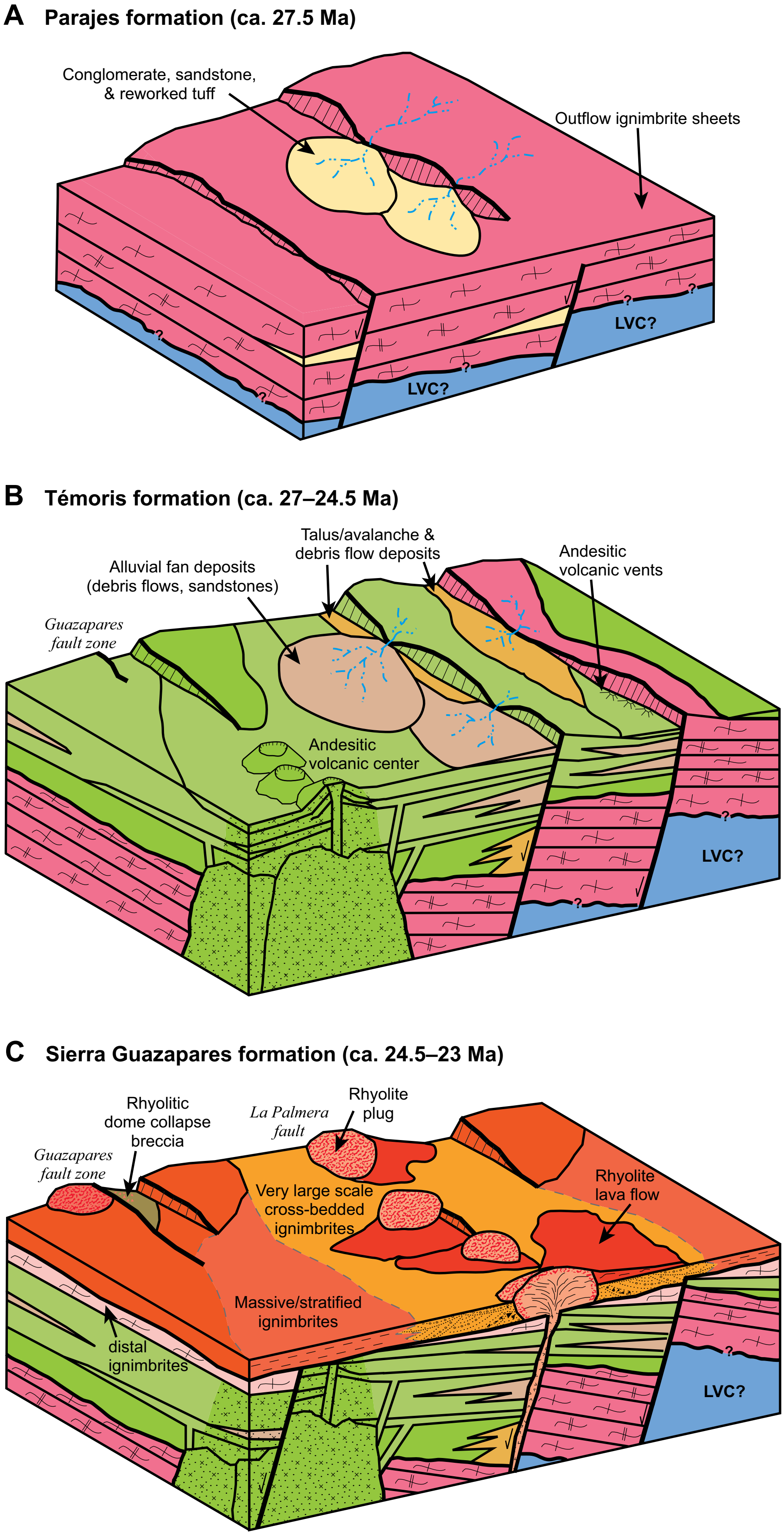

Figure 14. Schematic block diagrams illustrating the tectonic and volcanic evolution of the three formations in Guazapares Mining District region during the Late Oligocene to Early Miocene. The colors correspond to the geologic map units in Figure 3C. (A) By ca. 27.5 Ma, outflow ignimbrite sheets of the Parajes formation were erupted from medial sources during the end of the Early Oligocene pulse of the mid-Cenozoic ignimbrite flare-up in northern Mexico. The base of this stratigraphic division is not exposed in the field area; it is inferred that the Parajes formation is deposited over the pre-Oligocene Lower Volcanic Complex (LVC), based on regional studies (e.g., Ferrari et al., 2007). At least the upper part of the Parajes formation was deposited during crustal extension, indicated by reworked tuffs, cross-bedded sandstones, and pebble to cobble conglomerates with Parajes formation ignimbrite clasts interbedded between outflow ignimbrite sheets and thinning of ignimbrites on normal fault footwall blocks. Continued uplift and partial erosion of the formation occurred prior to eruption of the Témoris formation. (B) Between ca. 27 and 24.5 Ma, the Témoris formation was erupted from an andesitic volcanic center sited along the Guazapares fault zone and from smaller vents located along normal faults in the region. Primary volcanic rocks and volcaniclastic rocks derived from intrabasinal reworking of eruptive products were deposited into alluvial fan systems in synvolcanic half-graben basins. (C) Following a period of waning locally erupted mafic to intermediate volcanism in the region marked by an increase in distal ignimbrite deposition in the upper section of the Témoris formation, the Sierra Guazapares formation was erupted during the Early Miocene ignimbrite pulse of the mid-Cenozoic ignimbrite flare-up, ca. 24.5–23 Ma. Fissure vents are located along preexisting normal faults in the Guazapares Mining District region; there is a lateral volcanic facies transition away from the faults, from vent (very large scale cross-bedded ignimbrites, lavas, plugs) to proximal with slight fluvial reworking (massive to stratified ignimbrites). Rhyolitic plugs intrude normal faults and are the source for many of the rhyolitic lavas.

Geosphere, published online on 13 September 2013 as doi:10.1130/GES00862.1

(e.g., Aguirre-Díaz and Labarthe-Hernández, 2003). Each explosive and effusive volcanic event of the Sierra Guazapares formation may have progressed in a fashion similar to this fissure ignimbrite eruption model proposed by Aguirre-Díaz and Labarthe-Hernández (2003), with several silicic magma chambers interacting at high crustal levels with the Guazapares fault zone–La Palmera fault to develop a fissure-vent system. Further mapping is needed in the region to determine whether the fissure continues to the south of Témoris, where resistant silicic intrusions are obvious from a distance (Fig. 2; Supplemental Fig. 1 [see footnote 1]).

Regional Correlations

New stratigraphic and geochronologic data presented in this study indicate that mafic to intermediate volcanic rocks in the study area are not related to the Lower Volcanic Complex as proposed by previous workers (e.g., Ramírez Tello and Garcia Peralta, 2004; Roy et al., 2008; Wood and Durgin, 2009; Gustin, 2011, 2012). The Témoris formation instead represents a period of mafic to intermediate volcanism that occurred between two ignimbrite pulses of the mid-Cenozoic ignimbrite flare-up in the northern Sierra Madre Occidental and preceded local silicic ignimbrite flare-up magmatism in the study area.

The ca. 27.5 Ma Parajes formation is interpreted as medial welded to nonwelded silicic outflow ignimbrite sheets erupted at the end of the Early Oligocene pulse of the mid-Cenozoic ignimbrite flare-up in the Sierra Madre Occidental (ca. 36–27 Ma; Ferrari et al., 2007; Cather et al., 2009; McDowell and McIntosh, 2012), based on the similar eruption ages and physical characteristics to ignimbrite sequences described elsewhere in the region (e.g., Swanson et al., 2006; McDowell, 2007, and references therein). Possible sources for the outflow ignimbrites of the Parajes formation include (1) vent to proximal volcanic facies of similar ages previously identified ~100 km toward the north and northeast near Basaseachic and Tomóchic (e.g., McDowell, 2007, and references therein; McDowell and McIntosh, 2012), and (2) several calderas identified <50 km to the north, south, and east of the Guazapares Mining District region (e.g., Ferrari et al., 2007, and references therein) (Fig. 15).

Based on phenocryst assemblages and an eruption age older than 27.5 Ma, the oldest flow unit of the Parajes formation, the Chepe ignimbrite (Tpc; Table 1), is tentatively correlated with the regionally extensive Divisadero tuff of Swanson et al. (2006). The Divisadero tuff is distinctive for its crystal-rich nature (to ~40% phenocrysts) of mostly large (to 4 mm) grains of plagioclase and deeply embayed quartz. It is highly variable in thickness (~10–300 m) and has multiple cooling units with densely welded red-brown interiors that grade upward to poorly welded white tops (Swanson et al., 2006). We sampled the upper Divisadero tuff near Divisadero, southwest of Creel (sample DIV-2; Fig. 6), to compare it with the Chepe ignimbrite (Tpc) of this study. Both have a very similar crystal-rich nature with large plagioclase, biotite, and embayed quartz phenocrysts, and the Chepe ignimbrite, like the Divisadero tuff, is densely welded. However, further investigation is needed to confirm this regional correlation, such as pumice and zircon geochemistry, and U-Pb zircon geochronology on the Divisadero tuff, which was previously dated by Swanson et al. (2006) using the K-Ar method as 29.9 ± 0.7 and 29.8 ± 0.5 Ma (±1σ errors). The Divisadero tuff extends from San Juanito to Divisadero for a length of ~60 km (Swanson et al., 2006); our tentative correlation would expand the extent of the Divisadero tuff an additional ~75 km southwest, to a total length of ~135 km (Fig. 1).

In several localities in the northern Sierra Madre Occidental, mafic to intermediate composition volcanism followed the large-volume eruptions of the Early Oligocene ignimbrite pulse (the Southern Cordillera basaltic andesite province); the Témoris formation in the Guazapares Mining District region may be related to this period of mafic to intermediate composition volcanism. The mafic to intermediate composition volcanic rocks in other parts of the Sierra Madre Occidental are roughly coeval with or slightly younger than the ca. 27–24.5 Ma Témoris formation. In addition, the composition of Témoris formation rocks is similar to those of the Southern Cordillera basaltic andesite province (Fig. 7).

The age of the ca. 24.5–23 Ma Sierra Guazapares formation generally coincides with the onset of the regional Early Miocene (ca. 24–20 Ma) ignimbrite pulse of the mid-Cenozoic ignimbrite flare-up (e.g., Ferrari et al., 2002, 2007; McDowell and McIntosh, 2012; Bryan et al., 2013). Although the Early Miocene ignimbrite pulse is volumetrically significant in the southern Sierra Madre Occidental (Ferrari et al., 2002, 2007), in the northern and central Sierra Madre Occidental this ignimbrite pulse was previously thought to be less abundant and restricted to the westernmost part of the silicic large igneous province (Ferrari et al., 2007; McDowell and McIntosh, 2012; Bryan et al., 2013). The Sierra Guazapares formation thus represents a previously unrecognized part of the Early Miocene ignimbrite pulse that may have been more widespread, east of the area where rocks erupted during this pulse were previously recognized in the northern Sierra Madre Occidental.

Regional Timing of Volcanism and Extension

Previous studies have interpreted that a transition from andesitic arc magmatism in a compressional (Laramide) stress regime accompanying rapid plate convergence (Lower Volcanic Complex) to silicic ignimbrite flare-up magmatism in an extensional stress regime (Upper Volcanic Supergroup) was the result of decreased convergence between the Farallon and North American plates beginning in the Late Eocene ca. 40 Ma (Wark et al., 1990; Aguirre-Díaz and McDowell, 1991; Ward, 1991; Wark, 1991; Grijalva-Noriega and Roldán-Quintana, 1998; Ferrari et al., 2007). After the end of the Laramide orogeny in Mexico (Late Eocene), the Farallon plate was removed from the base of the North American plate by either steepening (slab rollback) and possible detachment of the deeper part of the subducted slab (e.g., Ferrari et al., 2007; Henry et al., 2010; Best et al., 2013; Busby, 2013), or through the development of a slab window (e.g., Wong et al., 2010). Based on the available age distribution of volcanic rocks in the southwestern U.S. and the Sierra Madre Occidental, the locus of magmatism is inferred to have migrated eastward (inboard) from the trench in Cretaceous to Eocene time, followed by a general southwestward migration of the arc-front magmatism toward the trench commencing by ca. 40 Ma in response to these Farallon–North American plate interactions (e.g., Coney and Reynolds, 1977; Damon et al., 1981; Ferrari et al., 1999; Gans et al., 2003; Ferrari et al., 2007; Henry et al., 2010; Wong et al., 2010; McDowell and McIntosh, 2012; Bryan et al., 2013; Busby, 2013). This plate tectonic interpretation is similar to space-time models of mid-Cenozoic volcanism proposed in the western U.S. (e.g., Coney and Reynolds, 1977; Damon et al., 1981; Gans et al., 1989; Best and Christiansen, 1991; Christiansen and Yates, 1992; Axen et al., 1993; Humphreys, 1995; Dickinson, 2002, 2006; Henry et al., 2010; Best et al., 2013; Busby, 2013). However, at a more detailed level this age trend shows greater complexity, as the Early Oligocene pulse of the ignimbrite flare-up occurred in a wide belt throughout the entire Sierra Madre Occidental at essentially the same age without internal migration patterns, and volcanism reappears in the rear-arc east of the arc front in the Middle to Late Miocene (Ferrari et al., 2007; Bryan et al., 2013).

The timing of the onset of extension relative to southwestward-migrating volcanism in

Geosphere, published online on 13 September 2013 as doi:10.1130/GES00862.1

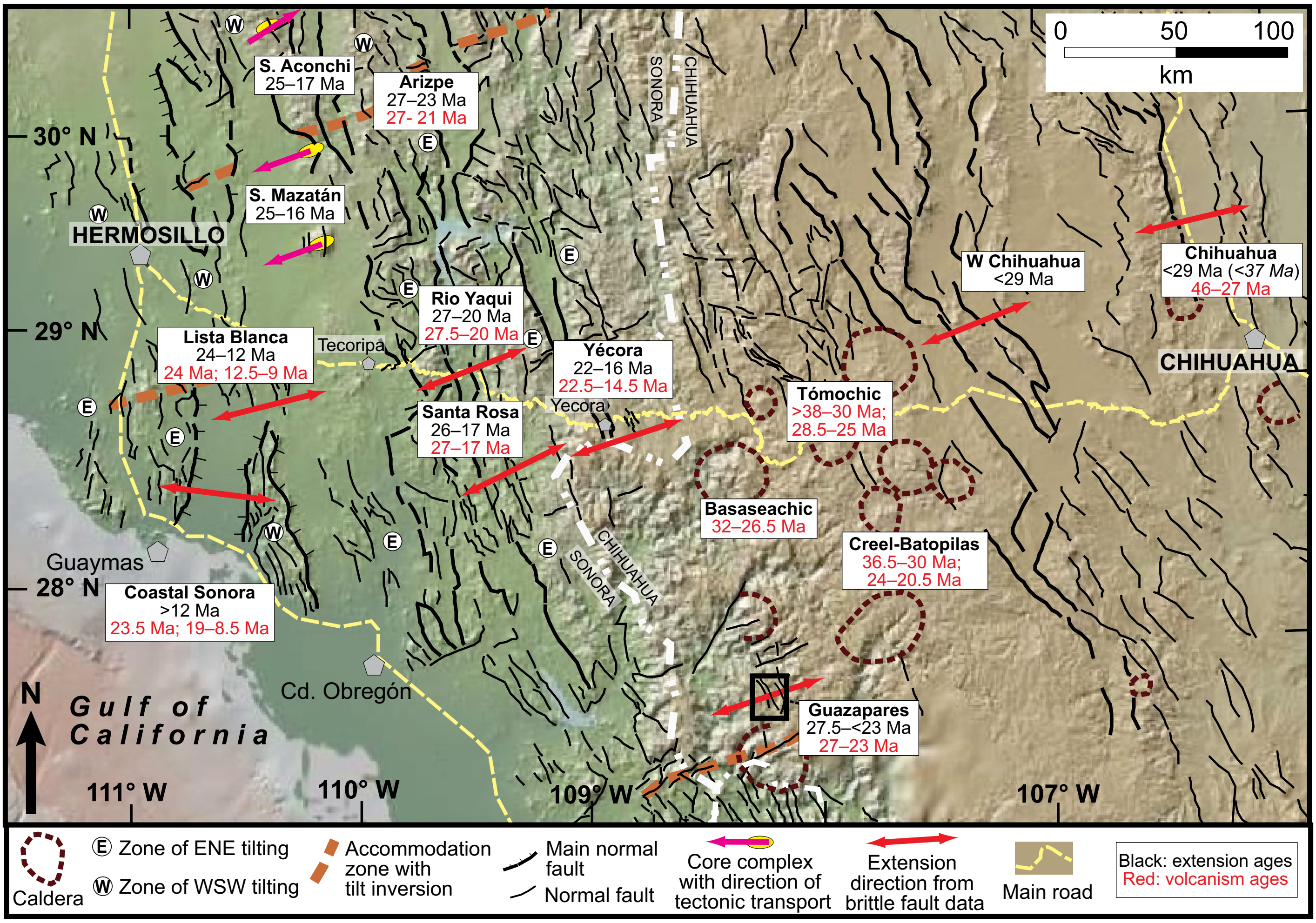

Figure 15. Map of the northern Sierra Madre Occidental showing the timing of extensional deformation and post–Lower Volcanic Complex locally derived volcanism (e.g., intracaldera facies, lavas) in the region relative to Guazapares (this study; black box in figure). Known and inferred calderas in the region are indicated, as well as main Tertiary faults and the direction of crustal extension (modified from Ferrari et al., 2007). Generally, the age of the volcanism is increasingly younger toward the southwest, and although the timing of extension is less constrained, there also appears to be an increasingly younger trend toward the southwest of the study area in the Gulf Extensional Province of Sonora. Ages of extension and volcanism are from Bagby (1979), Cameron et al. (1989), Wark et al. (1990), Swanson et al. (2006), González León et al. (2000), McDowell (2007), Ferrari et al. (2007, and references therein), Wong et al. (2010), McDowell and McIntosh (2012), Bryan et al. (2013), and this study. ENE—east-northeast; WSW—west-southwest.

the Sierra Madre Occidental has been poorly constrained, due at least in part to sparse map data. At the regional scale, the onset of extension possibly migrated episodically from east to west along the entire Sierra Madre Occidental, roughly corresponding to the southwestward migration of the arc front toward the trench; however, in detail volcanism in a given area may be preextensional, synextensional, or postextensional (Ferrari et al., 2007). Although no direct evidence has been found for Eocene extension in the eastern Sierra Madre Occidental proper, there is evidence of an initial episode of extensional faulting during the Early Eocene in the Mesa Central region to the east of the southern Sierra Madre Occidental (Aranda-Gómez and McDowell, 1998; Aguillón-Robles et al., 2009; Tristán-González et al., 2009) and at its easternmost boundary east of Durango during the Early Oligocene (32.3–30.6 Ma; Luhr et al., 2001), east of the unextended core. The earliest initiation of upper crustal extension that developed regionally is inferred to have occurred ca. 30 Ma, marked by the widespread eruption of the Southern Cordillera basaltic andesite province (Cameron et al., 1989). The timing of this event immediately followed the peak of ignimbrite flare-up volcanism of the Early Oligocene pulse and coincided with a decline in silicic explosive volcanism (Bryan and Ferrari, 2013). Following this regional event, extensional deformation generally became focused in the Gulf Extensional Province to the west of the unextended core of the Sierra Madre Occidental and the timing of initial extensional deformation appears to have migrated westward with time in this region (Fig. 15; Gans, 1997; Gans et al., 2003).

Our new geologic mapping and geochronological data from the Guazapares Mining District region is broadly consistent with the interpretations that the inception of volcanism and extension generally migrated southwestward with time across the Sierra Madre Occidental. The Late Oligocene age (ca. 27 Ma) of initial local volcanism in the study area is younger than Late Eocene to Early Eocene volcanism to the northeast, and older than to coeval with Late Oligocene to Early Miocene volcanism to the west (Fig. 15). Our data clearly show that extension in the study area not only preceded local mafic to intermediate volcanism ca. 27 Ma and local silicic ignimbrite flare-up magmatism during the Early Miocene pulse ca. 24.5 Ma, but also overlapped in time with the end of the Early Oligocene pulse of the ignimbrite flare-up in the northern Sierra Madre Occidental, which occurred ~50–150 km to the north and east ca. 32–28 Ma (Fig. 15). The Late Oligocene age (ca. 27.5 to after 23 Ma) of extension in the Guazapares Mining District region is slightly older than to roughly coeval with the onset of extension farther west in Sonora (Fig. 15), where sedimentation in fault-bound grabens and rapid footwall cooling of core complexes also began at the end of the Oligocene to Early Miocene (Gans, 1997; McDowell et al., 1997; Wong et al., 2010).

Extensional Effects on Volcanism

Although much more mapping and dating are needed, we suggest that widespread crustal extension in northwestern Mexico may have played an important role in the later stages of magmatic development of the Sierra Madre Occidental silicic large igneous province. As magmatism migrated southwestward during the Late Oligocene to Miocene toward the Gulf of California, previously extended or currently extending crust likely influenced the composition of melts and promoted the localization of volcanic vents along favorable structures. Extension has been inferred to favor the generation and storage of melt (e.g., Hildreth, 1981; McKenzie and Bickle, 1988; White and McKenzie, 1989; Wark, 1991; Hanson and Glazner, 1995), and crustal thinning and active normal faulting is inferred to promote the ascent of basaltic magma, which results in crustal melting and the formation of silicic magma compositions (e.g., Johnson and Grunder, 2000; Ferrari et al., 2010). Although much of the pre–30 Ma volcanic and structural relationships are unclear, the inferred relationship between lithospheric extension and magmatism is supported by the synextensional nature of the of the Late Oligocene to Early Miocene mid-Cenozoic ignimbrite flare-up in the Sierra Madre Occidental silicic large igneous province, as observed in the Guazapares Mining District region.

CONCLUSIONS

New geologic mapping and zircon U-Pb LA-ICP-MS ages indicate that the Late Oligocene to Early Miocene rocks of the Guazapares Mining District region record synextensional volcanism in the northern Sierra Madre Occidental. Three informal formations are recognized: (1) the Parajes formation, consisting of silicic outflow ignimbrite sheets erupted from distant sources by ca. 27.5 Ma, during the end of the Early Oligocene pulse of the mid-Cenozoic ignimbrite flare-up; (2) the ca. 27–24.5 Ma Témoris formation, comprising locally erupted mafic to intermediate composition volcanic rocks, including an andesitic volcanic center; and (3) the ca. 24.5–23 Ma Sierra Guazapares formation, consisting of vent to proximal silicic ignimbrites, lavas, and plugs erupted by fissure magmatism during the onset of the Early Miocene pulse of the mid-Cenozoic ignimbrite flare-up.

The main geologic structures in the Guazapares Mining District region are NNW–trending normal faults, several of which bound synvolcanic half-graben basins that began to form by the time of deposition of the upper part of the Parajes formation, and continued to develop during deposition of the Témoris and Sierra Guazapares formations. Much of the crustal extension occurred prior to the eruption of the Sierra Guazapares formation, with the earliest evidence of crustal extension by ca. 27.5 Ma. A minimum of 20% total horizontal extension is estimated in the Guazapares Mining District region. Preexisting extensional structures controlled the localization of andesitic and silicic volcanic vents and shallow level intrusions of the Témoris and Sierra Guazapares formations. The age of volcanism and extensional faulting in the Guazapares Mining District region generally corresponds to regional models inferring a post-Eocene southwestward migration of volcanism and crustal extension in the northern Sierra Madre Occidental.

In summary, this study presents direct evidence that crustal extension occurred in the western part of the northern Sierra Madre Occidental during the end of the Early Oligocene pulse of the ignimbrite flare-up. Extension in the Guazapares Mining District region preceded and continued during the onset of local magmatism, consisting first of mafic to andesitic magmatism, followed by silicic magmatism related to the Early Miocene pulse of the ignimbrite flare-up. Regional crustal extension in northwestern Mexico may have played an important role in the magmatic development of the Sierra Madre Occidental silicic large igneous province during the mid-Cenozoic ignimbrite flare-up, promoting the generation of silicic and intermediate magmas and the localization of volcanic eruptions along favorable preexisting geologic structures.

ACKNOWLEDGMENTS

We thank Paramount Gold & Silver Corp., Larry Segerstrom, Danny Sims, and Dana Durgin for financial, logistical, and intellectual contributions, and Denis Norton for arranging this support. Additional financial support was provided by a UC Mexus (University of California Institute for Mexico and the United States) grant (2009-2010) to Busby and Elena Centeno-García, National Science Foundation grant EAR-1019559 to Busby, and a Geological Society of America student research grant to Murray. Dana Roeber Murray, Jordan Lewis, Adrienne Kentner, and Angeles Verde-Ramírez assisted in the field. Carlos Ortega-Obregón and Ofelia Pérez-Arvizu (Universidad Nacional Autónoma de México, UNAM) assisted with laser ablation–inductively coupled plasma–mass spectrometry analyses. Rufino Lozano Santa Cruz (UNAM) assisted with whole-rock geochemical analyses. We thank Graham Andrews for a detailed informal review. Constructive formal reviews by Scott Bryan and an anonymous reviewer and comments by Carol Frost and Keith Putirka helped improve the manuscript.

REFERENCES CITED

Aguillón-Robles, A., Tristán-González, M., Aguirre-Díaz, G.J., and Bellon, H., 2009, Syn-extensional intra-plate trachydacite-rhyolitic dome volcanism of the Mesa Central, southern Sierra Madre Occidental volcanic province, Mexico: Journal of Volcanology and Geothermal Research, v. 187, p. 33–52, doi:10.1016/j.jvolgeores.2009.08.021.

Aguirre-Díaz, G.J., and Labarthe-Hernández, G., 2003, Fissure ignimbrites: Fissure-source origin for voluminous ignimbrites of the Sierra Madre Occidental and its relationship with Basin and Range faulting: Geology, v. 31, p. 773–776, doi:10.1130/G19665.1.

Aguirre-Díaz, G.J., and McDowell, F.W., 1991, The volcanic section at Nazas, Durango, Mexico, and the possibility of widespread Eocene volcanism within the Sierra Madre Occidental: Journal of Geophysical Research, v. 96, no. B8, p. 13373–13388, doi:10.1029/91JB00245.

Aguirre-Díaz, G.J., and McDowell, F.W., 1993, Nature and timing of faulting and synextensional magmatism in the southern Basin and Range, central-eastern Durango, Mexico: Geological Society of America Bulletin, v. 105, p. 1435–1444, doi:10.1130/0016-7606(1993)105<1435:NATOFA>2.3.CO;2.

Albrecht, A., and Goldstein, S.L., 2000, Effects of basement composition and age on silicic magmas across an accreted terrane-Precambrian crust boundary, Sierra Madre Occidental, Mexico: Journal of South American Earth Sciences, v. 13, p. 255–273, doi:10.1016/S0895-9811(00)00014-6.

Andersen, T., 2002, Correction of common lead in U-Pb analyses that do not report ^{204}Pb: Chemical Geology, v. 192, p. 59–79, doi:10.1016/S0009-2541(02)00195-X.

Aranda-Gómez, J.J., and McDowell, F.W., 1998, Paleogene extension in the southern basin and range province of Mexico: Syndepositional tilting of Eocene red beds and Oligocene volcanic rocks in the Guanajuato Mining District: International Geology Review, v. 40, p. 116–134, doi:10.1080/00206819809465201.

Armstrong, R.L., and Ward, P.L., 1991, Evolving geographic patterns of Cenozoic magmatism in the North American Cordillera: The temporal and spatial association of magmatism and metamorphic core complexes: Journal of Geophysical Research, v. 96, no. B8, p. 13201–13224, doi:10.1029/91JB00412.

Axen, G.J., Taylor, W.J., and Bartley, J.M., 1993, Space-time patterns and tectonic controls of Tertiary extension and magmatism in the Great Basin of the western United States: Geological Society of America Bulletin, v. 105, p. 56–76, doi:10.1130/0016-7606(1993)105<0056:STPATC>2.3.CO;2.

Bagby, W.C., 1979, Geology, geochemistry, and geochronology of the Batopilas quadrangle, Sierra Madre Occidental, Chihuahua, Mexico [Ph.D. thesis]: Santa Cruz, University of California, 271 p.

Best, M.G., and Christiansen, E.H., 1991, Limited extension during peak Tertiary volcanism, Great Basin of Nevada and Utah: Journal of Geophysical Research, v. 96, p. 13509–13528, doi:10.1029/91JB00244.

Geosphere, published online on 13 September 2013 as doi:10.1130/GES00862.1

Best, M.G., Christiansen, E.H., and Gromme, S., 2013, The 36–18 Ma southern Great Basin, USA, ignimbrite province and flareup: Swarms of subduction-related supervolcanoes: Geosphere, v. 9, p. 260–274, doi:10.1130/GES00870.1.

Blair, T.C., and McPherson, J.G., 1994, Alluvial fans and their natural distinction from rivers based on morphology, hydraulic processes, sedimentary processes, and facies assemblages: Journal of Sedimentary Research, v. A64, no. 3, p. 450–489, doi:10.1306/D4267DDE-2B26-11D7-8648000102C1865D.

Branney, M.J., and Kokelaar, P., 2002, Pyroclastic density currents and the sedimentation of ignimbrites: Geological Society of London Memoir 27, 150 p.

Brown, R.J., and Branney, M.J., 2004, Bypassing and diachronous deposition from density currents: Evidence from a giant regressive bed form in the Poris ignimbrite, Tenerife, Canary Islands: Geology, v. 32, p. 445–448, doi:10.1130/G20188.1.

Bryan, S., 2007, Silicic large igneous provinces: Episodes, v. 30, no. 1, p. 1–12.

Bryan, S.E., and Ernst, R.E., 2008, Revised definition of large igneous provinces (LIPs): Earth-Science Reviews, v. 86, p. 175–202, doi:10.1016/j.earscirev.2007.08.008.

Bryan, S.E., and Ferrari, L., 2013, Large igneous provinces and silicic large igneous provinces: Progress in our understanding over the last 25 yr: Geological Society of America Bulletin, doi:10.1130/B30820.1.

Bryan, S.E., Riley, T.R., Jerram, D.A., Stephens, C.J., and Leat, P.T., 2002, Silicic volcanism: An undervalued component of large igneous provinces and volcanic rifted margins, *in* Menzies, M.A., et al., eds., Volcanic rifted margins: Geological Society of America Special Paper 362, p. 97–118, doi:10.1130/0-8137-2362-0.97.

Bryan, S.E., Ferrari, L., Reiners, P.W., Allen, C.M., Petrone, C.M., Ramos-Rosique, A., and Campbell, I.H., 2008, New insights into crustal contributions to large-volume rhyolite generation in the mid-Tertiary Sierra Madre Occidental Province, Mexico, revealed by U-Pb geochronology: Journal of Petrology, v. 49, p. 47–77, doi:10.1093/petrology/egm070.

Bryan, S.E., Orozco-Esquivel, T., Ferrari, L., and López-Martínez, M., 2013, Pulling apart the mid to late Cenozoic magmatic record of the Gulf of California: Is there a Comondú arc?, *in* Gomez-Tuena, A., et al., eds., Orogenic andesites and crustal growth: Geological Society of London Special Publication 385, doi:10.1144/SP385 (in press).

Busby, C.J., 2013, Birth of a plate boundary ca. 12 Ma in the ancestral Cascades arc, Walker Lane belt of California and Nevada: Geosphere, doi:10.1130/GES00928.1.

Cameron, K.L., Nimz, G.J., Niemeyer, S., and Gunn, S., 1989, Southern Cordilleran basaltic andesite suite, southern Chihuahua, Mexico: A link between Tertiary continental arc and flood basalt magmatism in North America: Journal of Geophysical Research, v. 94, no. B6, p. 7817–7840, doi:10.1029/JB094iB06p07817.

Carey, S.N., 1991, Transport and deposition of tephra by pyroclastic flows and surges, *in* Fisher, R.V., and Smith, G.A., eds., Sedimentation in volcanic settings: SEPM (Society for Sedimentary Geology) Special Publication 45, p. 39–57, doi:10.2110/pec.91.45.0039.

Cather, S.M., Dunbar, N.W., McDowell, F.W., McIntosh, W.C., and Scholle, P.A., 2009, Climate forcing by iron fertilization from repeated ignimbrite eruptions: The icehouse–silicic large igneous province (SLIP) hypothesis: Geosphere, v. 5, p. 315–324, doi:10.1130/GES00188.1.

Charlier, B.L.A., Wilson, C.J.N., Lowenstern, J.B., Blake, S., Van Calsteren, P.W., and Davidson, J.P., 2004, Magma generation at a large, hyperactive silicic volcano (Taupo, New Zealand) revealed by U-Th and U-Pb systematics in zircons: Journal of Petrology, v. 46, p. 3–32, doi:10.1093/petrology/egh060.

Christiansen, R.L., and Yates, R.S., 1992, Post-Laramide geology of the western U.S. Cordillera, *in* Burchfiel, B.C., et al., eds., The Cordilleran orogen: Conterminous U.S.: Boulder, Colorado, Geological Society of America, Geology of North America, v. G-3, p. 261–406.

Cochemé, J.J., and Demant, A., 1991, Geology of the Yécora area, northern Sierra Madre Occidental, Mexico, *in* Pérez-Segura, E., and Jacques-Ayala, C., eds., Studies in Sonoran geology: Geological Society of America Special Paper 254, p. 81–94, doi:10.1130/SPE254-p81.

Coney, P.J., 1978, Mesozoic–Cenozoic Cordilleran plate tectonics, *in* Smith, R.B., and Eaton, G.P., eds., Cenozoic tectonics and regional geophysics of the Western Cordillera: Geological Society of America Memoir 152, p. 33–50, doi:10.1130/MEM152-p33.

Coney, P.J., and Reynolds, S.J., 1977, Cordilleran Benioff zones: Nature, v. 270, p. 403–406, doi:10.1038/270403a0.

Costa, A., Gottsmann, J., Melnik, O., and Sparks, R.S.J., 2011, A stress-controlled mechanism for the intensity of very large magnitude explosive eruptions: Earth and Planetary Science Letters, v. 310, p. 161–166, doi:10.1016/j.epsl.2011.07.024.

Damon, P.E., Shafiqullah, M., and Clark, K.F., 1981, Age trends of igneous activity in relation to metallogenesis in the southern Cordillera: Arizona Geological Society Digest, v. 14, p. 137–154.

Dickinson, W.R., 2002, The Basin and Range Province as a composite extensional domain: International Geology Review, v. 44, p. 1–38, doi:10.2747/0020-6814.44.1.1.

Dickinson, W.R., 2006, Geotectonic evolution of the Great Basin: Geosphere, v. 2, p. 353–368, doi:10.1130/GES00054.1.

Dreier, J., 1984, Regional tectonic control of epithermal veins in the western United States and Mexico, *in* Wilkins, J., ed., Gold and silver deposits of the Basin and Range Province, western U.S.A.: Arizona Geological Society Digest, v. 15, p. 28–50.

Ferrari, L., López-Martinez, M., Aguirre-Díaz, G., and Carrasco-Núñez, G., 1999, Space-time patterns of Cenozoic arc volcanism in central Mexico: From the Sierra Madre Occidental to the Mexican Volcanic Belt: Geology, v. 27, p. 303–306, doi:10.1130/0091-7613(1999)027<0303:STPOCA>2.3.CO;2.

Ferrari, L., López-Martínez, M., and Rosas-Elguera, J., 2002, Ignimbrite flare-up and deformation in the southern Sierra Madre Occidental, western Mexico: Implications for the late subduction history of the Farallon plate: Tectonics, v. 21, p. 17-1–17-24, doi:10.1029/2001TC001302.

Ferrari, L., Valencia-Moreno, M., and Bryan, S., 2007, Magmatism and tectonics of the Sierra Madre Occidental and its relation with the evolution of the western margin of North America, *in* Alaniz-Álvarez, S.A., and Nieto-Samaniego, Á.F., eds., Geology of México: Celebrating the centenary of the Geological Society of México: Geological Society of America Special Paper 422, p. 1–39, doi:10.1130/2007.2422(01).

Ferrari, L., Bryan, S., Rosique, A.R., Allen, C., Lopez, M., and Rankin, A., 2010, Relationships between rates of silicic magma generation, eruption and extensional tectonics: Insights from the Bolanos Graben, southern Sierra Madre Occidental, Mexico: Geophysical Research Abstracts, v. 12, EGU2010–3825–1.

Fisher, R.V., and Schmincke, H.U., 1984, Pyroclastic rocks: Berlin, Springer Verlag, 472 p.

Fisher, R.V., and Smith, G.A., eds., 1991, Sedimentation in volcanic settings: SEPM (Society for Sedimentary Geology) Special Publication 45, 257 p., doi:10.2110/pec.91.45.

Freundt, A., Wilson, C.J.N., and Carey, S.N., 2000, Ignimbrites and block-and-ash flow deposits, *in* Sigurdsson, H., et al., eds., Encyclopedia of volcanoes: San Diego, California, Academic Press, p. 581–600.

Gans, P.B., 1997, Large-magnitude Oligo-Miocene extension in southern Sonora: Implications for the tectonic evolution of northwest Mexico: Tectonics, v. 16, p. 388–408, doi:10.1029/97TC00496.

Gans, P.B., Mahood, G.A., and Schermer, E.R., 1989, Synextensional magmatism in the Basin and Range Province: A case study from the eastern Great Basin: Geological Society of America Special Paper 233, 53 p., doi:10.1130/SPE233-p1.

Gans, P.B., Blair, K.D., MacMillan, I., Wong, M.S., and Roldán-Quintana, J., 2003, Structural and magmatic evolution of the Sonoran rifted margin: A preliminary report: Geological Society of America Abstracts with Programs, v. 35, no. 4, p. 21.

Gertisser, R., Preece, K., and Keller, J., 2009, The Plinian Lower Pumice 2 eruption, Santorini, Greece: Magma evolution and volatile behaviour: Journal of Volcanology and Geothermal Research, v. 186, p. 387–406, doi:10.1016/j.jvolgeores.2009.07.015.

González León, C.M., McIntosh, W.C., Lozano-Santacruz, R., Valencia-Moreno, M., Amaya-Martínez, R., and Rodríguez-Castañeda, J.L., 2000, Cretaceous and Tertiary sedimentary, magmatic, and tectonic evolution of north-central Sonora (Arizpe and Bacanuchi quadrangles), northwest Mexico: Geological Society of America Bulletin, v. 112, p. 600–610, doi:10.1130/0016-7606(2000)112<600:CATSMA>2.0.CO;2.

Grijalva-Noriega, F.J., and Roldán-Quintana, J., 1998, An overview of the Cenozoic tectonic and magmatic evolution of Sonora, northwestern Mexico: Revista Mexicana de Ciencias, v. 15, no. 2, p. 145–156.

Gunderson, R., Cameron, K.L., and Cameron, M., 1986, Mid-Cenozoic high-K calc-alkalic volcanism in eastern Chihuahua, Mexico: Geology and geochemistry of the Benevides-Pozos area: Geological Society of America Bulletin, v. 97, p. 737–753, doi:10.1130/0016-7606(1986)97<737:MHCAAV>2.0.CO;2.

Gustin, M.M., 2011, Technical report on the San Miguel project, Guazapares Mining District, Chihuahua, Mexico, prepared for Paramount Gold and Silver Corp.: Reno, Nevada, Mine Development Associates, 149 p.

Gustin, M.M., 2012, Updated technical report on the San Miguel project gold and silver resources, Guazapares Mining District, Chihuahua, Mexico, prepared for Paramount Gold and Silver Corp.: Reno, Nevada, Mine Development Associates, 176 p.

Hampton, B.A., and Horton, B.K., 2007, Sheetflow fluvial processes in a rapidly subsiding basin, Altiplano plateau, Bolivia: Sedimentology, v. 54, p. 1121–1148, doi:10.1111/j.1365-3091.2007.00875.x.

Hanson, R.B., and Glazner, A.F., 1995, Thermal requirements for extensional emplacement of granitoids: Geology, v. 23, p. 213–216, doi:10.1130/0091-7613(1995)023<0213:TRFEEO>2.3.CO;2.

Henry, C., and Aranda-Gómez, J.J., 2000, Plate interactions control middle-late Miocene, proto-Gulf and Basin and Range extension in the southern Basin and Range: Tectonophysics, v. 318, p. 1–26, doi:10.1016/S0040-1951(99)00304-2.

Henry, C.D., and Fredrikson, G., 1987, Geology of part of southern Sinaloa, Mexico, adjacent to the Gulf of California: Geological Society of America Map and Chart Series MCH067, scale 1:250,000, 14 p.

Henry, C.D., McIntosh, W., McDowell, F.W., Lipman, P.W., Chapin, C.E., and Richardson, M.T., 2010, Distribution, timing, and controls of the mid-Cenozoic ignimbrite flareup in western North America: Geological Society of America Abstracts with Programs, v. 42, no. 5, p. 144.

Hildreth, W., 1981, Gradients in silicic magma chambers: Implications for lithospheric magmatism: Journal of Geophysical Research, v. 86, no. B11, p. 10153–10192, doi:10.1029/JB086iB11p10153.

Humphreys, E.D., 1995, Post-Laramide removal of the Farallon Slab, western United States: Geology, v. 23, p. 987–990, doi:10.1130/0091-7613(1995)023<0987:PLROTF>2.3.CO;2.

Irvine, T.N., and Baragar, W.R.A., 1971, A guide of the chemical classification of common volcanic rocks: Canadian Journal of Earth Sciences, v. 8, p. 523–548, doi:10.1139/e71-055.

Jicha, B.R., Scholl, D.W., and Rea, D.K., 2009, Circum-Pacific arc flare-ups and global cooling near the Eocene-Oligocene boundary: Geology, v. 37, p. 303–306, doi:10.1130/G25392A.1.

Johnson, J.A., and Grunder, A.L., 2000, The making of intermediate composition magma in a bimodal suite: Duck Butte Eruptive Center, Oregon, USA: Journal of Volcanology and Geothermal Research, v. 95, p. 175–195, doi:10.1016/S0377-0273(99)00125-0.

Kelly, S.B., and Olsen, H., 1993, Terminal fans—A review with reference to Devonian examples: Sedimentary Geology, v. 85, p. 339–374, doi:10.1016/0037-0738(93)90092-J.

Le Bas, M.J., Le Maitre, R.W., Streckeisen, A., and Zanettin, B., 1986, A chemical classification of volcanic rocks

Geosphere, published online on 13 September 2013 as doi:10.1130/GES00862.1

based on the total alkali–silica diagram: Journal of Petrology, v. 27, p. 745–750, doi:10.1093/petrology/27.3.745.

Lipman, P.W., 2007, Incremental assembly and prolonged consolidation of Cordilleran magma chambers: Evidence from the Southern Rocky Mountain volcanic field: Geosphere, v. 3, p. 42–70, doi:10.1130/GES00061.1.

Ludwig, K. L., 2008, Isoplot 3.70. A geochronological toolkit for Microsoft Excel: Berkeley Geochronology Center Special Publication 4, p. 1–77.

Luhr, J.F., Henry, C.D., Housh, T.B., Aranda-Gómez, J.J., and McIntosh, W.C., 2001, Early extension and associated mafic alkalic volcanism from the southern Basin and Range Province: Geology and petrology of the Rodeo and Nazas volcanic fields, Durango (Mexico): Geological Society of America Bulletin, v. 113, p. 760–773, doi:10.1130/0016-7606(2001)113<0760:EEAAMA>2.0.CO;2.

McDowell, F.W., 2007, Geologic transect across the northern Sierra Madre Occidental volcanic field, Chihuahua and Sonora, Mexico: Geological Society of America Digital Map and Chart Series 6, 70 p.

McDowell, F.W., and Clabaugh, S.E., 1979, Ignimbrites of the Sierra Madre Occidental and their relation to the tectonic history of western Mexico, *in* Chapin, C.E., and Elston, W.E., eds., Ash-flow tuffs: Geological Society of America Special Paper 180, p. 113–124, doi:10.1130/SPE180-p113.

McDowell, F.W., and Keizer, R.P., 1977, Timing of mid-Tertiary volcanism in the Sierra Madre Occidental between Durango City and Mazatlan, Mexico: Geological Society of America Bulletin, v. 88, p. 1479–1487, doi:10.1130/0016-7606(1977)88<1479:TOMVIT>2.0.CO;2.

McDowell, F.W., and Mauger, R.L., 1994, K-Ar and U-Pb zircon chronology of Late Cretaceous and Tertiary magmatism in central Chihuahua State, Mexico: Geological Society of America Bulletin, v. 106, p. 118–132, doi:10.1130/0016-7606(1994)106<0118:KAAUPZ>2.3.CO;2.

McDowell, F.W., and McIntosh, W.C., 2012, Timing of intense magmatic episodes in the northern and central Sierra Madre Occidental, western Mexico: Geosphere, v. 8, p. 1505–1526, doi:10.1130/GES00792.1.

McDowell, F.W., Roldán-Quintana, J., and Amaya-Martínez, R., 1997, Interrelationship of sedimentary and volcanic deposits associated with Tertiary extension in Sonora, Mexico: Geological Society of America Bulletin, v. 109, p. 1349–1360, doi:10.1130/0016-7606(1997)109<1349:IOSAVD>2.3.CO;2.

McDowell, F.W., Roldán-Quintana, J., and Connelly, J.N., 2001, Duration of Late Cretaceous–early Tertiary magmatism in east-central Sonora, Mexico: Geological Society of America Bulletin, v. 113, p. 521–531, doi:10.1130/0016-7606(2001)113<0521:DOLCET>2.0.CO;2.

McKenzie, D., and Bickle, M.J., 1988, The volume and composition of melt generated by extension of the lithosphere: Journal of Petrology, v. 29, p. 625–679, doi:10.1093/petrology/29.3.625.

Minjárez Sosa, I., Montaño Jiménez, T.R., Ochoa Granillo, J.A., Grijalva Noriega, F.J., Ochoa Landín, L.H., Herrera Urbina, S., Guzmán Espinosa, J.B., and Mancilla Gutiérrez, A.A., 2002, Carta Geológico-Minera Ciudad Obregón G12–3 Sonora, Chihuahua y Sinaloa: Servicio Geológico Mexicano, scale 1:250,000.

Murray, B.P., Horton, B.K., Matos, R., and Heizler, M.T., 2010, Oligocene–Miocene basin evolution in the northern Altiplano, Bolivia: Implications for evolution of the central Andean backthrust belt and high plateau: Geological Society of America Bulletin, v. 122, p. 1443–1462, doi:10.1130/B30129.1.

Nieto-Samaniego, Á.F., Ferrari, L., Alaniz-Álvarez, S.A., Labarthe-Hernández, G., and Rosas-Elguera, J., 1999, Variation of Cenozoic extension and volcanism across the southern Sierra Madre Occidental volcanic province, Mexico: Geological Society of America Bulletin, v. 111, p. 347–363, doi:10.1130/0016-7606(1999)111<0347:VOCEAV>2.3.CO;2.

Ramírez Tello, E., and Garcia Peralta, Á.A., 2004, Carta Geológico-Minera Témoris G12–B39 Chihuahua: Servicio Geológico Mexicano, scale 1:50,000.

Rowley, P.D., MacLeod, N.S., Kuntz, M.A., and Kaplan, A.M., 1985, Proximal bedded deposits related to pyroclastic flows of May 18, 1980, Mount St. Helens, Washington: Geological Society of America Bulletin, v. 96, p. 1373–1383, doi:10.1130/0016-7606(1985)96<1373:PBDRTP>2.0.CO;2.

Roy, D., Trinder, I.D., and Lustig, G., 2008, Report on the San Miguel project, Guazapares Mining District, Chihuahua, Mexico for Paramount Gold and Silver Corp.: Toronto, Ontario, A.C.A. Howe International Limited, 205 p.

Sambridge, M.S., and Compston, W., 1994, Mixture modeling of multi-component data sets with application to ion-probe zircon ages: Earth and Planetary Science Letters, v. 128, p. 373–390, doi:10.1016/0012-821X(94)90157-0.

Schermer, E.R., and Busby, C.J., 1994, Jurassic magmatism in the central Mojave Desert: Implications for preservation of continental arc volcanic sequences: Geological Society of America Bulletin, v. 106, p. 767–790, doi:10.1130/0016-7606(1994)106<0767:JMITCM>2.3.CO;2.

Sigurdsson, H., Houghton, B.F., McNutt, S.R., Rymer, H., and Stix, J., 2000, Encyclopedia of volcanoes: San Diego, California, Academic Press, 1471 p.

Silva Parejas, C., Druitt, T.H., Robin, C., Moreno, H., and Naranjo, J.-A., 2010, The Holocene Pucón eruption of Volcán Villarrica, Chile: Deposit architecture and eruption chronology: Bulletin of Volcanology, v. 72, p. 677–692, doi:10.1007/s00445-010-0348-9.

Sláma, J., and 13 others, 2008, Plešovice zircon—A new natural reference material for U-Pb and Hf isotopic microanalysis: Chemical Geology, v. 249, p. 1–35, doi:10.1016/j.chemgeo.2007.11.005.

Smith, R.L., 1960, Zones and zonal variations in welded ash flows: U.S. Geological Survey Professional Paper 354-F, p. 149–159.

Solari, L.A., and Tanner, M., 2011, UPb.age, a fast data reduction script for LA-ICP-MS U-Pb geochronology: Revista Mexicana de Ciencias Geológicas, v. 28, no. 1, p. 83–91.

Solari, L.A., Gómez-Tuena, A., Bernal, J.P., Pérez-Arvizu, O., and Tanner, M., 2010, U-Pb zircon geochronology by an integrated LA-ICPMS microanalytical workstation: Achievements in precision and accuracy: Geostandards and Geoanalytical Research, v. 34, p. 5–18, doi:10.1111/j.1751-908X.2009.00027.x.

Swanson, E.R., 1977, Reconnaissance geology of the Tomochic-Ocampo area, Sierra Madre Occidental, Chihuahua, Mexico [Ph.D. thesis]: Austin, University of Texas, 123 p.

Swanson, E.R., and McDowell, F.W., 1984, Calderas of the Sierra Madre Occidental volcanic field, western Mexico: Journal of Geophysical Research, v. 89, p. 8787–8799, doi:10.1029/JB089iB10p08787.

Swanson, E.R., and McDowell, F.W., 1985, Geology and geochronology of the Tomochic caldera, Chihuahua, Mexico: Geological Society of America Bulletin, v. 96, p. 1477–1482, doi:10.1130/0016-7606(1985)96<1477:GAGOTT>2.0.CO;2.

Swanson, E.R., Kempter, K.A., McDowell, F.W., and McIntosh, W.C., 2006, Major ignimbrites and volcanic centers of the Copper Canyon area: A view into the core of Mexico's Sierra Madre Occidental: Geosphere, v. 2, p. 125–141, doi:10.1130/GES00042.1.

Tera, F., and Wasserburg, G., 1972, U-Th-Pb systematics in three Apollo 14 basalts and the problem of initial Pb in lunar rocks: Earth and Planetary Science Letters, v. 14, p. 281–304, doi:10.1016/0012-821X(72)90128-8.

Tristán-González, M., Aguirre-Díaz, G.J., Labarthe-Hernández, G., Torres-Hernández, J., and Bellon, H., 2009, Post-Laramide and pre-Basin and Range deformation and implications for Paleogene (55–25 Ma) volcanism in central Mexico: A geological basis for a volcano-tectonic stress model: Tectonophysics, v. 471, p. 136–152, doi:10.1016/j.tecto.2008.12.021.

Umhoefer, P.J., Dorsey, R., Willsey, S., Mayer, L., and Renne, P., 2001, Stratigraphy and geochronology of the Comondú Group near Loreto, Baja California Sur, Mexico: Sedimentary Geology, v. 144, p. 125–147, doi:10.1016/S0037-0738(01)00138-5.

Ward, P.L., 1991, On plate tectonics and the geologic evolution of southwestern North America: Journal of Geophysical Research, v. 96, no. B7, p. 12,479–12,496, doi:10.1029/91JB00606.

Wark, D.A., 1991, Oligocene ash flow volcanism, northern Sierra Madre Occidental: Role of mafic and intermediate-composition magmas in rhyolite genesis: Journal of Geophysical Research, v. 96, no. B8, p. 13,389–13,411, doi:10.1029/90JB02666.

Wark, D.A., Kempter, K.A., and McDowell, F.W., 1990, Evolution of waning subduction-related magmatism, northern Sierra Madre Occidental, Mexico: Geological Society of America Bulletin, v. 102, p. 1555–1564, doi:10.1130/0016-7606(1990)102<1555:EOWSRM>2.3.CO;2.

White, R.S., and McKenzie, D.P., 1989, Magmatism at rift zones: The generation of volcanic continental margins and flood basalts: Journal of Geophysical Research, v. 94, p. 7685–7729, doi:10.1029/JB094iB06p07685.

Wong, M.S., Gans, P.B., and Scheier, J., 2010, The ^{40}Ar/^{39}Ar thermochronology of core complexes and other basement rocks in Sonora, Mexico: Implications for Cenozoic tectonic evolution of northwestern Mexico: Journal of Geophysical Research, v. 115, B07414, doi:10.1029/2009JB007032.

Wood, D.R., and Durgin, D.C., 2009, Technical report project update: San Miguel project, Chihuahua, Mexico, prepared for Paramount Gold and Silver Corp.: Sparks, Nevada, Delve Consultants, L.L.C., 86 p.

Wright, J.V., Self, S., and Fisher, R.V., 1981, Towards a facies model for ignimbrite-forming eruptions, *in* Self, S., and Sparks, R.S., eds., Tephra studies: Dordrecht, Netherlands, D. Reidel, p. 433–439.